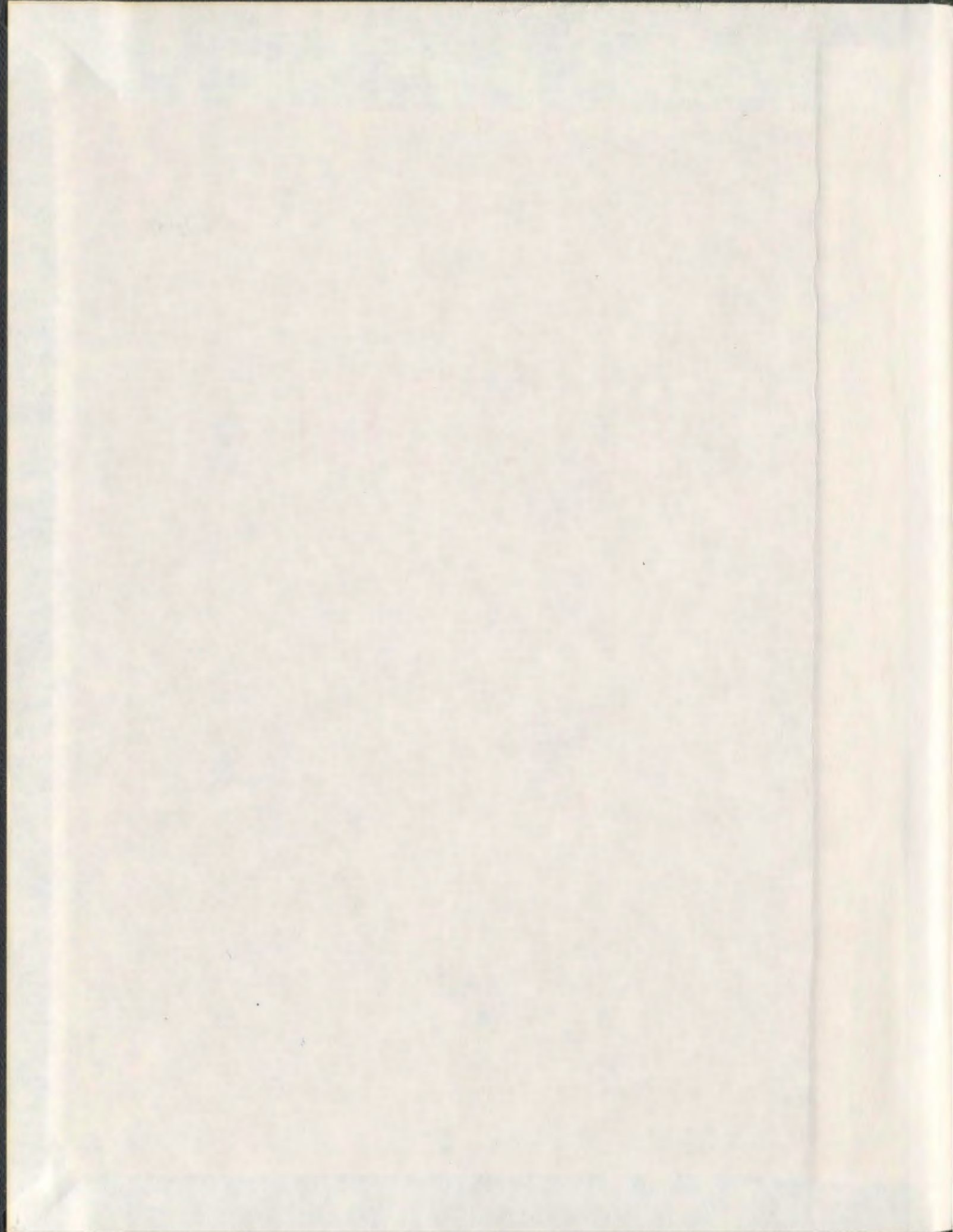


**CONSEQUENCE ANALYSIS FOR THE RISK-BASED  
DESIGN OF OFFSHORE SAFETY SYSTEM**

**MOHAMMAD DADASHZADEH**







**Consequence Analysis for the Risk-Based Design of Offshore Safety System**

by

© Mohammad Dadashzadeh

A Thesis submitted to the

School of Graduate Studies

in partial fulfillment of the requirements for the degree of

**Doctor of Philosophy**

**Faculty of Engineering and Applied Science**

Memorial University of Newfoundland

**March 2013**

St. John's

Newfoundland

## ABSTRACT

Safety measure design and accident predictive and prevention strategies are critical in the offshore process. The key area of concern in an offshore facility is a major event such as a fire, an explosion and the release of hazardous materials. The recent BP Transocean Deepwater Horizon accident is an example of safety protocols either being inadequate or response being inefficient and ineffective. Understanding the consequences of major release events is a key step in safety measure design and consequence assessment of major events. The assessment includes the definition of different release scenarios, release modeling, event modeling, and damage/loss quantification. The consequence assessment is an important step of risk estimation and is subsequently used to design safety measures.

To address release scenario modeling, a new methodology is developed in the current study to revise the emission factor estimation methods earlier developed by USEPA. Applying a non-linear regression approach, a new set of equations is introduced to estimate emission rates. Having  $\Delta AIC$  values of more than 10, in the categories of pump seals, connectors, flanges and others, the equations replace USEPA's proposed correlation equations for oil and gas facilities.

Computational Fluid Dynamics (CFD) is used to simulate different release scenarios, particularly to study fire, explosion and toxic dispersion. The Flame Acceleration Simulator (FLACS), a CFD tool, is used to model explosion and toxic dispersion of

combustion products. To improve the consequence modeling work, a systematic approach for CFD modeling of Vapour Cloud explosion (VCE) is also introduced. Fire Dynamic Simulator (FDS) is used to model pool and jet fires.

A novel integrated approach in modeling the evolving accident scenarios is also developed in the current study. To develop the toxic risk profile of combustion products of an installation, a risk-based approach is proposed, overcoming the shortcomings of a concentration-based approach.

The newly developed approaches and models are tested on real-life case studies.

## ACKNOWLEDGEMENTS

I would like to express my sincere and profound sense of gratitude and respect to my supervisor Dr. Faisal Khan for his expert guidance and untiring support throughout my research time at Memorial University of Newfoundland. I also wish to express my sincere sense of gratitude to my co-supervisor Dr. Kelly Hawboldt for her help and support. Without their encouragement and advice, this thesis might not have been completed successfully. I am also thankful to my supervisory committee member, Dr. Rouzbeh Abbassi, and my proposal examiners Drs Bing Chen and Helen Zhang for their critical comments and constructive suggestions.

I am grateful to my family members, especially my father, mother and sister for their unconditional love and affection during all these years.

## Table of Contents

ABSTRACT.....	ii
ACKNOWLEDGEMENTS.....	iv
Table of Contents.....	v
List of Tables .....	x
List of Figures .....	xi
List of Symbols, Nomenclature or Abbreviations .....	xiv
1 Introduction.....	1
1.1 Overview .....	1
1.2 Consequence analysis.....	1
1.3 Motivation .....	4
1.4 Organization of the Thesis .....	6
1.5 References .....	8
2 Novelty and contribution .....	12
2.1 Overview .....	12
2.1.1 Release modeling.....	12
2.1.2 Vapour cloud explosion (VCE) modeling .....	13

2.1.3	Integration of fire and explosion consequences .....	14
2.1.4	Combustion products toxicity risk assessment .....	14
3	Literature review .....	16
3.1	Consequence analysis.....	16
3.1.1	Defining the potential accident scenarios .....	16
3.1.2	Evaluating the event consequences.....	19
3.1.3	Event impact estimation.....	29
3.2	References .....	32
4	Emission factor estimation for oil and gas industry*.....	37
	Abstract .....	37
4.1	Introduction .....	38
4.2	Correlation equation development methodology .....	41
4.2.1	EPA correlation equation approach .....	41
4.2.2	Approach used in the current study.....	44
4.3	Application of the new approach: a case study .....	46
4.4	Results and discussion.....	50
4.5	Conclusion.....	55
4.6	References .....	56

5	Explosion modeling and analysis of BP deepwater horizon accident* .....	59
	Abstract .....	59
5.1	Introduction .....	60
5.1.1	Important vapour cloud explosion accidents .....	60
5.2	Vapour cloud explosion modeling .....	64
5.2.1	CFD modeling.....	66
5.3	Results and discussion.....	82
5.3.1	Dispersion .....	82
5.3.2	Explosion .....	86
5.4	Conclusion.....	90
5.5	References .....	92
6	An Integrated Approach for Fire and Explosion Consequence Modelling.....	98
	Abstract .....	98
6.1	Introduction .....	99
6.1.1	Hazards caused due to the release of hydrocarbons.....	102
6.1.2	Past major accidents and their analysis.....	104
6.2	Proposed methodology .....	106
6.3	Case studies .....	111

6.3.1	Case study 1: LNG vapour cloud explosion and the consequent pool fire	111
6.3.2	Case study 2: BP Deepwater Horizon vapour cloud explosion and the consequent fire .....	115
6.4	Results and discussions .....	119
6.4.1	Case study 1: Explosion.....	119
6.4.2	Case study 1: Pool fire .....	122
6.4.3	Case study 1: Integration of effects .....	124
6.4.4	Case study 2: Explosion.....	125
6.4.5	Case study 2: Jet fire .....	127
6.4.6	Case study 2: Integration of effects .....	129
6.5	Conclusion.....	130
6.6	References .....	132
7	Combustion Products Toxicity Risk Assessment in an Offshore Installation .....	138
	Abstract .....	138
7.1	Introduction .....	139
7.2	Toxicity risk assessment approach.....	141
7.2.1	Risk assessment .....	142
7.3	Results .....	148

7.4	Conclusion.....	154
7.5	References .....	156
8	Conclusions, and recommendations.....	160
8.1	Conclusions .....	160
8.1.1	New equations to model emission factors .....	160
8.1.2	Systematic approach to model vapour cloud explosion.....	160
8.1.3	Integration of the dispersion of flammable vapour with explosion modeling 161	
8.1.4	Integrated modeling of fire and explosion consequences .....	161
8.1.5	Risk-based approach for toxicity assessment .....	162
8.2	Recommendations .....	163
8.2.1	CFD explosion modeling .....	163
8.2.2	Integrated consequence modeling.....	163
8.2.3	Toxic dispersion modeling.....	164
8.2.4	Data uncertainty analysis .....	165

## List of Tables

Table 3.1. Damage estimates for common structures based on overpressure [Crowl and Louvar, 2001].....	21
Table 3.2. Comparison of the empirical models .....	22
Table 3.3. Comparison of the phenomenological models.....	24
Table 3.4. Comparison of the CFD models .....	25
Table 3.5. Comparison of the advanced CFD models .....	27
Table 3.6. Definition of D value in probit function .....	31
Table 4.1. Component categories with the number of data [USEPA, 1995].....	47
Table 4.2. Comparison of the equations developed by EPA and non-linear approach.....	51
Table 5.1. Damage estimates for common structures based on overpressure [Crowl and Louvar, 2001].....	65
Table 5.2. Simplified gas composition for FLACS analysis [BP, 2010].....	76
Table 5.3. Time dependent release points for scenario A [BP, 2010] .....	78
Table 5.4. Comparison of dispersion results.....	86
Table 6.1. Major human effects caused by fire and explosion [Assail and Kakosimos, 2010] .....	109
Table 6.2. Scores (S) for seven major human effects caused by fire and explosion.....	110
Table 7.1. Emission factors, fuel consumption and the flow rate of CO and NO <sub>2</sub> .....	143
Table 7.2. Adverse health effects [Abbassi et al., 2012; OSHA, 2003] .....	143

## List of Figures

Figure 1.1. Quantitative risk analysis flowchart .....	2
Figure 1.2. Focus of the current work.....	3
Figure 4.1. Application of linear regression with ISV and emission rate.....	43
Figure 4.2. Application of non-linear regression with ISV and leak rate.....	46
Figure 4.3. Trends of actual data and EPA and new equations' estimation of emission leak rate (Pump seals).....	53
Figure 4.4. Trends of actual data and EPA and new equations' estimation of emission leak rate (Flanges) .....	54
Figure 4.5. Trends of actual data and EPA and new equations' estimation of emission leak rate (Others) .....	54
Figure 5.1. The required steps for the CFD modeling of vapour cloud dispersion/explosion .....	72
Figure 5.2. Geographic location of the well [BP, 2010].....	73
Figure 5.3. BP Deepwater Horizon geometry used for dispersion/explosion simulation..	80
Figure 5.4. Second deck, configuration of engine rooms #1 to #6 .....	81
Figure 5.5. Gas concentration at engine rooms' ventilation inlets with no operating ventilation system .....	83
Figure 5.6. Gas concentration at engine rooms' ventilation inlets with operating ventilation system .....	84
Figure 5.7. Gas concentration at engine rooms' ventilation inlets.....	85

Figure 5.8. Overpressure due to explosion in engine room 6 .....	88
Figure 5.9. Overpressure vs. Distance from the Aft side to the Forward side of the platform.....	88
Figure 5.10. Maximum overpressure contour plot at the surface of the platform .....	90
Figure 6.1. Applied methodology to model the sequences of an evolving accident scenario and the integrated effect.....	108
Figure 6.2. The considered geometry.....	112
Figure 6.3. Dispersion of vapourized fuel over the plant (-) .....	113
Figure 6.4. LNG pool diameter and depth after the explosion (m).....	114
Figure 6.5. BP Deepwater Horizon geometry used for dispersion/explosion simulation	117
Figure 6.6. Second deck, configuration of engine rooms #1 to #6 .....	118
Figure 6.7. Explosion overpressure over the plant (bar).....	120
Figure 6.8. Explosion risk profile (-) .....	121
Figure 6.9. Temperature after the explosion over the pool of LNG (K).....	121
Figure 6.10. Heat radiation caused by the pool fire over the plant (kW/m <sup>2</sup> ) .....	123
Figure 6.11. Pool fire risk profile (-).....	124
Figure 6.12. Integrated risk profile (-) .....	125
Figure 6.13. Explosion overpressure over the plant (bar).....	126
Figure 6.14. Explosion risk profile (-) .....	127
Figure 6.15. Heat radiation caused by the jet fire over the plant (kW/m <sup>2</sup> ) .....	128
Figure 6.16. Jet fire risk profile (-).....	128
Figure 6.17. Integrated risk profile (-) .....	130

Figure 7.1. A methodology of toxic risk assessment .....	142
Figure 7.2. Schematic of offshore installation considered in modeling scenario .....	146
Figure 7.3. Time spent by a person during a day .....	147
Figure 7.4. Air flow over the plant due to wind effect.....	149
Figure 7.5. CO concentration ( $\text{mgm}^{-3}$ ).....	150
Figure 7.6. NO <sub>2</sub> concentration ( $\text{mgm}^{-3}$ ) .....	150
Figure 7.7. CH <sub>4</sub> concentration ( $\text{mgm}^{-3}$ ) .....	151
Figure 7.8. Hazard quotients ( $\text{Risk}_{\text{CO}}$ ) for CO inhalation over the plant .....	151
Figure 7.9. Hazard quotients ( $\text{Risk}_{\text{NO}_2}$ ) for NO <sub>2</sub> inhalation over the plant .....	152
Figure 7.10. Hazard quotients ( $\text{Risk}_{\text{CH}_4}$ ) for CH <sub>4</sub> inhalation over the plant .....	152
Figure 7.11. Final risk ( $\text{Risk}_f$ ) for NO <sub>2</sub> , CO and CH <sub>4</sub> inhalation over the plant .....	153

## **List of Symbols, Nomenclature or Abbreviations**

ACGIH: American Conference of Governmental Industrial Hygienists

AIC: Akaike's Information Criteria

API: American Petroleum Institute

ASME: American Society of Mechanical Engineers

BakerRisk: Baker Engineering and Risk

BOP: Blowout Preventer

BP: British Petroleum

BW: Body Weight

CASD: Computer Aided Scenario Design

CCPS: Center for Chemical Process safety

CFD: Computational Fluid Dynamic

CFLC: Courant-Friedrich-Levy number based on speed of sound

CFLV: Courant-Friedrich-Levy number based on flow velocity

CLICHE: Confined Link Chamber Explosions

CSB: Chemical Safety Board

DEA: Domino Effect Analysis

EDT: Emergency Drain Tank

FDS: Fire Dynamic Simulator

FLACS: Flame Acceleration Simulator

FPSO: Floating Production Storage and Offloading

FR: Flammable Range

GPSI: GraphPad Software Incorporation

HEX: High Expansion

HPCL: Hindustan Petroleum Corporation Limited

HSE: Health and Safety Executive

HSL: Health Sciences Library

ISFI: International Symposium on Fire Investigation Science and Technology

ISV: Individual Screening Value

LES: Large Eddie Simulation

LFL: Lower Flammable Limit

LNG: Liquefied Natural Gas

LPG: Liquefied Petroleum Gas

MAXCRED: MAXimum CREDible rapid risk assessment

MGS: Mud Gas Separator

MSE: Mean Square Error

NGL: Natural Gas Liquid

NIST: National Institute of Standards and Technology

NSERC: Natural Sciences and Engineering Research Council of Canada

NTNU: Norwegian University of Science and Technology

OSHA: Occupational Safety and Health Administration

PHAST: Process Hazard Analysis Software Tool

RANS: Reynold-Average Navier-Stokes

RDCT: R Development Core Team

RV: Relief Valve

SBCF: Scale Bias Correction Factor

SCOPE: Shell Code for Overpressure Prediction in gas Explosion

SIF: Simple Interface Flame

SIMPLE: Semi-Implicit Method for Pressure Linked Equations

SLIC: Simple Line Interface Calculation

SS: Sum of Squared errors

TLV: Threshold Limit Value

TNO: The Netherlands Organization for Applied Scientific Research

TNT: Trinitrotoluene

TWA: Time-Weight Average

UFL: Upper Flammable Limit

USEPA: United States Environmental Protection Agency

VCE: Vapour Cloud Explosion

WHO: World Health Organization

## Symbols

A (mass, volume, distance, duration of the activity emitting pollutant): Activity rate

a: Constant

b: Constant

C (ppm): Concentration

$c_1$ : Constant

$C_{10}H_{22}$ : n-Decane

$c_2$ : Constant

$C_2H_6$ : Ethane

$C_3H_8$ : Propane

$C_4H_{10}$ : Butane

$C_5H_{12}$ : Pentane

$C_6H_{14}$ : Hexane

$C_7H_{16}$ : Heptane

$C_8H_{18}$ : n-Octane

$C_9H_{20}$ : n-Nonane

CH<sub>4</sub>: Methane

C<sub>i</sub> (-): Fuel concentration fraction in the mixture of fuel, air and combustion products

CO<sub>2</sub>: Carbon monoxide

E (mass): Emission

EF (mass/mass, volume, distance, or duration of the activity emitting the pollutant):

Emission factor

ER (%): Overall emission reduction efficiency

F: Ratio explaining the variability

F<sub>α</sub>, numerator d.f., denominator d.f.: F-critical

k (Jkg<sup>-1</sup>): Turbulent kinetic energy

k: Number of parameters

M: number of data pairs-1

n: Number of data pairs

NO<sub>2</sub>: Nitrogen dioxide

P (-): Probability

P<sub>0</sub> (Pa): Overpressure

$P_i$  (bar): Explosion overpressure

$P_{MAX}$  (bar): Maximum overpressure

$P_r$ : Probit value

$q$  ( $W/m^2$ ): heat flux

$R^2$ : Parameter for the best fit of nonlinear regression

$R^2_a$ : Adjusted parameter for the best fit of nonlinear regression

$Risk_{CH_4}$  (-): Risk of methane inhalation

$Risk_{CO}$  (-): Risk of carbon monoxide inhalation

$Risk_e$  (-): Overpressure risk

$Risk_f$  (-): Final risk

$Risk_f$  (-): Heat radiation risk

$Risk_i$  (-): Risk index for  $i^{th}$  effect

$Risk_{NO_2}$  (-): Risk of nitrogen dioxide inhalation

$Risk_t$  (-): Overall risk

$S_i$  (-): Effect score for  $i^{th}$  effect

$S_{QL}$  ( $ms^{-1}$ ): Quasi-laminar burning velocity

xx

$SS_{reg}$ : Sum of the squares of distances of the points from the best fit of curve

$SS_{tot}$ : Sum of the squares of distances of the points from a horizontal line through the mean of all y values

$S_T$  ( $ms^{-1}$ ): Turbulent burning velocity

$S_u$  ( $ms^{-1}$ ): Burning velocity

$t$  (-): exposure time

$X_i$ : Natural logarithm of the screening value

$Y_i$ : Natural logarithm of the leak rate

$\alpha$ : Rejection region

$\beta_0$ : Intercept of the regression line

$\beta_1$ : Slope of the regression line

$\epsilon$  ( $m^2s^{-3}$ ): Dissipation of turbulent kinetic energy

# 1 Introduction

## 1.1 Overview

## 1.2 Consequence analysis

Increasing energy demand is driving offshore exploration to more remote, deeper, and harsher environments and as a result safety issues and accident prediction and prevention are becoming increasingly challenging.

The key areas of concern are major accidents, starting from a hydrocarbon release leading to dispersion, fire, and explosion that may likely occur. As shown in Figure 1.1, there are seven steps in a detailed quantitative risk analysis. Consequence analysis is the most important step. It begins with defining the potential accident scenarios, evaluating the event consequences, and estimating the event impacts. This approach can be used as a tool in prevention and/or mitigation of accidents.

The current study focuses on the following tasks:

- Development of a methodology for release scenarios and emission factors assessment.
- Development of an integrated methodology for dispersion, fire, and explosion scenario modeling.
- Development of an approach to integrate consequence assessment into a risk assessment framework.

- Development of a risk evaluation methodology and its integration with design of safety measures.

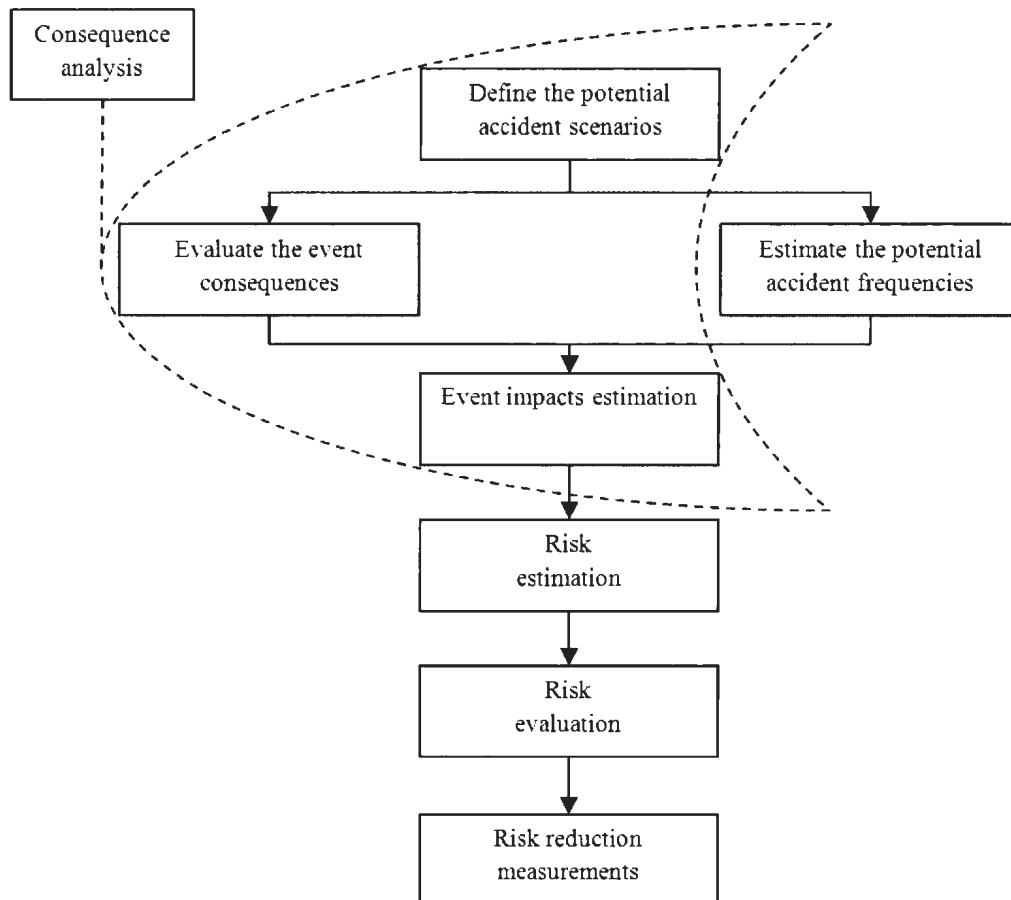


**Figure 1.1. Quantitative risk analysis flowchart**

Figure 1.2 demonstrates the focus of the current work presented in this thesis.

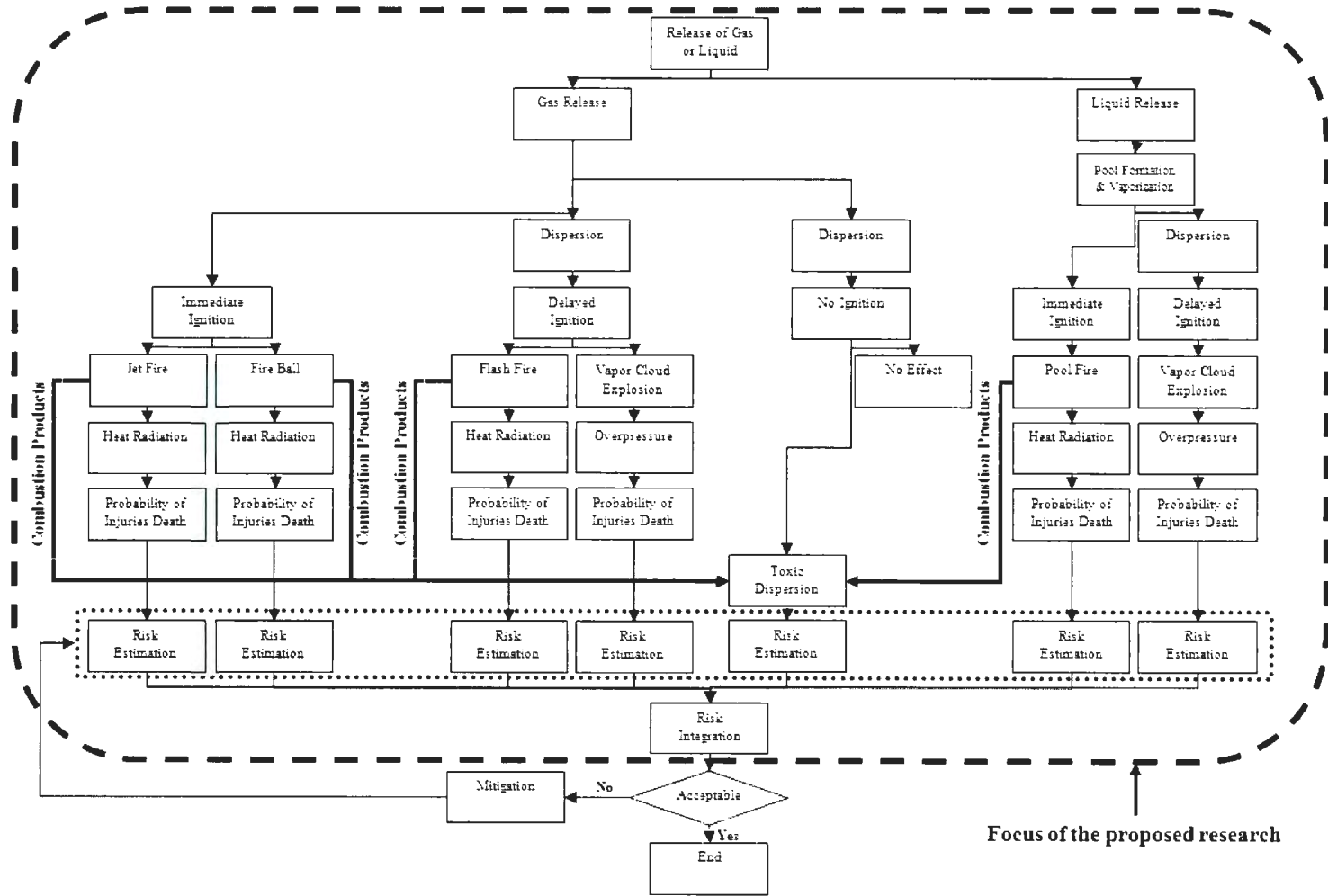


Figure 1.2. Focus of the current work

### 1.3 Motivation

Due to the lack of available detailed quantitative methods and tools for consequence assessment, this work explored the application of CFD codes FLCAS and FDS to analyze the consequences involving the release of hydrocarbons and the subsequent events in an offshore oil and gas installation. This work has also explored the interaction of different consequence events. The current work attempts to address the following points:

- Estimation of emission factor was extensively studied through various researches [USEPA, 1995; Dubose et al., 1982; API, 1993a; API, 1993b; API, 1995]. Methods for estimating emission factors include the average emission factor approach, screening range approach, USEPA's correlation approach and unit-specific correlation approach. However, the mentioned methods suffer from a lack of precision. In the present work, a methodology is proposed in order to better estimate emission factors in oil and gas facilities, optimizing USEPA's correlation approach.
- Using CFD codes to simulate the vapour cloud explosion (VCE) due to a hydrocarbon release is a common method and is applied in many studies; CFD codes were used in defining the obstacles' configuration on an installation to reduce the risk [Berg et al., 2000], to investigate the effects of natural and mechanical configurations on explosion overpressure [Moros et al., 1996] and to estimate the damages caused by explosion overpressure on a platform [Wingerden

and Salvesen, 1995]. However, these studies modeled the explosion phenomenon based only on stoichiometric volume of the flammable fuel vapour, ignoring the dispersion characteristics of the flammable vapour. Due to the importance of dispersion characteristics on the resulted explosion overpressure, the current study proposes a methodology to simulate VCE considering the dispersion of the flammable vapour.

- Comprehensive studies have been done to model the consequences of the release of hydrocarbons; these studies range from advanced CFD simulation to comparison of different tools in accident modeling [Hansen et al, 2009; Gavelli et al., 2010; Kim and Salvesen, 2002; Skarsbo, 2011; Suardin et al., 2009; Yun et al., 2011; Qi et al, 2010]. One shortcoming in above mentioned studies is that they only focus on assessing individual events such as fire or explosion, ignoring the interactions among events. The combination of events is very important, as one event may lead to another and escalate the overall consequence. Through the current study, the authors highlight the importance of integral accident scenarios and their use in consequence analysis.
- Offshore personnel spend most of their time in the semi enclosed processing area or the enclosed office/residential area. Thus, it is important to minimize harmful effects during an accidental event. According to Pula et al. (2005), fire is the most frequent accident occurring on offshore installations. One of the main sources of concern is the combustion of hydrocarbons due to accidents causing fire [Hartzell, 2001]. Thus, there is a need to carefully assess the hazards caused by a fire

accident such as heat radiation and airborne toxic contaminants (combustion products). Safety measure design and emergency preparedness is not very effective if they are only based on contaminants' concentration. Personnel spent different time durations in various locations of the plant (different exposure time), and the concentration of various toxic substances cannot be simply added. To overcome this shortcoming, the current research exploits a risk-based approach considering the time duration for which personnel are exposed to air pollutants in different sections of a plant. Additionally, it helps to combine the harmful effects caused by various toxic substances [Markatos, 2012].

#### **1.4 Organization of the Thesis**

The thesis is written in manuscript format (paper based) as explained below:

In chapter 2, the novelties and contributions this thesis has made to consequence analysis are discussed. Novel approaches to emission factor estimation, vapour cloud explosion modeling (VCE), integrated fire and explosion consequence analysis and combustion products toxicity assessment are explained in this chapter.

Chapter 3 discusses the literature review associated with this thesis. Release modeling approaches, dispersion modeling methods, and fire and explosion modeling related studies are presented in this chapter.

Chapter 4 presents the emission factor estimation methodology proposed through the present work. Past approaches of emission factor estimation and their shortcomings, and

a novel approach to precisely estimate the emission factors in oil and gas facilities are discussed. There is also a set of new equations, based on the proposed methodology, with a qualitative comparison with the USEPA equations to estimate the emission factors. This chapter is published in the *Journal of Process Safety and Environmental Protection* 2011; 89: 295–299.

In chapter 5, a systematic approach to model the VCE through the application of CFD codes is introduced. The limitations of associated studies and how the current work overcomes these shortcomings are also presented in detail with a real case study. This chapter is published in the *Journal of Safety Science* 2013; 57: 150-160.

Chapter 6 discusses an integrated approach to fire and explosion consequence analysis. The limitations of past consequence modeling methodologies are explained in this chapter. The main contribution of this work is the consideration of interactions of events in an evolving accident scenario. This chapter presents the approach with two case studies; a hypothetical case study with the focus on VCE and the consequent pool fire, and a real case study with the focus of VCE and the consequent jet fire. The chapter is submitted to the *fire safety journal* for publication.

Chapter 7 presents a risk-based approach in combustion products' toxicity risk assessment. The advantages of a risk-based approach over a concentration-based one in toxicity risk assessment are mapped in an offshore installation. The chapter is submitted to the *journal of process safety and environmental protection* for publication.

Chapter 8 presents the conclusions of the current research. There are also recommendations provided for future work towards the end of this chapter.

## 1.5 References

American Petroleum Institute (API). (1993a). *Development of fugitive emission factors and emission profiles for petroleum marketing terminals*. Health and environmental sciences. Washington, D.C.: American Petroleum Institute.

American Petroleum Institute (API). (1993b). *Fugitive hydrocarbon emissions from oil and gas production operations*. Health and environmental sciences. Washington, D.C.: American Petroleum Institute.

American Petroleum Institute (API). (1995). *Emission factors for oil and gas production operations*. Health and environmental sciences. Washington, D.C.: American Petroleum Institute.

Berg, J. T., Bakke, J. R., Fearnly, P., & Brewerton, R. B. (2000). CFD layout sensitivity study to identify optimum design of a FPSO. *Offshore technology conference*. Houston, Texas.

Dubose, D. A., Steinmetz, J. I., & Harris, G. E. (1982). *Frequency of leak occurrence and emission factors for natural gas liquid plants*. U. S. Environmental Protection Agency, Research triangle park, NC 27711.

Gavelli, F., Davis, S. G., & Hansen, O. R. (2010). Evaluating the potential for overpressures from the ignition of an LNG vapour cloud during offloading. *Journal of Loss Prevention in the Process Industries*, 24, 908-915.

Hansen, O. R., Ichard, M., & Davis, S. G. (2009). Validation of FLACS against experimental data sets from the model evaluation database for LNG vapour dispersion. *Journal of loss prevention in the process industries*, 23, 857-877.

Hartzell, G. E. (2001). Engineering analysis of hazards to life safety in fires: the fire effluent toxicity component. *Safety science*, 38, 147-155.

Koo, J., Kim, H. S., So, W., Kim, K. H., & Yoon, E. S. (2009). Safety assessment of LNG terminal focused on the consequence analysis of LNG spills. *Proceeding of the 1st annual gas processing symposium*, (pp. 325-311). Doha, Qatar.

Markatos, N. C. (2012). Dynamic computer modeling of environmental systems for decision making, risk assessment and design. *Asia-Pacific journal of chemical engineering*, 7, 182-205.

Moros, A., Tam, V., Webb, S., Paterson, K., & Coulter, C. (1996). The effect of ventilation and gas cloud size on explosion overpressure. *International conference on health, safety and environment*. New Orleans.

- Pula, R., Khan, F. I., Veitch, B., & Amyotte, P. (2005). Revised fire consequence models for offshore quantitative risk assessment. *Journal of loss prevention in the process industries*, 18, 443-454.
- Qi, R., Ng, D., Cormier, B. R., & Mannan, M. S. (2010). Numerical simulations of LNG vapour dispersion in Brayton fire training field tests with ANSYS CFX. *Journal of Hazardous Materials*, 183, 51-61.
- Skarsbo, L. R. (2011). *An experimental study of pool fires and validation of different CFD fire models*. Master thesis submitted to the Department of physics and technology, University of Bergen, Bergen, Norway.
- Suardin, J. A., Wang, Y., Willson, M., & Mannan, M. S. (2009). Field experiments on high expansion (HEX) foam application for controlling LNG pool fire. *Journal of Hazardous Materials*, 165, 612-622.
- U. S. Environmental Protection Agency (USEPA). (1995). *Protocol for equipment leak emission estimates*. Office of air quality planning and standards, research triangle park, , NC 27711.
- Wingerden, K. V., & Salvesen, H. C. (1995). Simulation of an accidental vapour cloud explosion. *Process safety progress*, 14, 173-181.

Yun, G., Ng, D., & Mannan, M. S. (2011). Key findings of liquefied natural gas pool fire outdoor tests with expansion foam application. *Industrial and Engineering Chemistry Research*, 50, 2359-2372.

## **2 Novelty and contribution**

### **2.1 Overview**

This thesis is comprised of four main topics: i) release modeling, ii) vapour cloud explosion modeling, iii) integration of evolving fire and explosion consequence modeling, and iv) toxicity risk assessment. The novelties and contributions made for each topic are detailed below.

#### **2.1.1 Release modeling**

In this research, a non-linear regression method is used to better estimate the emission factors in oil and gas facilities. Although the emission factor estimation approaches were developed by the USEPA, they lack accuracy. This study optimizes the existing methods and models used for hydrocarbon emission assessment in oil and gas facilities by:

- introducing a new set of equations to estimate leak rates in oil and gas facilities.
- developing a quantitative comparison of the proposed equations and the ones proposed by USEPA, and
- defining a set of recommendations for the use of a specific leak rate equation.

This contribution is discussed in chapter 4.

### 2.1.2 Vapour cloud explosion (VCE) modeling

In the current work, a systematic procedure is introduced to model the VCE with the application of CFD tools. CFD codes are only recently beginning to be used in associated studies to simulate the VCE phenomenon and they suffer the following limitations:

- lack of a systematic approach to model the VCE presenting associated consequences.
- use of stoichiometric volume of the flammable fuel for explosion modeling, ignoring the dispersion characteristics of the flammable vapour.

Dispersion behaviour of the flammable vapour plays a significant role in the consequences of the VCE. Thus, the current study proposes a VCE modeling algorithm based on:

- recreating the sequence of the vapour cloud dispersion and explosion during a recent VCE accident, and
- integrating of dispersion and explosion using CFD code FLACS.

Consideration of the dispersion characteristics of the flammable fuel helps to precisely estimate the explosion overpressure and to overcome uncertainties associated with damage impacts that directly feed into the risk assessment. Considering the extent and location of the overpressure helps to design risk controls and mitigative measures. The research aims for a better understanding of how to use CFD in the modeling of VCE. This contribution is explained in chapter 5.

### **2.1.3 Integration of fire and explosion consequences**

There are extensive studies to model the consequences involved in the release of hydrocarbons. The main limitation of these studies is that they consider only an individual event such as fire or explosion independently, ignoring the interactions of these events. The current study proposes a novel approach to model the consequences considering the interaction of different events using CFD codes FLACS and FDS. An integrated approach is also adopted to evaluate the cumulative impact of the explosion overpressure and the fire heat load.

There are many studies exploring chains of accidents starting from one unit and spreading to different units, such as the release of hydrocarbon from a pipeline causing an explosion, and subsequently involving reactors, storage vessels and others units. The major difference between the current study and the studies based on the domino effects is that the current study focuses on an evolving accident scenario of one unit and the occurrence of more than one event. The domino effects studies, however, focus on the escalation of events from one unit to other units and may include different hazardous chemicals. The integrated scenario and the assessment of the cumulative risk makes the current research unique. This contribution is presented in chapter 6.

### **2.1.4 Combustion products toxicity risk assessment**

In the current research, a risk-based methodology is proposed to monitor and manage dispersion of combustion products. Evaluating the toxic dispersion at an offshore installation based only on concentrations misses the impact of dispersion and the additive

effects of the gas mixture. Personnel spend different amounts of time at different locations of the facility, including the processing area, the office area and the accommodation area. Combustion products are gas mixtures such as carbon monoxide, nitrogen dioxide, methane and smoke and thus cannot be simply added together. A risk-based approach considers the exposure duration that any individual spends at different parts of an installation in assessing the risk of exposure. As risk has an additive characteristic, this approach takes into account the cumulative impacts caused by various combustion products. The proposed approach helps to develop effective monitoring and safety measures design to minimize the effects of toxic substances, and also provides a tool for effective emergency management. This contribution is discussed in chapter 7.

### **3 Literature review**

#### **3.1 Consequence analysis**

Consequence analysis includes three major steps as follows (Figure 1.1):

- Defining the potential accident scenarios
- Evaluating the event consequences
- Estimating the event's impact

##### **3.1.1 Defining the potential accident scenarios**

After a hydrocarbon release on an offshore installation, there are several potential accident scenarios, depending on conditions such as fuel type, surrounding ventilation conditions and ignition time and location. Fire, explosion and toxic dispersion are likely accident scenarios after a hydrocarbon release [Assael and Kakosimos, 2010].

###### **3.1.1.1 Toxic dispersion**

The airborne transport of toxic material beyond the release point and into the region or exposed community is described by dispersion phenomenon. Parameters such as wind speed, atmospheric stability, ground conditions, height of the release, and momentum and buoyancy of the initial material released influence the atmospheric dispersion of toxic materials (Crowl and Louvar, 2001).

### **3.1.1.2 Fire**

An exothermic oxidation which occurs in the gas phase is called fire. The mixing of flammable gases with air or other oxidants results in a fire. Fire types are classified as pool fire, fire ball, jet fire and flash fire which are explained as follows:

#### **3.1.1.2.1 Pool fire**

Pool fires are the formation of a pool of a flammable substance through a liquid state outflow followed by an ignition. The occurrence of this type of fire is due to the release of jet fuels and diesel oils, hydrocarbons (heavier than hexane), glycols, oils and hydraulic fluids. Meteorological conditions play a significant role in the characteristics of this type of fire. The amount of the evaporated flammable material is also an important parameter determining the pool fire duration. There are three categories of pool fires: confined pool fires, unconfined pool fires, and fires on water [Khan and Abbassi, 1999].

#### **3.1.1.2.2 Fire ball**

A very rapid pressurized outflow of flammable gas followed by an ignition could lead to the fire ball. Due to the high pressure of the flammable material, the formation of the fire ball does not depend on the meteorological conditions. This type of fire has a short duration [Assael and Kakosimos, 2010].

#### **3.1.1.2.3 Jet fire**

The formation of the jet fire is through the immediate ignition of a high-pressurized outflow of a flammable gas. The release of light hydrocarbons, natural gas, gases with

flammable condensates, high-pressure hydrocarbon gases, and fuels could lead to a jet fire. Like the fire ball, the formation of the jet fire is not influenced by meteorological conditions, due to the high pressure release of the flammable substance [Pula et al., 2005].

#### **3.1.1.2.4 Flash fire**

An immediate ignition of a sudden high-pressurized outflow of a flammable substance could result in a flash fire. The condition under which the flash fire occurs is not perfectly understood. The shock wave through this type of fire is negligible while the duration of fire is short. The impact on compartments/equipment outside the vapour cloud is limited. However, the facilities inside the cloud are exposed to the burning part of the cloud. In risk analysis studies, this type of fire is considered because of its consequences for people [Pula et al., 2006].

#### **3.1.1.3 Vapour Cloud Explosion (VCE)**

The leakage of a flammable gas could form a flammable vapour cloud. The resulting damage is a function of the conditions of the accident. If there is no ignition, the flammable vapour could be dispersed depending on the congestion/ventilation condition of the geometry. However, there could be a flash fire through an immediate ignition. If a delayed ignition (5-10 minutes) happens, a VCE is a probable consequence. The composition of the flammable gases and the ability of the ignition source to supply the required energy are the effective parameters for VCE [Assael and Kakosimos, 2010].

The VCE behaviour is influenced by several parameters which have been evaluated through different qualitative studies. The ignition probability increases with an increase in the size of the vapour cloud. The probability of explosion rather than fire is another effective parameter. Furthermore, the impact of the explosion could be affected by the turbulent mixing of vapour and air, and also by the location of ignition sources [Crowl and Louvar, 2001].

### **3.1.2 Evaluating the event consequences**

The following sections review the available tools to model the consequences caused by toxic dispersion, fire and explosion.

#### **3.1.2.1 Toxic dispersion modeling**

To evaluate the consequences caused by toxic substances at an offshore installation, the concentrations of toxic substances are estimated by the use of dispersion models. Dispersion models are classified as empirical, Lagrangian, and Eulerian models [Assael and Kakosimos, 2010].

##### **3.1.2.1.1 Empirical models**

Empirical models are classified as Gaussian models and Box models. The basic assumption in Gaussian models is the occurrence of steady dispersion in an infinite ideal medium. These models are simple to use and computationally rapid. Box models are even simpler than empirical ones, as their main assumption is the box shape of the region of interest. The emission concentration distribution in Box models is assumed to be

homogenous. Due to this simplicity, these models are not suitable to predict the distribution of emission concentrated over an airshed.

#### **3.1.2.1.2 Lagrangian models**

In Lagrangian models, the motion of pollution plume particles is mathematically modeled as a random walk during the time while these particles move in the atmosphere. Thus, by calculating the statistics of a large number of particles' tracks, the emission dispersion is predicted.

#### **3.1.2.1.3 Eulerian models**

The mathematical approach in Eulerian models is based on the solution of the common differential equations of continuity integrated over the turbulent time scale. These models are well established for the condition under which the atmospheric characteristics or the pollution distribution are complex. Though Eulerian models are more accurate, the computational time and the complexity of the equation limit application to large-scale spatial calculations due to cost limits.

#### **3.1.2.2 Fire modeling**

Radiation heat is the consequence of a fire causing damage. Thus, in order to assess the radiation heat flux, the characteristics of the fire should be known. Fire models are capable of estimating the characteristics such as fire diameter, flame length, and flame drag. Fire models are categorized as point source models, solid flame models, field models, and zone models. Solid flame models have the advantage of flame geometry and

external thermal radiation, which is important for offshore fires. These models are simple to apply and easy to program and have a short run time. Offshore fires are categorized as four major types: pool fires, jet fires, flash fires, and fire balls [Pula et al., 2005].

### 3.1.2.3 VCE modeling

Most of the explosion damage is caused by the blast wave as a consequence of the explosion; the blast is made up of the combination of the pressure wave, the change in overpressure during the period of explosion, and subsequent wind. Table 3.1 demonstrates the estimated damages based on different overpressure intensities.

**Table 3.1. Damage estimates for common structures based on overpressure [Crowl and Louvar, 2001]**

<b>Pressure (bar)</b>	<b>Damage</b>
0.17	50% destruction of brickwork of houses
0.21	Heavy machines (3000 lb) in industrial building suffer little damage; Steel frame buildings distort and pull away from foundations
0.21-0.28	Frameless, self-framing steel panel buildings demolished; rupture of oil storage tanks
0.28	Cladding of light industrial buildings ruptures
0.34	Wooden utility poles snap; tall hydraulic presses (40,000 lb) in buildings slightly damaged
0.34-0.48	Nearly complete destruction of houses
0.48	Loaded train wagons overturned
0.48-0.55	Brick panels, 8-12 in. thick, not reinforced, fail by shearing or flexure

<b>Pressure (bar)</b>	<b>Damage</b>
0.62	Loaded train boxcars completely demolished
0.69	Probable total destruction of buildings; heavy machine tools (7000 lb) moved and badly damaged, very heavy machine tools (12,000 lb) survive

VCE models are categorized as empirical models, phenomenological models, CFD models and advanced CFD models.

### 3.1.2.3.1 Empirical models

Empirical models were developed based on correlations obtained using experimental data [Ledin, 2002]. The TNT equivalency method, the TNO Multi-Energy method, the Baker-Strehlow method, and the congestion assessment method are the most common empirical methods. Table 3.2 demonstrates the advantages and disadvantages of these models.

**Table 3.2. Comparison of the empirical models**

<b>Model</b>	<b>Advantages</b>	<b>Disadvantages</b>
TNT Equivalency method [Bjerkedvedt et al., 1997]	Simple to use Validated use of empirical data	Difficulty in choosing the yield factor Weak representation of weak gas explosions Only representation of the positive phase duration Not suitable for gas explosions Difficulty in defining the

Model	Advantages	Disadvantages
		sensible charge centre
<p>TNO Multi-Energy method [Mercx and Van Den Berg, 1997]</p>	<p>Fast method Conservative approximations</p>	<p>Difficulty to define a sensible value of the charge strength Difficulty to define a sensible value of the total combustion energy Not suitable for weak explosions Dealing with several congested regions is not clear Dealing with multiple blast waves is not clear</p>
<p>Baker-Strehlow method [Baker et al., 1994]</p>	<p>Considering some geometrical/confinement details Handling multi-ignition points</p>	<p>Over conservative</p>
<p>Congestion assessment method [Cates and Samuels, 1991]</p>	<p>Easy to use with short run times Applicable to a large number of experiments due to the calibration Sensible maximum over-pressure when the severity goes to infinity Applicable to non-symmetrical congestion and long, narrow plant</p>	<p>Only a crude representation of the geometry Non-uniqueness in the specification of level of congestion/confinement</p>

### 3.1.2.3.2 Phenomenological models

As simplified physical models, phenomenological models represent the essential physics of explosions. The greatest simplification is made in geometry which is replaced by an idealized system instead of the actual scenario geometry. However, these models are not appropriate under the condition of more complex geometries (Ledin, 2002). The Shell Code for Overpressure Prediction in gas Explosions (SCOPE) and Confined Linked Chamber Explosions (CLICHE) are common phenomenological models with their strengths and weaknesses as explained in Table 3.3.

**Table 3.3. Comparison of the phenomenological models**

<b>Model</b>	<b>Advantages</b>	<b>Disadvantages</b>
SCOPE [Puttock et al., 2000]	<ul style="list-style-type: none"> <li>Handling venting and external explosions</li> <li>Sensible flame speeds</li> <li>Validated against different scales of experiments/different gases/different degrees of congestion</li> <li>Less geometrical detail than CFD models</li> <li>Fast tool to evaluate different scenarios during the design phase</li> </ul>	<ul style="list-style-type: none"> <li>Less flow field information compared to CFD models</li> <li>Not appropriate for complex geometries with high degrees of details</li> <li>Dealing only with single enclosures</li> </ul>
CLICHE [Fairweather and Vasey, 1982]	<ul style="list-style-type: none"> <li>Ignition location could be anywhere in the cuboidal volume</li> <li>Simple combustion model</li> </ul>	<ul style="list-style-type: none"> <li>Representation of geometries is simplified</li> <li>Less flow field information compared to CFD models</li> </ul>

<b>Model</b>	<b>Advantages</b>	<b>Disadvantages</b>
	Representation of the flame distortion due to vents  Handling external explosions  Input parameters could be imported from an obstacle database  Short run times	

### 3.1.2.3.3 Computational fluid dynamic (CFD) models

Applying CFD models, the partial differential equations governing the explosion process are solved by finding their numerical solutions. Through the application of these models, the solution domain is discretized to sub-domains in order to generate the numerical solutions. Then, a series of coupled algebraic equations are generated through the application of conservative equations to each sub-domain [Ledin, 2002]. Some common CFD models with their advantages and disadvantages are explained in Table 3.4.

**Table 3.4. Comparison of the CFD models**

<b>Model</b>	<b>Advantages</b>	<b>Disadvantages</b>
EXSIM [Ledin, 2002]	Spatial resolution of obstacles  Validated against different scales of experiments  Applicable to congested/unconfined	Using standard k-ε model  No local grid refinement

Model	Advantages	Disadvantages
	geometries Applicable to external explosions Readable in CAD data	
FLACS [Hanna et al., 2004]	Validated against different scales scenarios Second order accurate discretization scheme for the reaction process Applicable to congested, but confined geometries Applicable to external explosions Readable in CAD data Water deluge model	First order accurate for all variables except for the reaction progress variables Calibrated for 1 m cube grid cell size (versions up to 1993) No recent development in the open literature
AutoReaGas [Ledin, 2002]	Validated against different scales scenarios Water deluge model Readable in CAD data Acceptance of a large number of objects	First order accurate for all variables Using standard k-ε model

In the current study, Flame Acceleration Simulator (FLACS) is used to model dispersion and explosion phenomenon. Using a finite volume method on a Cartesian grid, FLACS solves the conservation equations of mass, momentum, enthalpy, and mass fraction of

species which are closed by the ideal gas law. Equation 3.1 represents the conservation equations:

$$\frac{\partial}{\partial t}(\rho\phi) + \frac{\partial}{\partial x_j}(\rho u_j \phi) - \frac{\partial}{\partial x_j} \left( \rho \Gamma_\phi \frac{\partial}{\partial x_j}(\phi) \right) = S_\phi \quad (3.1)$$

where  $t$ ,  $\rho$ ,  $u$  and  $\phi$  represent time (s), density ( $\text{kgm}^{-3}$ ), velocity (m/s) and general variable. The numerical model resolves diffusive fluxes with second order scheme and convective fluxes with a second order k scheme. FLACS uses a first order backward Euler time stepping scheme [GEXCON, 2010].

#### 3.1.2.3.4 Advanced CFD models

The advanced CFD models are capable of presenting the explosion process in a more descriptive way. The exact geometric representation throughout the explosion simulation is one of the valuable features in advanced CFD models. However, this presents a problem which is the limitation of the available computer memory (Ledin, 2002). The accuracy of the numerical scheme is another advantage of advanced CFD models. CFX-4, COBRA, NEWT, REACFLOW, and Imperial College Research Code are some common advanced CFD models with the strengths and weaknesses as explained in Table 3.5.

**Table 3.5. Comparison of the advanced CFD models**

<b>Model</b>	<b>Advantages</b>	<b>Disadvantages</b>
CFX-4	Multi-block capability	Not suitable for gases other

Model	Advantages	Disadvantages
[Pritchard et al., 1999]	<p>Different options for discretization</p> <p>Readable in CAD data</p> <p>Integrated geometry building</p> <p>Suitable for CH<sub>4</sub> and H<sub>2</sub> deflagration</p>	<p>than CH<sub>4</sub> and H<sub>2</sub></p> <p>Thin flame model which is not suitable for explosion</p> <p>Deficiencies with the ignition model</p> <p>Explosion and ignition models are poorly validated</p>
<p>COBRA</p> <p>[Popat et al., 1996]</p>	<p>Second order accurate spatial and temporal discretization</p> <p>Cartesian mesh and also handling cylindrical polar or arbitrary hexahedral meshes</p> <p>Advanced grid refinement/de-refinement facility</p> <p>Readable in CAD data</p>	<p>Using the standard k-e model and offering Wolfshtein's two layer k-e model</p> <p>Time-consuming and difficult when the geometry is complex</p> <p>Lack of a model for transition from laminar to turbulent flow</p> <p>Slow and difficult visualization of the flow field</p>
<p>NEWT</p> <p>[Watterson et al., 1998]</p>	<p>Adaptive mesh algorithm</p> <p>Less effort during the mesh generation than with the use of unstructured meshes</p> <p>Use of any tetrahedral mesh generator</p>	<p>Standard k-e model, but with a better near wall damping</p> <p>Crude ignition model</p> <p>Crude transition model</p>
<p>REACFLOW</p> <p>[Wilkenings and Huld, 1999]</p>	<p>Easier meshing than with the use of unstructured meshing</p> <p>Adaptive mesh capability</p> <p>Accurate solver and second</p>	<p>Standard k-e model</p> <p>Simple combustion model</p>

Model	Advantages	Disadvantages
	order, Van Leer discretization scheme	
Imperial College Research Code [Lindstedt and Vaos, 1999]	Higher order spatial and temporal discretization techniques Adaptive meshing capability Detailed chemical kinetics Realistic method of obtaining the PDF Available in parallelized form	Long run times for large scale problems Great requirements for computer memory Not readily available as a research code

### 3.1.3 Event impact estimation

The explosion overpressure damages to people are categorized as lung damage, eardrum rupture, head impact, whole body displacement and injury from fragments and debris [Assael and Kakosimos, 2010]. In lung damage, the sudden extreme pressure difference causes the pressure increase in the lung leading to lung damage and possible death. This sudden pressure difference can also lead to eardrum rupture injury. As a tertiary effect, the head impact can occur due to the shock wave pushing the head backward and leading to skull rupture or fracture and possible death. Another tertiary effect is due to throwing the whole body backwards and causing injuries/death because of the impact with other objects. There is also a possibility of death/injuries due to fragments or debris which is a secondary indirect effect.

Thermal damages to people caused due to fire heat load are categorized as a first degree burn, second degree burn and third degree burn [Wieczorek and Nicholas, 2001]. The severity of damage depends on the level of tissue death and the depth of damage. In a first degree burn, the epidermis is affected and it is red and painful with no blisters. In a second degree burn, the epidermis and part of the dermis layer of the skin are burned; the skin is red, blistered, red and painful. A third degree injury burns both the epidermis and the dermis layer of the skin and sometimes the severity of the damage affects bones, muscles and tendons; the burned parts of the skin appear white and charred with no sensation in the area due to the total destruction of nerve endings [Assael and Kakosimos, 2010].

Toxic combustion substances such as carbon monoxide, nitrogen dioxide and unburned methane also have adverse effects on exposed people. A low level of carbon monoxide is harmful for those suffering from heart diseases (cardiovascular effects). Higher levels of carbon monoxide affect the central nervous system, causing vision problems, reducing the ability to work/learn, and also causing difficulties in the performance of complex tasks. Carbon monoxide at extremely high levels is toxic and may lead to death. Nitrogen dioxide at low levels can cause chronic respiratory symptoms such as coughing and phlegm. At extremely high levels, nitrogen dioxide is toxic and may cause death. Methane is not toxic at low levels, but it is an asphyxiant gas displacing oxygen, and causes hypoxia leading to death [Khan and Sadiq, 2005; WHO, 2003; OSHA, 2003].

To quantify the personal damage, the probit function is used where the personal harm due to a specific event is expressed as the percentage of people affected in a bounded region of interest [TNO, 1989]. In this method, the dose is first calculated as a function of the heat flux, explosion overpressure or toxic concentration. Then, the probit value is obtained as follows:

$$Pr = a + b \ln D \quad 3.1$$

where  $D$  is expressed as shown in table 3.6.

**Table 3.6. Definition of  $D$  value in probit function**

<b>Event</b>	<b>D</b>	<b>Definition</b>
Fire	$t \times q^{4/3}$	t: exposure time (s) q: heat flux (W/m <sup>2</sup> )
Explosion	$P_0$	$P_0$ : overpressure (Pa)
Toxic dispersion	$C \times t$	C: concentration (ppm) t: exposure time (s)

The values of  $a$  and  $b$  are available for various damage types in TNO (1989). Finally, the probability of damage is calculated through the following expression:

$$P = \frac{1}{2} \left[ 1 + \frac{Pr - 5}{|Pr - 5|} \operatorname{erf} \left( \frac{|Pr - 5|}{\sqrt{2}} \right) \right] \quad 3.2$$

The probit model has commonly been used in impact assessment studies such as Khan and Abbasi (1998), Pula et al. (2006) and Pasman and Duxbury (1992) to calculate the probability of damage due to fire, explosion and toxic dispersion.

### 3.2 References

Assael, M. J., & Kakosimos, K. E. (2010). *Fires, Explosions, and Toxic Gas Dispersions: Effects Calculation and Risk Analysis*. Boca Raton: CRC Press/Taylor and Francis.

Baker, Q. A., Tang, M. J., Scheier, E. A., & Silva, G. J. (1994). Vapour cloud explosion analysis. *AIChE loss prevention symposium*. Atlanta, Georgia, USA.

Bjerketvedt, D., Bakke, J. R., & Wingerden, K. (1997). Gas explosion handbook. *Journal of hazardous materials*, 52, 1-150.

Cates, D. A., & Samuels, B. (1991). A simple assessment methodology for vented explosions. *Journal of loss prevention in the process industries*, 4, 287-296.

Crowl, D. A., & Louvar, J. F. (2001). *Chemical process safety: fundamentals with applications*. New Jersey: Prentice Hall PTR.

Fairweather, M., & Vasey, M. W. (1982). A mathematical model for the prediction of overpressure generated in totally confined and vented explosions. *19th symposium (international) on combustion*. Pittsburgh, Pennsylvania, USA: The combustion institute.

GEXCON. (2010). FLACS v9.1 user's manual. Retrieved from [www.bp.com/sectiongenericarticle.do?categoryId=9034902&contentId=7064891](http://www.bp.com/sectiongenericarticle.do?categoryId=9034902&contentId=7064891)

Hanna, S. R., Hansen, O. R., & Dharmavaram, S. (2004). FLACS CFD air quality model performance evaluation with Kit Fox, Must, Prairie Grass, and EMU observations. *Atmospheric environment*, 38, 4675-4687.

Khan, F. I., & Abbasi, S. A. (1998). Rapid quantitative risk assessment of a petrochemical industry using a new software package MAXCRED. *Journal of Cleaner Production*, 6, 9-22.

Khan, F. I., & Abbasi, S. A. (1999). Assessment of risks posed by chemical industries-application of a new computer automated tool MAXCRED-III. *Journal of loss prevention in the process industries*, 12, 455-469.

Khan, F. I., & Sadiq, R. (2005). Risk-Based Prioritization of Air Pollution Monitoring Using Fuzzy Synthetic Evaluation Technique. *Environmental Monitoring and Assessment*, 105, 261-283.

Ledin, H. S. (2002). A review of the State-of-the-Art in gas explosion modeling. HSL report No. HSL/2002/02.

Lindstedt, R. P., & Vaos, E. M. (1999). Modeling of premixed turbulent flames with second moment methods. *Combustion and flame*, 116, 461-485.

Mercx, W. P., & Van Den Berg, T. (1997). The explosion blast prediction model in the revised CPR 14E (Yellow Book). *Process safety progress*, 16, 152-159.

Occupational Safety and Health Administration (OSHA). (2003). Safety and health topics: methane. Retrieved from [http://www.osha.gov/dts/chemicalsampling/data/CH\\_250700.html](http://www.osha.gov/dts/chemicalsampling/data/CH_250700.html)

Pasman, H. J., Duxbury, H. A., & Bjordal, E. N. (1992). Major hazards in the process industries: Achievements and challenges in loss prevention. *Journal of Hazardous Materials*, 30, 1-38.

Popat, N. R., Catlin, C. A., Arntzen, B. J., Lindstedt, R. P., Hjertager, B. H., Solberg, T., Van Den Berg, A. C. (1996). Investigations to improve and assess the accuracy of computational fluid dynamic based explosion models. *Journal of hazardous materials*, 45, 1-25.

Pritchard, D. K., Lewis, M. J., Hedley, D., & Lea, C. J. (1999). *Prediction the effects of obstacles on explosion development*. HSL report No. EC/99/41-CM/99/11.

Pula, R., Khan, F. I., Veitch, B., & Amyotte, P. R. (2005). Revised fire consequence models for offshore quantitative risk assessment. *Journal of loss prevention in the process industries*, 18, 443-454.

Pula, R., Khan, F. I., Veitch, B., & Amyotte, P. R. (2006). A grid based approach for fire and explosion consequence analysis. *Process safety and environmental protection*, 84, 79-91.

Puttock, J. S., Yardley, M. R., & Cresswell, T. M. (2000). Prediction of vapour cloud explosions using the SCOPE model. *Journal of loss prevention in the process industries*, 13, 419-430.

TNO. (1989). Methods for the determination of possible damage to people and objects resulting from releases of hazardous materials. Roos A. J. (Ed.), Green Book, Report CPR 16E, Chapter 1.

Watterson, J. K., Savill, A. M., & Dawes, W. N. (1998). A solution adaptive mesh producer for predicting confined explosions. *International journal for numerical methods in fluids*, 26, 235-247.

Wieczorek, C. J., & Nicholas, A. D. (2001). Human Variability Correction Factors for Use with Simplified Engineering Tools for Predicting Pain and Second Degree Skin Burns. *Journal of Fire Protection Engineering*, 11, 88-111.

Wilkenings, H., & Huld, T. (1999). An adaptive 3-D CFD solver for explosion modeling on large scales. *17th international colloquium on the dynamics of explosions and reactive systems*. Heidelberg, Germany.

World Health Organization (WHO). (2003). *Health aspects of air pollution with particulate matter, ozone and nitrogen dioxide*. Bonn, Germany: Report on a WHO working group.

#### 4 Emission factor estimation for oil and gas industry\*

Mohammad Dadashzadeh<sup>1</sup>, Faisal Khan<sup>1</sup>, Rouzbeh Abbassi<sup>2</sup>, Kelly Hawboldt<sup>1</sup>

1. Process Engineering, Faculty of Engineering and Applied Science, Memorial

University of Newfoundland, St. John's, NL, Canada, A1B 3X5

2. Department of Civil and Environmental Engineering, Princeton University, Princeton,

NJ 08544

##### **Abstract**

Quantification of the fugitive emission rate in an oil and gas facility is an important step in risk management. There are several studies conducted by the United States Environmental Protection Agency (USEPA) and American Petroleum Institute (API) proposing methods of estimating emission rates and factors. Four major approaches of estimating these emissions, in the order of their accuracy, are: average emission factor approach, screening ranges emission factor approach, USEPA correlation equations approach, and unit-specific correlation equations approach. The focus of this study is to optimize the USEPA correlation equations to estimate the emission rate of different units in an oil and gas facility. In the developed methodology, the data available from USEPA [USEPA, 1995] is used to develop new sets of equations. A comparison between USEPA correlation equations and the proposed equations is performed to define the optimum sets of equations. It is observed that for pumps, flanges, open-ended lines, and others, the

\* Dadashzadeh M, Khan F, Hawboldt K, and Abbassi R. (2010). Emission factor estimation for oil and gas facilities. *Journal of Process Safety and Environmental Protection*, 89, 295-299.

proposed developed equations provides a better estimation of the emission rate, whereas for other sources, USEPA equations gives a better estimate of the emission rate.

**Keywords:** *oil and gas industry, emission factor, linear regression, non-linear regression*

#### 4.1 Introduction

Fugitive emissions are any type of leak from sealed surfaces of equipment from oil and gas facilities [USEPA, 2007]. The major fugitive emissions are hydrocarbons; aromatic hydrocarbons including benzene, toluene, ethyl-benzene, and xylene; non-aromatic hydrocarbons including methane, ethane, propane, butane, pentane, and hexane [API, 1993].

Valves, pump seals, connectors, flanges, and open-ended lines are the main sources of equipment leaks in oil and gas facilities while instruments, loading arms, pressure relief valves, stuffing boxes, and vents are considered "others" [API, 1993].

To estimate the emission, a factor representing the relationship between the emission and the activity associated with the release of that particular emission or emission factor, is used (Equation 4.1).

$$E = A \times EF \times (1 - ER / 100) \quad 4.1$$

Where,

E = emission (mass)

A = activity rate (mass, volume, distance, or duration of the activity emitting the pollutant)

EF = emission factor (mass/ mass, volume, distance, or duration of the activity emitting the pollutant)

ER = overall emission reduction efficiency (%)

Emission factors are represented by units such as the mass of pollutant per unit mass, volume, distance, duration of activity, or other aspects associated with the activity of concern.

Emission factors are applied for a variety of situations, such as emission estimates for inventories associated with large industries. The inventories are also applicable in ambient dispersion modeling and analysis, management methodologies, and screening sources where required [USEPA, 2010].

Generally, there are four approaches to equipment emission estimation. These approaches, in order of increasing the accuracy, are the average emission factor approach, screening range approach, EPA correlation approach, and unit-specific correlation approach. The first two methods, the average emission factor and the screening range approach, estimate emissions by combining the emission factors with equipment counts. The EPA correlation factor estimates the emissions using the measured concentrations (screening values) of different equipments and correlation equations. In the unit-specific correlation approach, the measured screening and leak rate

data of a selected set of components of an equipment is used to develop the correlation equations. Subsequently, the leak rate is estimated using these correlation equations [USEPA, 1995].

Studies on emission factors development have been conducted on refineries, gas plants, marketing terminal equipments, and oil and gas production facilities. Studies on refineries' fugitive emissions were based on equipment leak data collected from 13 refineries. The collected data has been used to develop average emission factors and correlations. The above studies defined the components as valves, pumps, and pressure relief valves which operate in gas/vapour, light liquid and heavy liquid services [USEPA, 1995]. In another study, based on the data screened by EPA and API from six gas plants, the average emission factors including emissions of ethane and methane have been developed [Dubose et al., 1982]. In API (1993), the data screened from four marketing terminals has been used to develop new average emission factors, default zero emission factors, and emission correlation equations for the components of petroleum marketing terminals. In addition to the above, API (1993) and API (1995) provided two more reports, including data from 24 oil and gas production facilities. The services in these facilities were gas/vapour, light liquid, and heavy liquid streams in different components including connectors, flanges, open-ended lines, pumps, valves, instruments, loading arms, pressure relief valves, stuffing boxes, vents, compressors, dump lever arms, diaphragms, drains, hatches, meters, and polished rods. The results from these studies were used to develop emission correlation equations in two different categories of

onshore and offshore oil and gas production facilities [API, 1995; API, 1993]. In the last, data from refineries, marketing terminals and oil and gas production facilities was used to develop the new correlation equations, which are applicable in the whole petroleum industry. New equations are in six different equipment categories: valves, pump seals, connectors, flanges, open-ended lines, and others [USEPA, 1995].

The focus of this study is to optimize the emission rate estimation with the use of EPA correlation equations. The EPA approach of developing correlation equations will be outlined and a non-linear regression conducted. In this approach, the parameters for the non-linear regression are estimated with the target of minimizing the sum of the squared errors. Subsequently, the new approach is applied to a case study and the results are compared with those of EPA to optimize the selection of the most appropriate equations.

## **4.2 Correlation equation development methodology**

For a particular equipment type, an equation is developed to estimate the leak rate as a function of screening value which is the screened concentration of emission from the equipment. Compared with two previous methods, this approach is a strong function of the screening value, which provides an auditable basis and enhances emission rate prediction ability [USEPA, 1995].

### **4.2.1 EPA correlation equation approach**

According to EPA protocol [USEPA, 1995], when developing correlation equations, two sets of data are required:

- Individual Screening Value (ISV) which is the screened concentration of emission from the equipment with unit of ppmv.
- Emission Leak Rate (kg/hr)

The natural logarithm of both data (screening value (ppmv) and leak rate (kg/hr)) is applied as these values span several orders of magnitude and are not normally distributed. Subsequently, simple linear regression is performed as follows [USEPA, 1995]:

$$Y_i = \beta_0 + \beta_1 \times X_i \quad 4.2$$

Where  $Y_i$  and  $X_i$  are the natural logarithm of the leak rate measured by bagging equipment piece  $i$  and the natural logarithm of the screening value for equipment piece  $i$ , respectively. The intercept and the slope of the regression line ( $\beta_0$  and  $\beta_1$ ) are calculated as explained in Figure 4.1.

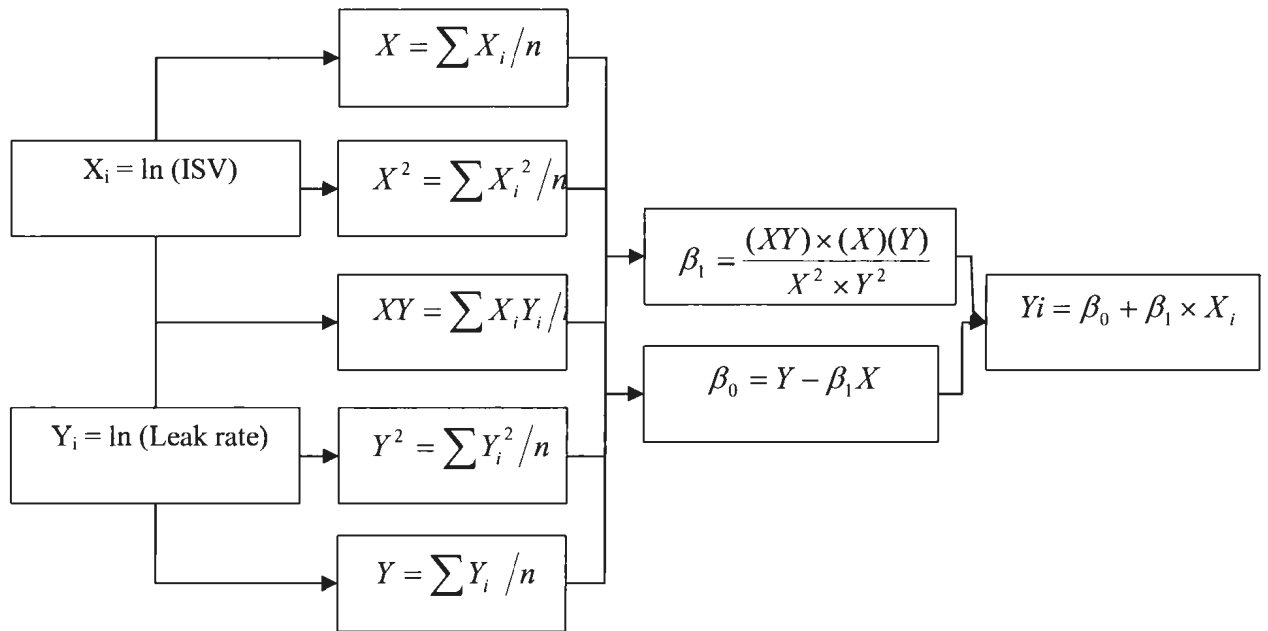


Figure 4.1. Application of linear regression with ISV and emission rate

Finally, equation 4.2 is converted from log-space to arithmetic space as follows:

$$\text{LeakRate}(\text{kg} / \text{hr}) = \text{SBCF} \times \text{Exp}(\beta_0)(\text{ISV})^{\beta_1} \quad 4.3$$

Where, SBCF is a function of the mean square error of the correlation in log-space. The equation for this factor is as follows [USEPA, 1995]:

$$\text{SBCF} = 1 + \frac{(m-1) \times T}{m} + \frac{(m-1)^3 \times T^2}{m^2 \times 2! \times (m+1)} + \frac{(m-1)^5 \times T^3}{m^3 \times 3! \times (m+1) \times (m+3)} + \dots \quad 4.4$$

Where:

$$T = (\text{MSE}/2) \times ((\ln 10)^2) \quad \text{when regression performed using base 10 logarithms;}$$

$T = (\text{MSE}/2)$  when regression performed using natural logarithms;

MSE = mean square error from the regression;

$\ln 10$  = natural logarithm of 10; and

$m$  = number of data pairs – 1

#### **4.2.2 Approach used in the current study**

In some cases of nonlinear models, the equation is transformable to a linear model. A good example of this situation is the EPA correlation equation format ( $Y = a X^b$ ) where by obtaining the natural logarithm of both sides and converting the model to a linear format, the parameters have been estimated as explained in the EPA correlation equation approach. The detransformation (equation is transformed back to the arithmetic space) is often applied when the equation is used to estimate the value of one variable (leak rate) from the other variable (ISV) [Smith, 1993]. However, through the conversion from logarithmic space to the arithmetic space, a bias occurs. This bias is due to the compression of the largest values in logarithmic space tending to have less effect than small values in estimating the leak rate [Beauchamp and Olson, 1973; Finney, 1941].

On the other hand, applying this approach is a useful tool to estimate the initial values of the model parameters that are required in non-linear regression analysis [Smyth, 2002]. Therefore, the focus of this section is to use the initial values of parameters “a” and “b”, estimated through EPA correlation equation approach, in order to develop new sets of correlation equations with better accuracy.

The non-linear approach is applied to the same sets of data as the EPA to develop correlation equations [RDCT, 2009]. The methodology is focused to minimize the sum of the squared errors estimated by the equation  $Y = a X^b$ . This non-linear approach used by R software considers the following steps (Figure 4.2):

- The sets of data are selected as Y (emission rate) and X (screening value).
- Estimation of the initial values of a and b is an important step as the final estimation of two parameters is a strong function of initial estimates. In this case, the EPA suggested values are used as initial values.
- Estimating the sum of the squared errors
- If  $\sum (Y_i - a \times X_i^b)^2$  is less than  $\sum (Y_{i-1} - a \times X_{i-1}^b)^2$ , the parameters a and b are set to  $a_k$  and  $b_k$  and if it is not, try another values of  $a_k$  and  $b_k$ .

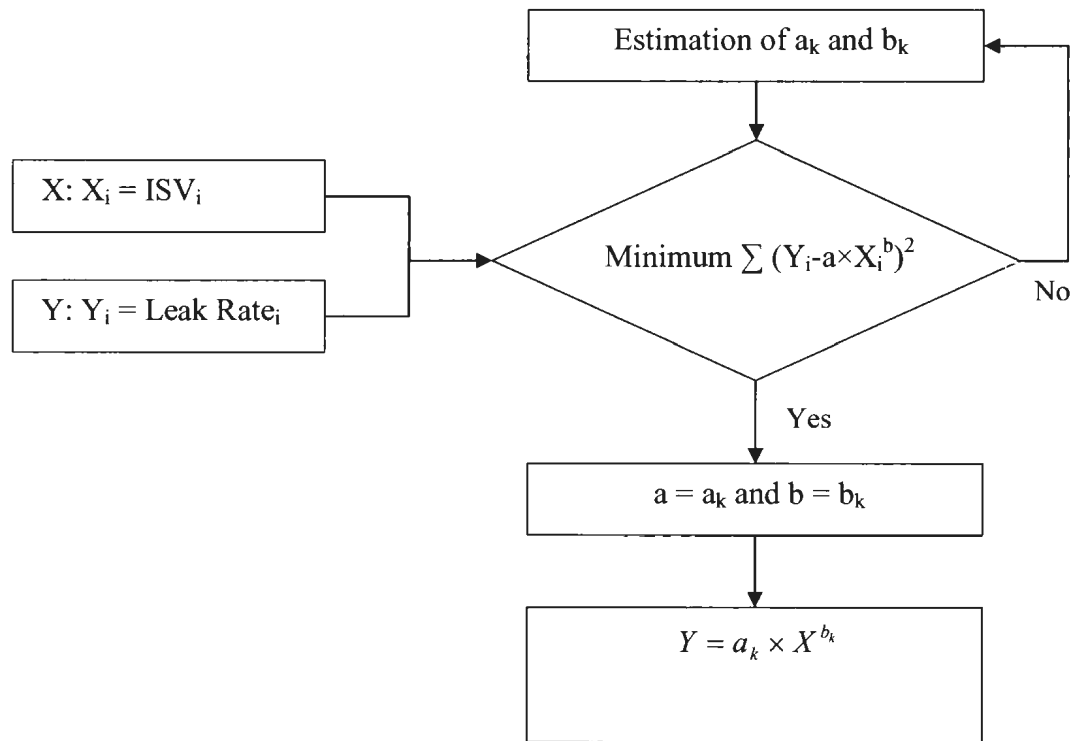


Figure 4.2. Application of non-linear regression with ISV and leak rate

After applying the non-linear regression analysis to the sets of data, the parameters  $a$  and  $b$  are optimized.

### 4.3 Application of the new approach: a case study

Both methodologies are applied to the sets of data, ISV and emission leak rate available from USEPA [USEPA, 1995]. Table 4.1 shows the group of components with the number of data available in each group.

**Table 4.1. Component categories with the number of data [USEPA, 1995]**

Compound Category	Number of data pairs
Valves	337
Pump seals	53
Connectors	118
Flanges	56
Open-Ended lines	141
Others	70

In this case study, the data from onshore/offshore oil and gas operations, refineries, and marketing terminals are combined. Six different categories are used, as shown in Table 4.1. The types of services in all categories include heavy liquid, light liquid, and gas services.

Detailed statistics, such as the sum of squared errors,  $R^2$ , F-ratio, and  $\Delta$  Akaike's information criterion ( $\Delta$  AIC), are used to compare the results from the EPA correlation equation approach and the non-linear approach used in this paper.

The sum of squared errors (SS) is estimated as:

$$SS = \sum_{i=1}^n (Y_i - f(X_i))^2 \quad 4.5$$

Where,  $Y_i$  and  $f(X_i)$  are observed and predicted values of sample  $i$ , respectively. This parameter is an unexplained variation of the model. In the other words, the smaller the SS estimated with a regression model, the better the model fits the sets of data [Berthouex Brown, 2002].

The  $R^2$  value is the parameter for the best fit of nonlinear regressions estimated as follows [GPSI, 2007]:

$$R^2 = 1 - \frac{SS_{reg}}{SS_{tot}} \quad 4.6$$

Where,  $SS_{reg}$  is the sum of the squares of distances of the points from the best fit of curve determined by non-linear regression and  $SS_{tot}$  is the sum of the squares of distances of the points from a horizontal line through the mean of all  $y$  values. Obtaining a higher value of  $R^2$  for a model does not necessarily mean the model shows a good estimation of all data points from the variables. As an example, if there are  $n$  data points and also  $n$  parameters, then the value of  $R^2$  will be 1. However, adding new data points to such a model will strongly affect  $R^2$  value. To overcome this, the  $R^2$  value is adjusted as follows [Mendenhall and Sincich, 1993]:

$$R_a^2 = 1 - \frac{n-1}{n-(p+1)} \times \left( \frac{SS_{reg}}{SS_{tot}} \right) \quad 4.7$$

Where  $n$  is the number of data points and  $p$  is the number of parameters. Compared to  $R^2$ ,  $R_a^2$  is affected by both the sample size and the number of parameters in the model [Mendenhall and Sincich, 1993].

Rather than conducting a hypothesis test on each parameter individually (t test), it is more appropriate to use a global test applicable to all parameters. Thus, the F test is a more useful approach to test the utility of the non-linear regression model [Mendenhall and Sincich, 1993]. The F ratio is as follows:

$$F = \frac{(SS_{tot} - SS_{reg}) / p}{SS_{tot} / [n - (p + 1)]} \quad 4.8$$

The F ratio explains the variability. Thus, if the model meets the following condition:

$$F\text{-ratio} > F\text{-critical} \quad 4.9$$

The following null hypothesis is rejected:

$$H_0 : \beta_1 = \beta_2 = \dots = \beta_p = 0 \quad 4.10$$

F-critical is  $F_{\alpha, \text{numerator d.f.}, \text{denominator d.f.}}$ , where the numerator d.f. is the number of parameters ( $k$ ), denominator d.f. is  $n-(k+1)$ ,  $\alpha$  is the rejection region (0.05 in this study), and  $\beta$  represents the parameters. In other words, F-critical is the minimum value of F-

ratio at which the null hypothesis could be rejected. Therefore, the larger F value shows the more usefulness of the model [Mendenhall and Sincich, 1993].

$\Delta$  Akaike's information criterion ( $\Delta$  AIC) is the value which can be estimated as follows:

$$\Delta AIC = p \times \ln\left(\frac{SS_{EPA}}{SS_{new}}\right) \quad 4.11$$

Where,  $SS_{EPA}$  is the sum of squared errors from the EPA approach and  $SS_{new}$  is the sum of squared errors from the new regression approach. When  $\Delta$  AIC is more than 1, it shows that the non-linear model is a better choice. According to [Burnham and Anderson, 2002], when  $\Delta$  AIC is more than 10, the non-linear equation is strongly recommended.

#### **4.4 Results and discussion**

Table 4.2 shows the equations provided through the application of both approaches; EPA correlation equation approach and the proposed approach.

**Table 4.2. Comparison of the equations developed by EPA and non-linear approach**

Component type	Approach	Equation	F Ratio	F Critical	Sum of squared errors	R <sup>2</sup>	Ra <sup>2</sup>	Δ AIC
Valves	EPA	$LR = 2.29 \times 10^{-6} \times ISV^{0.746}$	56	3.87	3.46E-03	0.142	0.139	6
	Proposed	$LR = 1.78 \times 10^{-6} \times ISV^{0.747}$	63	3.87	3.40E-03	0.158	0.157	
Pump seals	EPA	$LR = 5.03 \times 10^{-5} \times ISV^{0.610}$	0	4.03	7.48E-03	0	0	14
	Proposed	$LR = 5.53 \times 10^{-4} \times ISV^{0.2906}$	6	4.03	5.70E-03	0.107	0.090	
Connectors	EPA	$LR = 1.53 \times 10^{-6} \times ISV^{0.735}$	5	3.94	2.38E-02	0.039	0.031	10
	Proposed	$LR = 5.62 \times 10^{-6} \times ISV^{0.754}$	16	3.94	2.18E-02	0.120	0.112	
Flanges	EPA	$LR = 4.61 \times 10^{-6} \times ISV^{0.703}$	0	4.03	9.41E-05	0	0	37
	Proposed	$LR = 5.52 \times 10^{-5} \times ISV^{0.353}$	13	4.03	4.87E-05	0.198	0.184	
Open-ended lines	EPA	$LR = 2.20 \times 10^{-6} \times ISV^{0.704}$	2	3.91	4.58E-03	0.014	0.007	3
	Proposed	$LR = 9.93 \times 10^{-5} \times ISV^{0.347}$	5	3.91	4.49E-03	0.032	0.025	
Others	EPA	$LR = 1.36 \times 10^{-5} \times ISV^{0.589}$	0	3.98	9.79E-05	0	0	21
	Proposed	$LR = 7.72 \times 10^{-5} \times ISV^{0.320}$	12	3.98	7.29E-05	0.148	0.136	

It is evident from F-ratio, compared to F-critical, that for the pumps, flanges, and others categories the non-linear approach demonstrates better estimations of emission rate. Also, in open-ended lines, the F-ratio obtained for the EPA equation is less than F-critical, thus confirming the acceptance of the null hypothesis. In other words, the new equation represents a better estimation. In other categories, the F-ratio of both approaches are almost the same.

Comparing the sum of squared errors demonstrates those obtained through non-linear approach are less than those of EPA approach. In pumps, flanges, and others categories

where the sum of squared errors with non-linear approach are several times lower than those of EPA, the non-linear equations are proposed.

Similar to the F-ratio results, in pumps, flanges, and others categories,  $R_a^2$  is zero. In connectors and open-ended lines,  $R_a^2$  is several times higher than those of EPA while  $R_a^2$  for valves is similar in both approaches. Thus, the non-linear equations are proposed for the categories of pumps, connectors, flanges, open-ended lines, and others.

The  $\Delta AIC$ s obtained for the pump seals, connectors, flanges, and others are equal or higher than 10, confirming the better estimation of emission rate by applying the non-linear equations [Burnham and Anderson, 2002].

The statistical analysis of both approaches confirms that with the existence of new sets of data (ISV and emission rate), the non-linear approach is more accurate to develop the correlation equations.

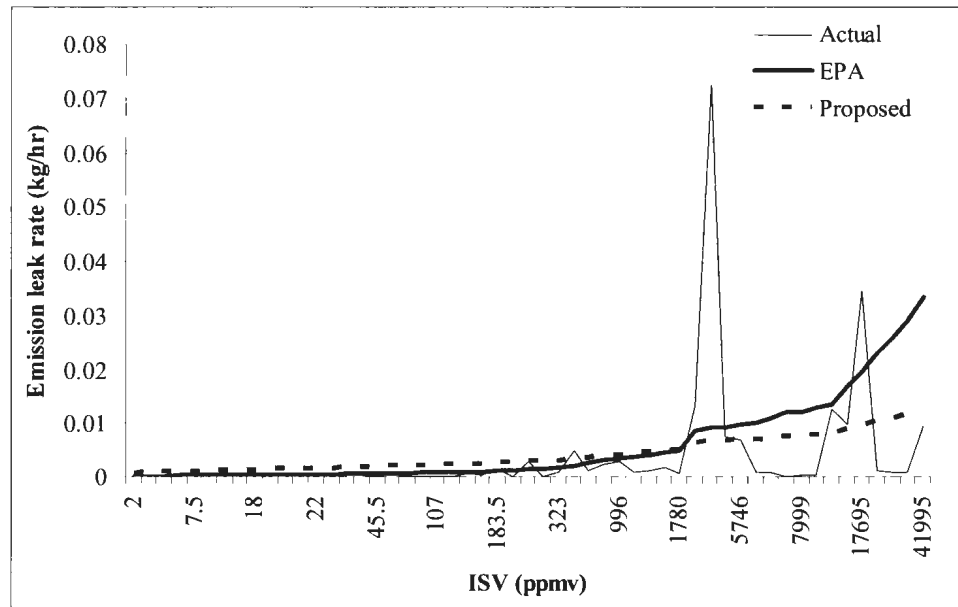
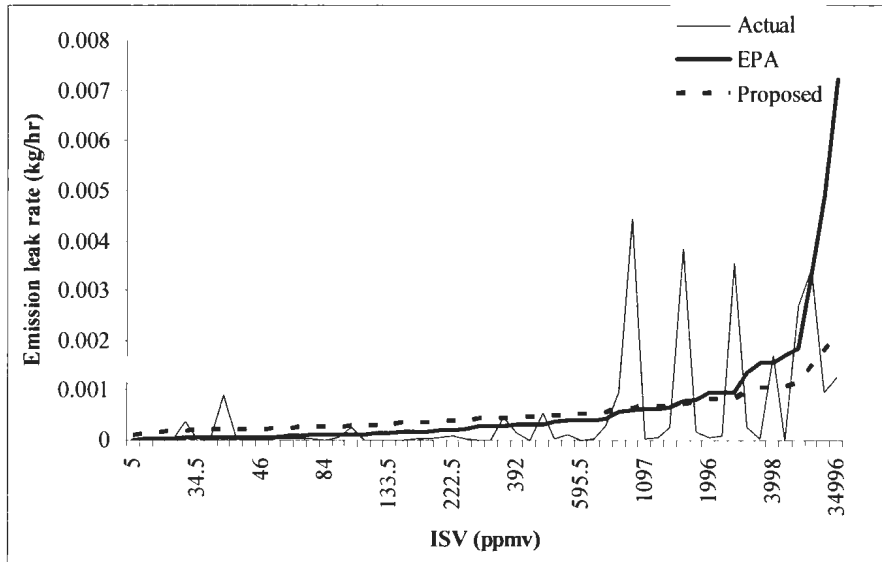
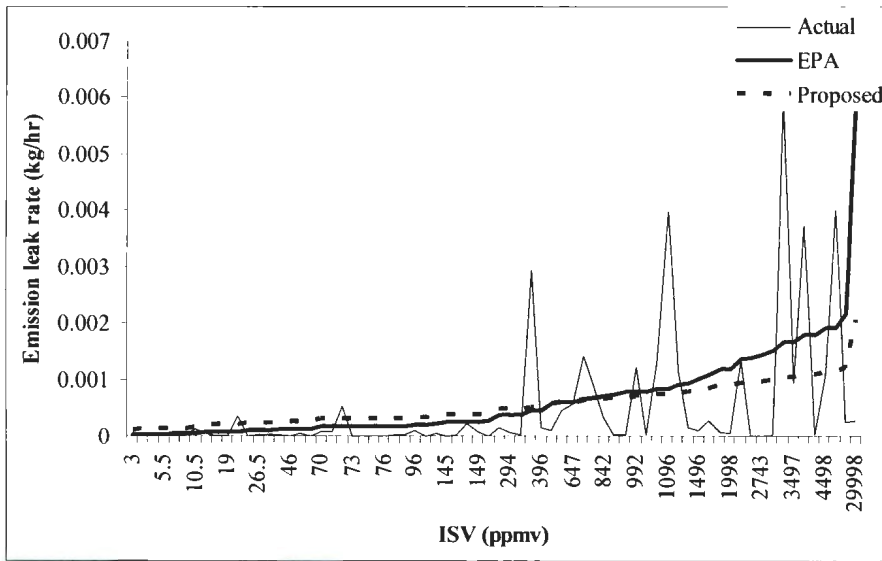


Figure 4.3. Trends of actual data and EPA and new equations' estimation of emission leak rate (Pump seals)



**Figure 4.4. Trends of actual data and EPA and new equations' estimation of emission leak rate (Flanges)**



**Figure 4.5. Trends of actual data and EPA and new equations' estimation of emission leak rate (Others)**

Figures 4.3 to 4.5 show the trends for the actual data, EPA equations' estimate, and also the new equation estimate of emission leak rate. Compared with the trend of actual data, both approaches show almost the same trend at lower ISV points. However, as the ISV values increase, the proposed equations show a better fit to the trend compared to EPA proposed methodology, which shows an overestimation.

#### **4.5 Conclusion**

Applying a non-linear regression to the screening values and leak rate, new sets of emission correlation equations for different equipment categories were developed. The purpose of developing such equations was to better estimate the emission rate based on the screening value for different series of valves, pump seals, connectors, flanges, open-ended lines, and others associated with oil and gas operations. Comparing the results estimated by EPA correlation equations with the proposed model show a better estimation of emission rate in pump seals, connectors, open-ended lines, and others. Finally, it is observed as new data gets available for different components the new approach is a better method of revising correlation equations as compared to EPA. The release rate equations are used to estimate concentration profile of the chemicals in and around the facility. The concentration profile is used to assessment environmental impact and associated risk. Precise estimation of the emission rate helps to overcome uncertainty associated with environmental impact and risk assessment. This paper would help readers to understand the methodology and choose better equations to estimate emission rate and assess associated risk.

### **Acknowledgment**

The financial support provided by Natural Sciences and Engineering Research Council of Canada (NSERC) is highly appreciated by the authors.

### **4.6 References**

American Petroleum Institute (API). (1993). *Development of fugitive emission factors and emission profiles for petroleum marketing terminals*. Health and environmental sciences. Washington, D.C.: American Petroleum Institute.

American Petroleum Institute (API). (1993). *Fugitive hydrocarbon emissions from oil and gas production operations*. Health and environmental sciences. Washington, D.C.: American Petroleum Institute.

American Petroleum Institute (API). (1995). *Emission factors for oil and gas production operations*. Health and environmental sciences. Washington, D.C.: American Petroleum Institute.

Beauchamp, J. J., & Olson, J. S. (1973). Corrections for bias in regression estimates after logarithmic transformation. *Ecology*, 54, 215-228.

Berthouex, P. M., & Brown, L. C. (2002). *Statistics for environmental engineers* (second ed.). Florida: CRC press LLC.

- Burnham, K. P., & Anderson, D. R. (2002). *Model Selection and Multimodel Inference: A Practical Information-Theoretic Approach* (2nd ed.). Fort Collins: Springer-Verlag.
- Dubose, D. A., Steinmetz, J. I., & Harris, G. E. (1982). *Frequency of leak occurrence and emission factors for natural gas liquid plants*. U. S. Environmental Protection Agency, Research triangle park, NC 27711.
- Finney, D. J. (1941). On the Distribution of a Variate Whose Logarithm is Normally Distributed. *Supplement to the Journal of the Royal Statistical Society*, 7, 155-161.
- GraphPad Software Inc. (GPSI). (2007). *Goodness of fit of non-linear regression*. Retrieved from [http://www.graphpad.com/help/Prism5/prism5help.html?reg\\_diagnostics\\_tab\\_7\\_2.htm](http://www.graphpad.com/help/Prism5/prism5help.html?reg_diagnostics_tab_7_2.htm)
- Mendenhall, W., & Sincich, T. (1993). *A second course in business statistics: regression analysis* (4th ed.). New York: Macmillan.
- R Development Core Team (RDCT). (2009). *The R Manual*. Retrieved from <http://www.r-project.org/>
- Smith, R. J. (1993). Logarithmic transformation bias in allometry. *American journal of physical anthropology*, 90, 215-228.
- Smyth, G. K. (2002). Nonlinear Regression. In A. H. El-Shaarawi, & W. W. Piegorsch (Eds.), *Encyclopedia of environmetrics* (pp. 1405-1411). Chichester: John Wiley & Sons Ltd.

U. S. Environmental Protection Agency (USEPA). (1995). *Protocol for equipment leak emission estimates*. Office of air quality planning and standards, research triangle park, NC 27711.

U. S. Environmental Protection Agency (USEPA). (2007). *Emission Inventory Improvement Program*. Retrieved from <http://www.epa.gov/ttn/chief/eiip/techreport/>

U. S. Environmental Protection Agency (USEPA). (2010). *Emission factors and AP 42, Compilation of air emission factors*. Retrieved from <http://www.epa.gov/ttnchie1/ap42/>

## **5 Explosion modeling and analysis of BP deepwater horizon accident\***

Mohammad Dadashzadeh, Rouzbeh Abbassi, Faisal Khan, Kelly Hawboldt

Process Engineering,

Faculty of Engineering and Applied Science,

Memorial University of Newfoundland, St.John's, NL, Canada

### **Abstract**

The BP Deepwater Horizon blowout not only resulted in an oil release over several months but also caused an explosion topside which took 11 lives. The details of the causes of the accident and a computational fluid dynamics (CFDs) modeling of the dispersion of flammable gas was given in the BP investigation report [BP, 2010]. However, the explosion consequence was not studied in the BP report. In this study, a CFD model was used to simulate the dispersion of flammable gas and integrated with the explosion consequences. The simulation includes modeling of the dispersion of the vapour cloud in the first section and modeling the resulting explosion based on the dispersion results. Through the modeling, it was determined that the overpressure in the engine room and in highly congested areas of the platform are 1.7 (bar) and 0.8 (bar), respectively. The model also identified overpressure regions on the platform and the effect of the area's congestion on overpressure intensity: lower overpressure in lower congested areas and higher overpressure in higher congested/confined areas.

\* Dadashzadeh M, Abbassi R., Khan F, and Hawboldt K. (2013). Explosion Modeling and Analysis of BP Deepwater Horizon Accident. *Journal of Safety Science*, 57, 150-160.

**Keywords:** Explosion modeling, explosion analysis, BP accident modeling, risk assessment, accident modeling

## **5.1 Introduction**

Increasing energy demand is driving offshore exploration to more remote, deeper, and harsh environments and as a result safety and accident control is becoming increasingly challenging. One of the key areas of concern is vapour cloud explosions (VCE) which occur due to the release of flammable gases and ignition. Thus, the understanding of the consequences of a VCE and using a safety design based on the consequences could prevent and/or mitigate accidents.

### **5.1.1 Important vapour cloud explosion accidents**

In June 1974, an explosion occurred in the Nypro plant at Flixborough resulting in 28 fatalities and 36 injuries. The explosion brought severe damage to the plant, while damage to the surrounding area was also significant. There was scattered debris as far as 32 km from the location of the plant. The main cause of the accident was the release of cyclohexane at 150 °C and a pressure of 1 MPa in the plant area due to the failure of one of the pipes between five interconnected oxidation vessels. The vapour cloud formed was then mixed with the air. Being in a flammable range, the vapour cloud was ignited through a source of ignition which was most likely the reformer furnace of the nearby hydrogen plant. Consequently, a vapour cloud explosion (VCE) occurred in the plant [Sadee and Samuels, 1977]. The highly destructive overpressure was caused due to the highly congested/confined area of the plant [Venart, 2007]. A CFD simulation of the

Flixborough incident was performed and results indicate that while the maximum overpressure of 15 bar was approached, the ignition location had no significant effect on the magnitude of the maximum overpressure [Høiset et al., 2000]. The magnitude was calculated to be equal to the detonation of 16 tons of TNT with an overpressure distribution radius of over 3 km [Sadee and Samuels, 1977].

In 1988, the Piper Alpha platform, located in the North Sea, experienced an explosion causing 165 deaths and total destruction of the platform. Investigations revealed the release of light hydrocarbons (condensate propane, butane, and pentane) occurred due to the restart of a pump which was out of service for maintenance. A relief valve (RV) was also replaced by a blank on the piping flange for the service. Then, due to the restart of the pump, with no knowledge of the removal of the RV, the flange leaked releasing hydrocarbon gases. The subsequent presence of an ignition source caused the explosion [CCPS, 2005]. Investigation reports revealed that the most likely sources of ignition were hot surfaces, broken light fittings, electrostatic sparks, and electric motors. Through the propagation of the fire to module B, the rupture of the B/C firewall caused the breaking of a pipe. Consequently, a large amount of crude oil was leaked in module B causing a fireball in this module. The fire then reached 1200 barrels of fuel stored on the deck above modules B and C while it was spreading back to module C. Thus, the second explosion occurred. The heat load in module B also caused the rupture of the riser followed by an impinging jet fire under the platform [Pate-Conell, 1993].

In October 1989, an explosion occurred at the Houston chemical complex of Philips Company, Pasadena, Texas. The complex was a polyethylene plant, and the accident was

caused through the release of about 39,000 kg of flammable vapour composed of ethylene, isobutene, hexane, and hydrogen. Due to the high pressure and temperature in the process, the flammable vapour cloud formed very fast, followed by ignition in less than 2 minutes after the release [Betha, 1996]. The actual source of ignition was unknown. However, there were several potential sources of ignition such as a small diesel crane used by a maintenance crew, an operating forklift, a gas-fired catalyst activator with an open flame, welding and cutting operations, vehicles parked near the polyethylene plant office building, and ordinary electrical gear in the control building and the finishing building. Around 90 seconds after the release, the flammable vapour was ignited followed by an explosion. Then, the flame reached two 20,000 gallon isobutene storage tanks and the second explosion occurred. There was also another polyethylene plant reactor exposed to the consequent fire which made the third explosion [OSHA, 1990].

In September 1997, an explosion occurred in a Liquefied Petroleum Gas (LPG) storage vessel at the refinery of Hindustan Petroleum Corporation Limited (HPCL) in Vishakhapatnam, India; it resulted in 60 deaths and over \$15 million damage. The cause of the accident was a leak from a corroded pipeline around a storage tank. The resulting vapour cloud formed a continuous fire that led to the subsequent explosion. The major reasons for the incident were that no decisive steps were taken during the period of the leak occurrence (1 hour 25 minutes), the LPG was getting unloaded without a proper safety system, there was no management plan, and no response to the warning signals [Khan and Abbasi, 1999].

In March 2001, an accident occurred on the Petrobras platform 36, located offshore from Rio de Janeiro, Brazil. The accident caused the loss of 11 lives. The platform sank after five days [USEPA, 2001]. Investigation showed the accident was started by the rupture of an Emergency Drain Tank (EDT) in the starboard aft column because of excessive overpressure. Consequently, the damage to the equipment led to the release of water, oil, and gas on the platform. Then, due to an ignition of dispersed gas through an unknown source of ignition, a major explosion occurred which resulted in a massive destruction of the platform [Barusco, 2002].

In March 2005 at BP's Texas City refinery an explosion resulted in 15 lives lost and 180 injuries. In this accident, a flammable liquid hydrocarbon was released to the ground around a drum stack. Then, the flammable liquid was vapourized, forming a vapour cloud at the top of the liquid pool. Atmospheric wind pushed the vapours and droplets downwind, causing them to mix with air. Some portions of the vapour cloud also went upwind and crosswind. The vapour cloud then reached an ignition source which was most likely an idling pickup truck near the area. The truck caught fire, followed by a vapour cloud explosion (VCE). Rather than the blast pressure causing a disaster, the flame-front through the VCE reached the accumulated vapour above the liquid pool and caused a pool fire [Kalantarnia et al., 2010; Khan and Amyotte, 2007; CSB, 2007]. According to Broadribb [Broadribb, 2006], the failure to control the liquid which escaped from the tower and the failure to respond appropriately resulted in the explosion. The severity of the incident was compounded by the presence of people in the vicinity of the release and the lack of rigour in safety management.

The previous accidents could have been minimized in terms of financial and human loss through better prediction of the dispersion of the flammable gases and resulting overpressure. With this information mitigation measures could be put in place and better safety management plans (e.g. “safe” areas) developed. The BP Deepwater Horizon accident in April 2010 is another, more recent example. Using FLACS CFD modeling, BP conducted a gas dispersion analysis to simulate the flammable concentration of the released hydrocarbons on the platform [BP, 2010]. However, the dispersion of the gas was only the initial step which resulted in the explosion.

This study focuses on integrating dispersion of flammable hydrocarbon release and explosion consequences using the FLACS model. While the dispersion modelling predicts cloud behaviour, the inclusion in the model of the resulting explosion and overpressure predictions can minimize damage and losses by identifying hazardous areas and using the information to optimize platform design.

## **5.2 Vapour cloud explosion modeling**

The extent of damage from the release of flammable gases is in part a function of the dispersion of the cloud. If there is no immediate ignition, the flammable vapour is dispersed through structure geometry and ventilation systems and ignition may be delayed. Ignition and resulting vapour cloud explosion (VCE) occur if the flammability limits of the gas are met (based on gas composition) and an ignition source with enough energy is presented [Assael and Kakosimos, 2010].

A VCE is influenced by several factors that have been analyzed in various studies [Mannan, 2005; Prugh, 1987]. In general, the ignition probability increases with the size of the vapour cloud. The explosion efficiency and impact are affected by the turbulent mixing of vapour and air and the location of ignition sources [Crowl and Louvar, 2001].

When an explosion occurs, there is a transient air pressure greater than the surrounding atmospheric pressure referred to as overpressure. During such a phenomenon, the gas expands rapidly due to the energy released and the surrounding gas is forced back, initiating a pressure wave that moves rapidly from the blast source. The propagation of a pressure wave in air, or blast wave, is the source of most of the damage caused by explosions. The blast is the composite of the pressure wave, the change in overpressure during the period of explosion, and subsequent wind. Table 5.1 outlines damages from various overpressure intensities. The dispersion and explosion are complex transport phenomena and tools such as computational fluid dynamic models are typically used to simulate incidents.

**Table 5.1. Damage estimates for common structures based on overpressure [Crowl and Louvar, 2001]**

<b>Pressure (bar)</b>	<b>Damage</b>
0.17	50% destruction of brickwork of houses
0.21	Heavy machines (3000 lb) in industrial building suffer little damage; steel frame buildings distort and pull away from foundations
0.21-0.28	Frameless, self-framing steel panel buildings demolished; rupture of oil storage tanks

Pressure (bar)	Damage
0.28	Cladding of light industrial buildings ruptures
0.34	Wooden utility poles snap; tall hydraulic presses (40,000 lb) in buildings slightly damaged
0.34-0.48	Nearly complete destruction of houses
0.48	Loaded train wagons overturned
0.48-0.55	Brick panels, 8-12 in. thick, not reinforced, fail by shearing or flexure
0.62	Loaded train boxcars completely demolished
0.69	Probable total destruction of buildings; heavy machine tools (7000 lb) moved and badly damaged; very heavy machine tools (12,000 lb) survive

### 5.2.1 CFD modeling

Computational Fluid Dynamics (CFDs) are able to model complex transport phenomena (momentum, mass and heat) in complicated flow geometries. The level of congestion/confinement in an industrial facility is an important parameter in VCE phenomena. The Flame Acceleration Simulator (FLACS) is a general purpose CFD model that is used in offshore/onshore studies of hydrocarbon dispersion and explosion modeling [Berg et al., 2000; Moros et al., 1996; Qiao and Zhang, 2010; Wingerden and Salvesen, 1995].

In the current study, FLACS CFD software [GEXCON, 2010] was used to model the dispersion and explosion of the flammable vapour cloud. Using a finite volume method in a Cartesian grid, the concentration equations of mass, momentum, and enthalpy are solved in FLACS. Mixture fraction and mass fraction equations are also solved in FLACS

and the combustion model is used to close the set of equations. For turbulence, FLACS uses a Reynold-averaged Navier-Stokes (RANS) approach based on the standard  $k-\epsilon$  model to close the equations. As obstacles with small details play a significant role during dispersion and explosions, the representation of such details is a key aspect of modeling. There is however a balance between the need to represent geometric details and the resulting increase in computational time. In order to satisfy these issues, a distributed porosity concept is used and obstacles are represented by area and volume porosity [Hanna et al., 2004; Launder and Splading, 1974].

There are two different modes for the combustion of gaseous fuel in air. One is where fuel and oxygen are mixed during the combustion process when the fire occurs. The other one is where the fuel and air are premixed and the combustion occurs when the fuel concentration is within the flammability limit. A vapour cloud explosion is initiated with the ignition of a premixed cloud of fuel and oxidants. Then, the premixed vapour will burn with a laminar burning velocity in a steady non-turbulent situation which may escalate to an explosion with turbulent burning velocity [Bjerketvedt, 1997].

The combustion model of a premixed combustion, like a vapour cloud explosion, is divided into two major parts; localizing the reaction zone (flame model); and conversion of reactants at a similar rate to what happens in a real explosion (Burning velocity rate). Modeling the flame is essential in a combustion model due to the thin premixed flame in the reaction zone compared to grid resolution. FLACS uses  $\beta$  flame model [Arntzen, 1998] in order to model the flame. In  $\beta$  flame model, the reaction zone is thickened by

increasing the diffusion with a factor  $\beta$  and decreasing the reaction rate with a factor  $1/\beta$ . There are three different modes of burning velocity from the beginning of the ignition up to the escalation to an explosion. These are laminar burning, when the flame is smooth and governed by molecular diffusion, and quasi-laminar, when there is wrinkling of the flame due to instabilities and the turbulent regime, after a transition period. FLACS calculates the burning velocity ( $S_u$ ) as  $S_u = \text{Max}(S_{QL}, S_T)$ . Turbulent burning velocity ( $S_T$ ) is calculated through a developed correlation [Bray, 1990] while quasi-laminar burning velocity is dependent on laminar burning velocity, the flame radius, and the fuel dependent constant [Arntzen, 1998].

Using several grid cells is the disadvantage of the  $\beta$  flame model. As an alternative, the Simple Line Interface Calculation (SLIC) was introduced by Arntzen (1998) in a 2D version of FLACS. In 3D, the SLIC is modified to SIF (Simple Interface Flame) as the flame is a surface in 3D compared to a line in 2D. In this model, the reactants and products are compounds of the gas while the flame is the interface between these two. Thus, the flame separates the zone into reactants and products. The reactants then convert to the products at a rate depending on burning velocity and flame area. The SIF algorithm starts with the update and calculation of values on the boundaries. Then, with a rate depending on flame area and burning velocity, reactants are converted to products resulting in an increase in the mass fraction of products. Using calculated pressures from previous steps, a velocity field is estimated using the momentum equation. In this step,  $\beta$  flame model uses a pressure correction routine for compressible flows to satisfy the

continuity equation. However, in a reactive flow, the equation of state is not satisfied with the normal pressure correction routine. Thus, SIF uses a modified pressure correction routine to satisfy the equation of state in a reactive flow [Arntzen, 1998].

Compared to other dispersion models, FLACS has some advantages; primarily it gives reasonably good predictions that have been validated for different scenarios. The distributed porosity concept is another key advantage as it results in simulations of dispersion and explosion in large and complex facilities which are computationally faster than other conventional models. Additionally, the well-established turbulence model (k- $\epsilon$ ) with fewer equations and constants, compared to other alternative models, is a key advantage. The k- $\epsilon$  model has some shortcomings such as the over prediction of turbulence intensities in the stagnation region of impinging jets. This causes the over prediction of wall heat transfer and poor prediction of boundary layers around bluff bodies. Lack of predicting the secondary swirling flows in non-circular ducts is another drawback in k- $\epsilon$  model which causes the faster spreading of the plane two-dimensional jets than that of round jets while in fact they are slower. Regardless of such shortcomings, the k- $\epsilon$  model is widely used in CFD studies [HSE, 2010].

The impact of grating between lower and upper process decks, different configuration of barrier walls, and different configuration of separation gaps in risk reduction have been studied in a floating production storage and offloading (FPSO) platform using the FLACS CFD code [Berg et al., 2000]. In another study, the methodologies of estimating the maximum achievable gas cloud for different releases, wind and ventilation conditions,

and probabilities of explosions were outlined through the application of the FLACS code [Moros et al., 1996]. In a study by Wingerden and Salvesen (1995), the damage as a result of a VCE in a naphtha cracker installation was simulated with FLACS. The trends between the actual explosion and the CFD model were similar. However, the explosion simulation in this study was sensitive to the characteristics of the flammable cloud and therefore a more realistic model of the dispersion process of the flammable vapour is critical. There was also a difference between the estimated overpressure from stoichiometric to excess ratio [Wingerden and Salvesen, 1995]. In a related study, FLACS was used to develop the potential gas build-up due to an accidental gas release and the resulting potential overpressure caused by VCE in offshore/onshore oil and gas production facilities [Qiao and Zhang, 2010].

The FLACS CFD code has been validated against a range of experiments through several studies [Middha et al., 2010; Davis et al., 2010]. Using the FLACS CFD code, a study was performed using simulations to predict the results of combined release and ignition scenarios. The simulation results were compared to the results achieved through the experiments carried out with the ignition of vertically upward hydrogen releases, different release rates, and different geometry configurations. There was good correlation between the simulated dispersion results and the experimental gas concentrations. In terms of explosion overpressure, the pressure levels obtained through the simulation results were similar to those of experiments, though the ignition locations were somewhat different in CFD simulation [Middha et al., 2010]. Another study was conducted to simulate the Buncefield Oil Storage Depot incident (2005). The FLACS CFD code was used to model

the geometry of the Buncefield site. There were also sets of experiments to validate the simulation results. The correlation between the FLACS simulation results and the observed blast damage compared well with experimental results [Davis et al., 2010].

In this study the BP Deepwater Horizon gas release, dispersion, and explosion are modelled. After a brief description of the main causes of the accident, a description of the CFD tool FLACS is described. In order to simulate explosion, the dispersion analysis is essential. Therefore, the first section of the modeling focuses on simulation of the dispersion of the flammable vapour cloud using the BP reported data [BP, 2010]. In the second section, the dispersion results are used in the FLACS explosion simulation to predict the overpressure caused by the explosion.

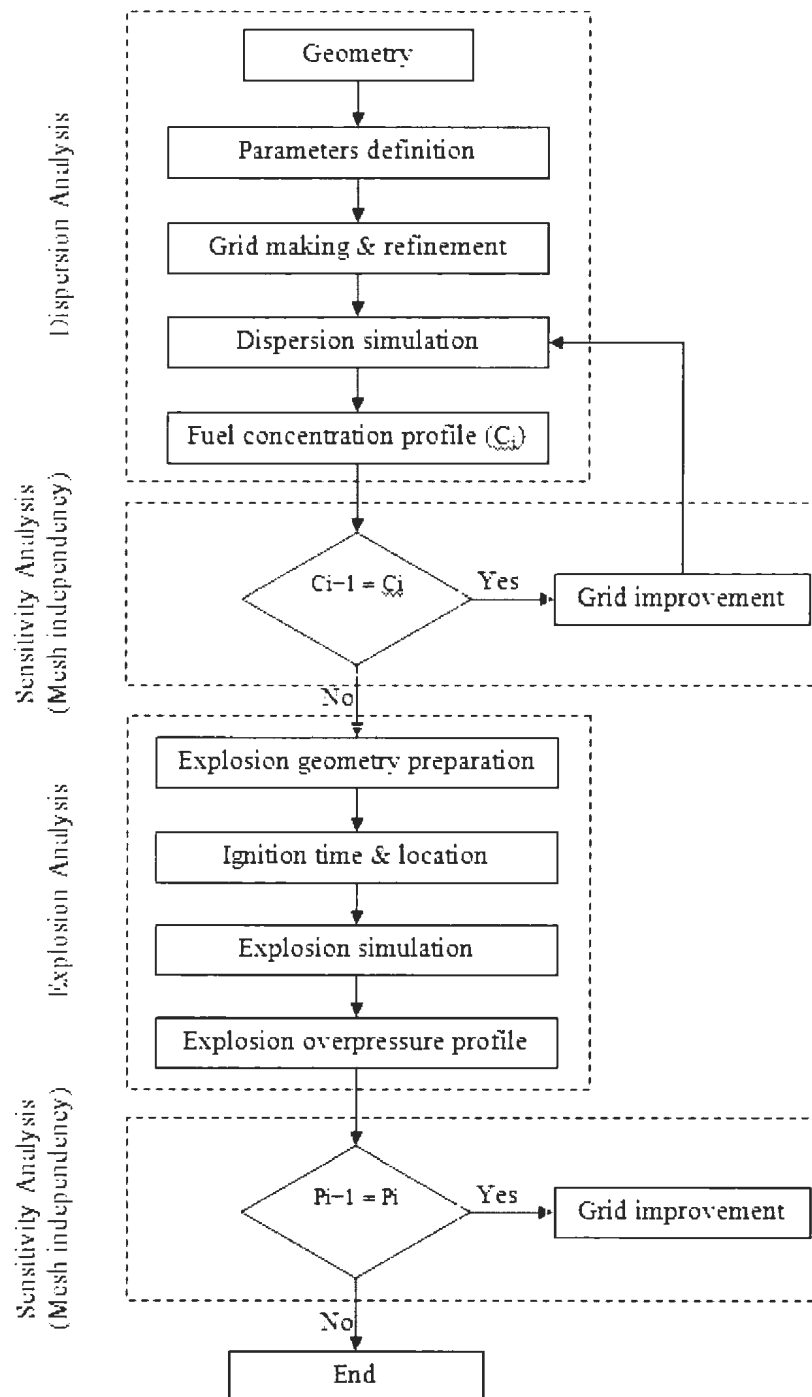


Figure 5.1. The required steps for the CFD modeling of vapour cloud dispersion/explosion

Figure 5.1 outlines the steps in the CFD modeling of the vapour cloud dispersion and explosion. Based on the construction plans/data, the geometry of the simulation is built followed by the input of simulation time, ventilation and wind conditions, boundary conditions, leak rates and their locations. The simulation volume and the dimensions of the grids are defined based on grid refinement for specific points such as leak positions. The dispersion model is then run and based on the results a sensitivity analysis is used to define the optimum size of grids. Based on these results the explosion simulation is run after adding the required changes in the geometry. The ignition time and location are selected followed by the explosion simulation. There will also be a sensitivity analysis after explosion modeling to make the simulation mesh independent.

#### 5.2.1.1 The history of BP Deepwater Horizon oil rig

Macondo well is located in Mississippi Canyon Block 252, 48 miles from the shoreline; 114 miles from the shipping supply point of Port Fourchon, Louisiana; and 154 miles from the Houma, Louisiana helicopter base (Figure 5.2).

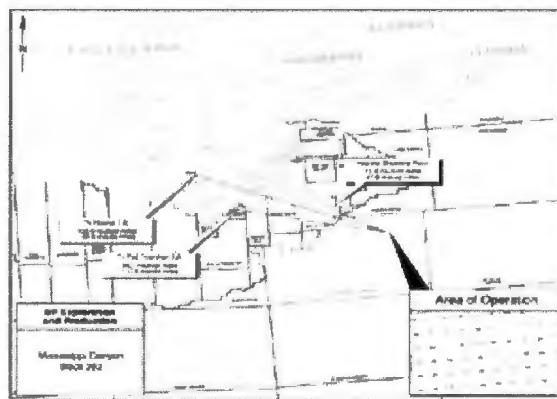


Figure 5.2. Geographic location of the well [BP, 2010]

Exploratory drilling initially began with Transocean's semi-submersible Marianas on October 2009. On February 2010, the semi-submersible Marianas was replaced by Transocean's Deepwater Horizon. On April 2010, the well's final depth of 18,360 ft was approached and well logging, cleanout, and open hull verification was conducted [BP, 2010].

#### **5.2.1.1.1 Accident description**

On the evening of April 20, 2010, a hydrocarbon release from the Macando well onto the platform resulted in an explosion and fire on the rig. Eleven people lost their lives, while 17 others were injured. The fire continued for 36 hours until the rig sank. The BP investigation team provided an accident investigation report based on partial real time data from the rig, documents from the well's development and construction, witness interviews and also information provided by other companies including Transocean, Halliburton and Cameron. According to the BP report [BP, 2010], there was a well integrity failure resulting in a loss of hydrostatic control of the rig. Failure to control the flow from the well with the Blowout Preventer (BOP) resulted in the release of hydrocarbons, followed by the subsequent ignition. After the initial explosion, the failure of the BOP emergency functions did not allow the well to be sealed.

Applying fault tree analysis, the BP investigation team defined eight major key findings related to the cause of the accident as follows:

- Failure of the annulus cement barrier to isolate hydrocarbons

- Failure of shoe track barriers to isolate the hydrocarbons
- Failure to establish the well integrity
- Failure to observe the influx of hydrocarbons into the riser
- Failure of well control response actions
- Venting of the gas diverted from the mud gas separator to the rig
- Failure of fire and gas systems to prevent the ignition
- Failure of the Blowout Prevention (BOP) mode to seal the well after the initial explosion

#### **5.2.1.1.2 BP investigation report: vapour cloud dispersion**

Using FLACS, Baker Engineering and Risk (BakerRisk) performed a flammable gas dispersion analysis of the accident. According to the BP, the most important release location points were as follows:

- Riser bore at the drill floor
- Mud gas separator vent at the top of the rig
- Mud Gas Separator (MGS) rupture disk/Diverter outlet
- Slip joint below the moon pool
- Mud processing

A simplified geometry of the Deepwater Horizon was built in FLACS pre-processor (CASD). The key building/structures included in the simplified geometry were the hull, the main deck structure, the key buildings around the drill floor, the helideck, the catwalk

aft of the drill floor, the partial walls around the drill floor, the bottle rack forward of the drill floor, a simplified representation of the drilling pipe and risers on the platform, and a simplified representation of the derrick.

The released gas composition is outlined in Table 5.2, and the wind was set at the speed of 2 m/s from port to starboard based on the information provided by BP.

**Table 5.2. Simplified gas composition for FLACS analysis [BP, 2010]**

Component	Symbol	Concentration (%)
Carbon Dioxide	CO <sub>2</sub>	0.84
Methane	CH <sub>4</sub>	57.18
Ethane	C <sub>2</sub> H <sub>6</sub>	5.53
Propane	C <sub>3</sub> H <sub>8</sub>	3.85
Butane	C <sub>4</sub> H <sub>10</sub>	2.60
Pentane	C <sub>5</sub> H <sub>12</sub>	1.62
Hexane	C <sub>6</sub> H <sub>14</sub>	1.16
Heptane	C <sub>7</sub> H <sub>16</sub>	1.68
n-Octane	C <sub>8</sub> H <sub>18</sub>	1.81
n-Nonane	C <sub>9</sub> H <sub>20</sub>	1.33
n-Decane	C <sub>10</sub> H <sub>22</sub>	22.38

As the engine rooms were the most probable ignition areas, the flammable gas concentration at the engine rooms' ventilation inlets are key monitoring points. General ventilation conditions for different areas of the oil rig were set by leak points in the FLACS geometry. Additionally, there were six extra monitor points to observe the flammable gas concentration in the ventilation inlets of engine rooms 1 through 6.

As the dispersion results show, a flammable gas cloud could develop in the moon pool and BOP house, on the drill floor, and on the vast majority of the main deck. In the engine room area, critical due to the probability of ignition occurrence, the formation of the flammable vapour cloud in engine rooms #3 through #4 occurred [BP, 2010].

### **5.2.1.2 CFD-based modeling of BP Deepwater Horizon explosion: application of FLACS as a validated CFD tool**

#### **5.2.1.2.1 Scenario definition**

The geometry, wind condition, gas composition and ventilation system are as outlined in Figure 5.3. The geometry details were extracted from recent BP investigation report [BP, 2010]. However, due to the high concentration of the gas at the ventilation inlets of the engine rooms, instead of two scenarios, three possible scenarios were defined in the explosion section. In the first scenario, the dispersion simulation was performed with non-operating ventilation systems at the engine rooms' ventilation inlets. In the second, an operating ventilation system was given. The difference between the concentrations of gas from the scenarios was assumed to be the mixture ratio that entered the engine rooms. In

the third scenario (explosion scenario), engine rooms 1 through 6 were created in the second deck of the platform. The dispersion simulation in the later scenario was defined as the main scenario for the explosion.

**Table 5.3. Time dependent release points for scenario A [BP, 2010]**

Phase No.	Time at Start of Phase	Phase Duration (min.)	Flowrate over phase (MMSCF/d)	Path of gas release
1	21:40:30	0.5	0-10	Mud System
2	21:41:00	0.5	10-50	Mud System
3	21:41:30	0.5	50-160	Mud System
			0-40	MGS Vent
4	21:42:30	0.5	160	Mud System
			40-20	MGS Vent
			150-75	Riser
5	21:42:30	1	160-50	Mud System
			20	MGS Vent
			75-30	Riser
6	21:43:30	0.5	50	Mud System
			20-40	MGS Vent
			30-40	Riser
7	21:44:00	0.6	50-320	Mud System
			40-240	MGS Vent
			40-180	Riser

Phase No.	Time at Start of Phase	Phase Duration (min.)	Flowrate over phase (MMSCF/d)	Path of gas release
8	21:44:36	1.4	320-100	Mud System
			240-60	MGS Vent
			160-50	Riser
9	21:46:00	3	100-10	Mud System
			60-5	MGS Vent
			50-2	Riser

The simulation volume was assumed to be 116m×71m×104m and the grid size was set as 1 (m) (obtained through sensitivity analysis). There were also some grid refinements around the leak areas and some ventilation points. The time of simulation was assumed to be 570 seconds, while the first 60 seconds were the start up period where only the ventilation points were in operation. The release of flammable gas started after 60 seconds. The leaks were time dependent during the time of simulation as outlined in Table 5.3.

In order to control the time steps, CFLC and CFLV numbers of 5 and 0.5 were selected, respectively. CFLC and CFLV are Courant-Friedrich-Levy numbers based on the sound velocity and the fluid flow velocity, respectively. The CFLC and CFLV control the sound waves and the fluid flow propagation distance in each time step, which is the average control volume length multiplied by the value of CFLC and CFLV. As an example, by

defining a CFLC value of 5 and a CFLV value of 0.5, the pressure will propagate 5 cells while the fluid flow propagates 0.5 cells in each time step [GEXCON, 2010]. The CFLC and CFLV numbers determined were optimized to guarantee convergence. Figure 5.2 outlines the geometry based on the data available in BP's investigation report for this modeling scenario.

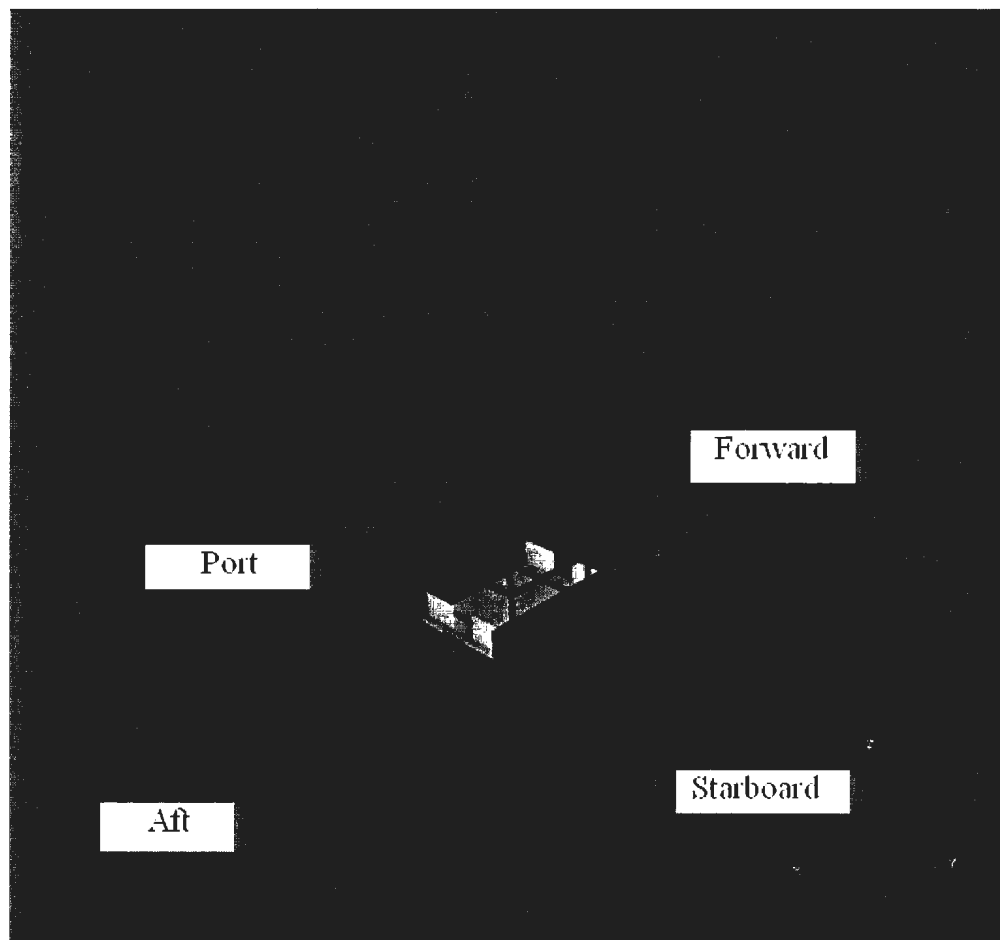


**Figure 5.3. BP Deepwater Horizon geometry used for dispersion/explosion simulation**

After the dispersion simulation, some geometry details were changed in order to initiate the explosion simulation of the flammable vapour cloud which was the focus of this study. In order to be flammable, the fuel cloud formed through the dispersion simulation should be in the flammable limit. Based on the gas composition (Table 5.2), the gas mixture has a Low Flammable Limit (LFL) of 0.02 and an Upper Flammable Limit (UFL) of 0.12. The flammable cloud then was used in explosion simulation. The maximum gas concentration was observed after 320 seconds and set as the time of ignition. The ignition location was set in engine room 6 where the highest concentration of flammable gas was observed. After 320 seconds, the simulation was re-started to observe the overpressure caused by the ignition. Figure 5.4 illustrates the location of engine rooms under the first deck of the second floor.

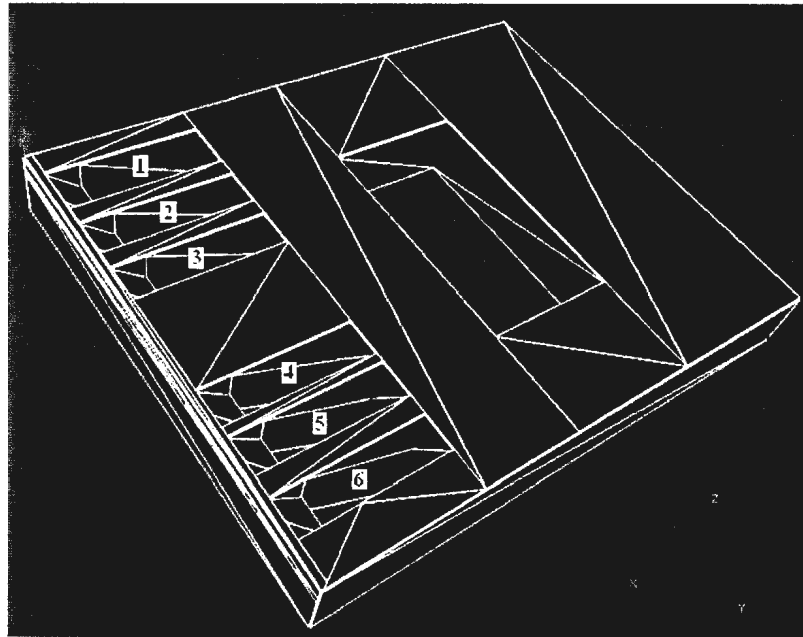


**Figure 5.4. Second deck, configuration of engine rooms #1 to #6**

Highly congested areas result in turbulence generation. Consequently, the combustion rate is enhanced leading to higher overpressure. Hence, the congestion parameter is an important factor in complex geometry which is calculated through dividing the total length (m) of all items on the main deck (cylinders and boxes) by the total volume ( $\text{m}^3$ ) of the area of interest. Extracting the total length of cylinders and boxes on the main deck, the congestion parameter of the BP Deepwater Horizon oil rig was estimated to be  $0.48 \text{ (m/m}^3\text{)}$  which is categorized as a low congestion level [Huser et al., 2009].

### **5.3 Results and discussion**

In section 5.3.1, the flammable gas concentration in different locations of the platform is presented and discussed. There is also a comparison between the dispersion results achieved through the current study and those of the BP investigation report. In section 5.3.2, the explosion overpressure results, which is the contribution of the current study, is presented and discussed.

#### **5.3.1 Dispersion**

Monitor points 71 and 72 in engine rooms #5 and #6 give the gas concentration at engine room ventilation inlets for Scenario 1 (Figure 5.5). FUEL in Figure 5.5 and 5.6 stands for the mass fraction of fuel in the mixture of fuel, air, and combustion products. The gas concentration starts to increase after 60 seconds when the first leak points occur. At 120 seconds, the first peak point of 24% is approached. There is a sharp decrease to 3% after the first peak point due to the decrease in gas released from the peak points.

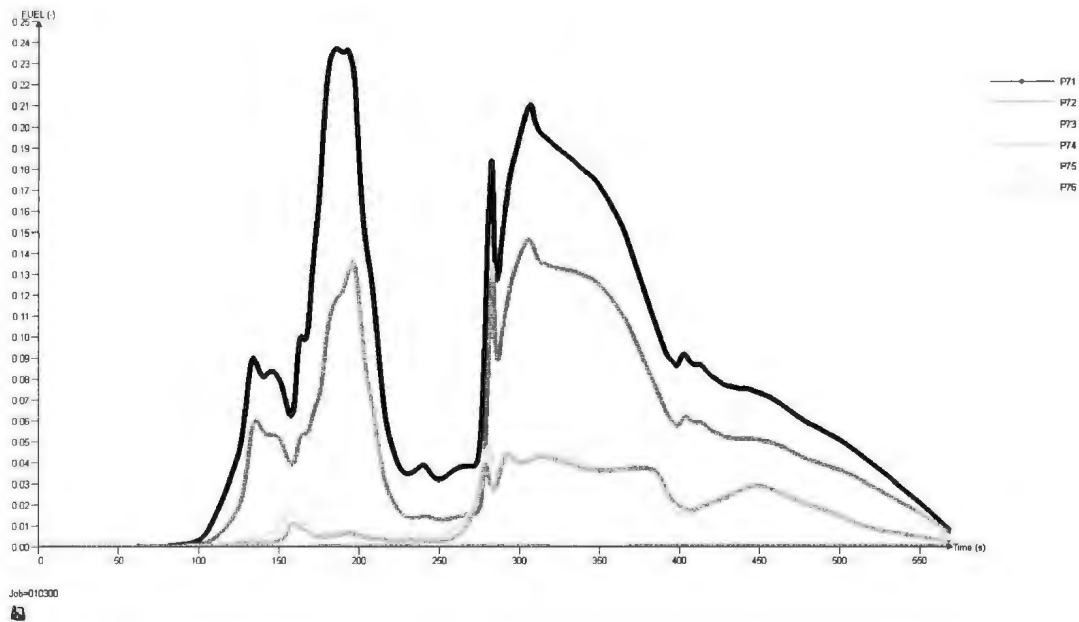


**Figure 5.5. Gas concentration at engine rooms' ventilation inlets with no operating ventilation system**

The second peak point occurs after 320 seconds of simulation when all leak points are released with their highest leak rate. There is a gradual decrease over 250 seconds to around 1% due to the gradual decrease of leak rates from sources. The higher gas concentration for engine rooms 5 and 6 compared to other rooms could be due to their closer proximity to the mud pit exhaust. The direction of wind, from port to starboard (the side where engine room 6 is located) of the platform could be another reason for higher gas concentration at these points.

Figure 5.6 outlines the gas concentration at the same inlets for Scenario 2. Through the extraction of data from both simulation results, the average gas concentration (in air) entering the engine rooms was estimated to be 7.5 %. Thus, in the third scenario the 6

leak points had the same leak rate as ventilation inlets; however, the composition of 7.5 % gas was added into the engine rooms.

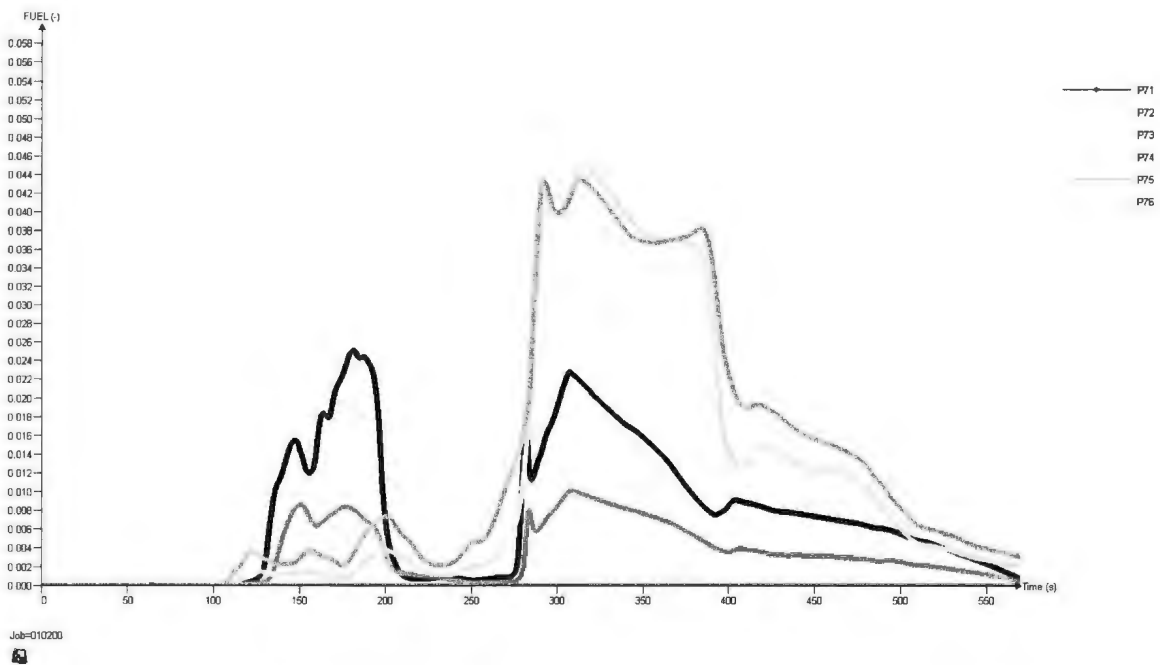


**Figure 5.6. Gas concentration at engine rooms' ventilation inlets with operating ventilation system**

Figure 5.7 shows the gas concentration released to the platform after 320 seconds when the maximum gas released was observed through the dispersion simulation. Due to the direction of wind and also ventilation, the gas concentrations at engine rooms 5 and 6 and also the starboard side of the platform were close to the flammable range for this gas composition (0.02 to 0.12). The gas released from engine rooms 5 and 6 also affect the high concentration of gas in starboard area.

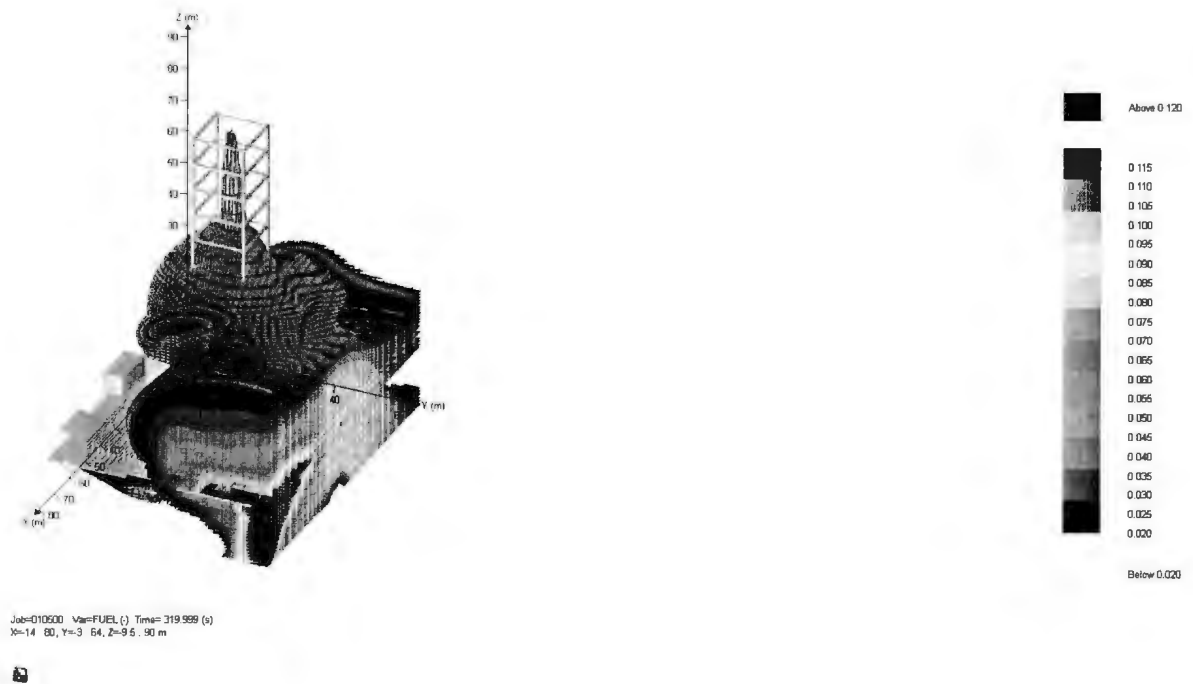


Figure 5.7. Gas concentration at engine rooms' ventilation inlets

### 5.3.1.1 Comparison with BP dispersion results

According to the BP investigation report [BP, 2010], approximately 300 seconds after the start of release, the fuel concentration at supply air intakes of engine rooms #5 and #6 was over 20%. In this study the fuel concentrations were 21% and 15% at the same time for engine rooms 5 and 6 respectively. However, at approximately 120 seconds after the start of release, the BP investigation report indicates a fuel concentration of 3-5% at engine rooms #5 and #6 inlets, while this study indicates an average fuel concentration of 19% for both engine rooms 5 and 6. This difference could be due to the lack of detailed data on the ventilation condition on the platform causing different turbulent conditions in the current study's simulation. As shown in Table 5.4, for durations of 200-300 and 400-

600 seconds after the start of simulation, the fuel concentration for both the BP investigation report and the current study are in the flammable range.

**Table 5.4. Comparison of dispersion results**

Time Duration after the start of simulation (s)	100-200	200-300	300-400	400-500	500-600
BP Investigation Report	FR*	FR*	Peak 21%	FR*	FR*
Current Study	Peak 19%	FR*	Peak 18.5%	FR*	FR*

\*FR: Flammable Range

### 5.3.2 Explosion

Figure 5.8 plots overpressure caused due to the explosion in engine room 6, where the ignition occurred. Monitor points 98 and 99 are in the middle of the confinement, monitor point 97 is located at the end of engine room and monitor point 100 is outside the engine room in front of the exhaust opening. The maximum overpressure of 1.7 bar occurred 1.5 seconds after the ignition happened in the middle of the engine room. According to Table 5.1, this overpressure is in the range of probable total destruction of the engine room. Figure 5.9 illustrates the maximum overpressure from the beginning of the platform (the location of engine rooms) to the end of the platform (heliboard location).

The release of flammable fuel on the platform caused the formation of the vapour fuel at the plant. The vapour hydrocarbon then dispersed on the main deck due to the wind effect and also the ventilation condition. A part of the fuel entered the engine rooms where the

most likely source of ignition was available. Due to high confinement of the engine room, the vapour fuel accumulated and ignited caused an intensive explosion with an overpressure of 1.7 (bar) (Figure 5.8). The explosion overpressure ranges between few mbar to several bar for deflagration and 15 to 20 bar for detonation [Assael and Kakosimos, 2010; Bjerketvedt, 1997]. The severity of the overpressure (at most 1.7 bar in this study) demonstrates the occurrence of deflagration. Moreover, the current version of FLACS is not capable of simulating detonation. Then, the flame front reached the vapour hydrocarbon on the main deck of the platform causing another explosion. Starting from aft to forward of the platform, the trends of overpressure are shown in Figure 5.9. The overpressure is low on the aft side due to low congestion in this area. Then, it increased gradually to 0.1 (bar) around the drill floor. The increased overpressure at this location is due to the higher congested area because of buildings on the drill floor. Moreover, all sources of release were around the drill floor, making this the most vulnerable place for the higher concentration of fuel, which affected the overpressure. The explosion overpressure reached 0.3 (bar) when it passed drill floor in an area where the congestion was high due to the existence of some storage vessels and instruments. Then, the overpressure dropped to 0.1 (bar) at the forward side because of the lower congestion and lower concentration of flammable vapour.

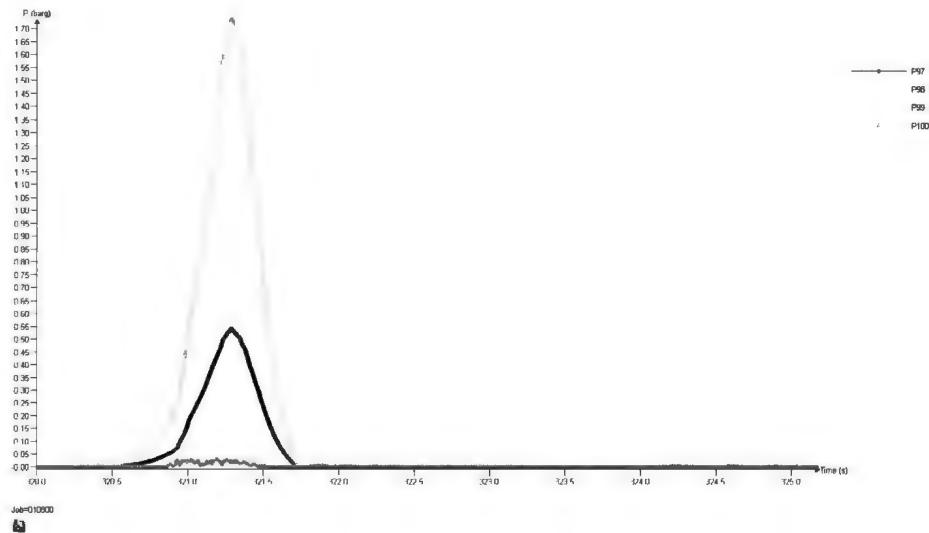


**Figure 5.8. Overpressure due to explosion in engine room 6**

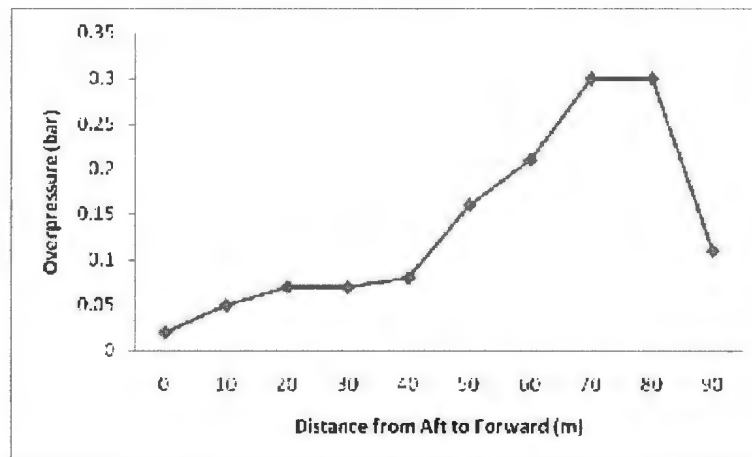


**Figure 5.9. Overpressure vs. Distance from the Aft side to the Forward side of the platform**

According to Figures 5.8 and 5.9, there is a significant difference between the explosion overpressure monitored in the engine room (1.7 bar) and over the platform (0.3 bar). The higher overpressure in the engine room is due to high confinement where the

concentration of the trapped flammable vapour is high and the reflection from the sidewalls also affects the resulting overpressure. On the other hand, the low overpressure over the platform is because of the open area where the confinement/congestion is low and the vapour cloud that dispersed due to natural ventilation (Figure 5.10). Unlike the dispersion model discussion, there is no data or modelling to compare these results to; however, the focus of this study was to demonstrate the utility of integrating the dispersion modelling with the explosion modelling. While the prediction of peak concentrations locations and times through dispersion modelling is important, the potential explosion and overpressure impacts are critical to the efficient and safe design of platforms.

While the focus of this study was on consequence modeling of the explosion accident which occurred in BP Deepwater Horizon, the application of CFD codes to prevent such types of disasters or reducing the harmful effects is in progress. One important parameter affecting the explosion consequence is ventilation condition. Investigating different wind and ventilation conditions to reduce the accumulation of flammable vapour is suggested by Moros et al. [Moros et al., 1996]. The effectiveness of congestion/confinement on explosion overpressure and the use of blast walls or pressure relief panels to reduce the impacts of the accident were also investigated in some associated studies [Bakke and Wingerden, 1992; Middha and Wingerden, 2010]. CFD codes could be used to analyze the ventilation rate, configuration of congestion/confinement and the use of blast walls or

pressure relief panels. This study confirms that CFD codes are helpful tools to test and design safety measures for offshore petroleum facilities.

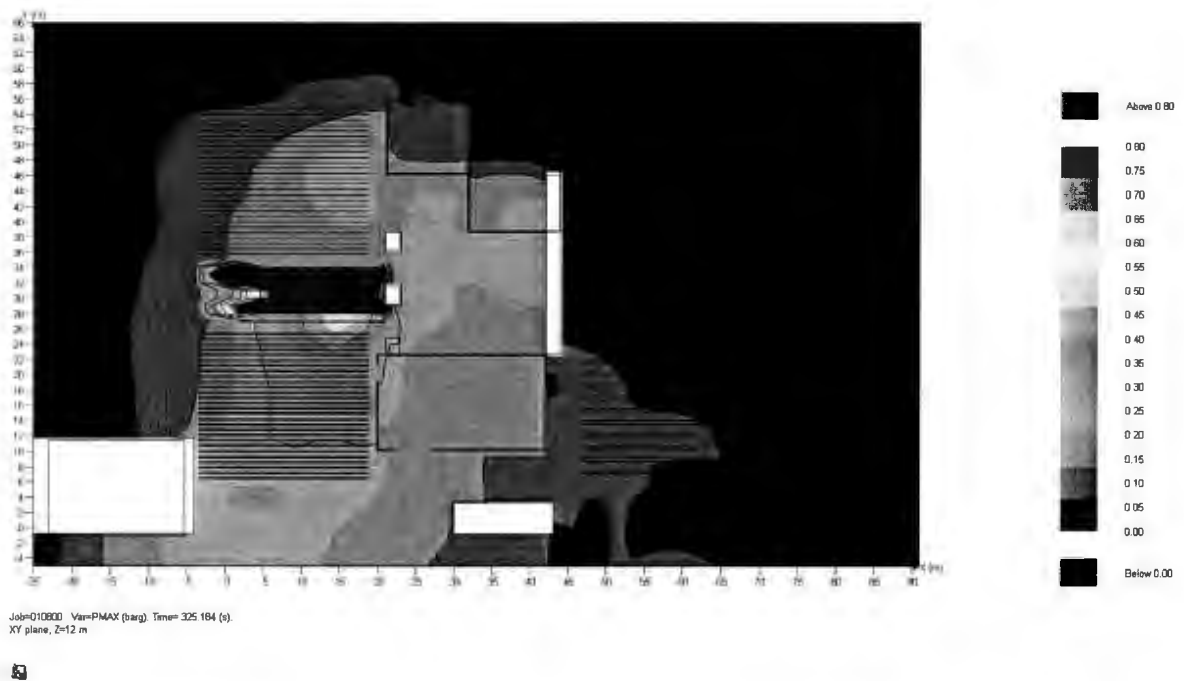


Figure 5.10. Maximum overpressure contour plot at the surface of the platform

#### 5.4 Conclusion

The BP Deepwater Horizon accident occurred in April 2010 through the release and ignition of flammable hydrocarbons, and resulted in the loss of 11 lives. Using the FLACS CFD code, a BP investigation team analyzed the dispersion of the flammable hydrocarbons released to the platform [BP, 2010]. However, the consequences of the explosion were not studied by BP and in this study the dispersion of the flammable gas was integrated with the explosion consequence. The results from the dispersion simulation showed the same trend as the analysis from the BP study [BP, 2010]. The

explosion modelling, which is the contribution of the current study, predicted a high overpressure of 1.7 (bar) in the engine room and around 0.8 bar on the platform. The effect of confinement/congestion on the explosion overpressure was also studied, where lower overpressure was observed in the low congested/confined area and higher overpressure in the highly congested/confined area. The overpressure on the platform was determined to be 0.07 bar, 0.21 bar, and 0.3 bar in low congestion areas, highly confined areas, and high congestion areas respectively. These overpressures are destructive as explained in Table 5.1. As the dispersion characteristics of the flammable vapour are important factors influencing the low and high limits of flammable concentration, considering this issue is a key point in the current study, while in other related studies with FLACS [Berg et al., 2000; Moros et al., 1996; Qiao and Zhang, 2010; Wingerden and Salvesen, 1995], the explosion phenomena were simulated only with the uniform stoichiometric volume of the dispersed gas. By integrating these two phenomena (vapour cloud dispersion and explosion) in the current study, the model was able to track the gas concentration and also determine the resulting risk of different areas. The application of the CFD code in order to prevent such accidents in offshore operations is another important aspect of such studies. Thus, focusing on parameters such as the congestion/confinement configuration and also ventilation conditions are of interest in such studies. While the current study focused on modeling the consequence of the BP Deepwater Horizon explosion, it is recommended to use the CFD code to analyze the parameters such as ventilation rate, configuration of confinement/congestion and the use of blast walls or pressure relief panels. The effectiveness of such parameters to prevent

accidents or reduce the harmful effects caused after accidents has been reported by associated studies [Moros et al., 1996; Bakke and Wingerden, 1992; Middha and Wingerden, 2010]. Smoke and heat radiation caused by the consequent fire also affect human health and offshore structures which are matter of concerns. This study confirms that the CFD code could be used as a tool to test and design safety measures.

### **Acknowledgement**

The financial support provided by Natural Sciences and Engineering Research Council of Canada (NSERC) is highly appreciated by the authors. Author, Mohammad Dadashzadeh thankfully acknowledges Mr. Vitor Eugênio Toledo Junior from Dalhousie University for his valuable technical support.

### **5.5 References**

Arntzen, B. J. (1998). Modeling of turbulence and combustion for simulation of gas explosions in complex geometries. *Dr. Ing, Thesis, NTNU*. Trondheim, Norway.

Assael, M. J., & Kakosimos, K. E. (2010). *Fires, Explosion, and Toxic Gas dispersion: Effects calculations and risk analysis*. Boca Raton: CRC Press/Taylor and Francis.

Bakke, J R; Wingerden, K V; Christian Michelsen Inst. (1992). Guidance for designing offshore modules evolving from gas explosion research. *67th annual technical conference and exhibition of the society of petroleum engineers*. Washington.

Barusco, P. (2002). The accident of P-36 FPS. *Offshore technology conference*. Houston.

Berg, J. T., Bakke, J. R., Fearnly, P., & Brewerton, R. B. (2000). CFD layout sensitivity study to identify optimum design of a FPSO. *Offshore technology conference*. Houston, Texas.

Betha, R. M. (1996). *Explosion and fire at Pasadena, Texas*. New York: Amsterdam Institute of Chemical Engineers.

Bjerketvedt, D., Bakke, J. R., & Wingerden, K. (1997). Gas explosion handbook. *Journal of hazardous materials*, 52, 1-150.

Bray, K. N. (n.d.). Studies of the turbulent burning velocity. *Proceedings of the Royal Society of London, Series A*, 431, (pp. 315-335).

British Petroleum (BP). (2010). Deepwater Horizon Accident Investigation Report. Retrieved from [http://www.bp.com/liveassets/bp\\_internet/globalbp/globalbp\\_uk\\_english/gom\\_response/STAGING/local\\_assets/downloads\\_pdfs/Deepwater\\_Horizon\\_Accident\\_Investigation\\_Report.pdf](http://www.bp.com/liveassets/bp_internet/globalbp/globalbp_uk_english/gom_response/STAGING/local_assets/downloads_pdfs/Deepwater_Horizon_Accident_Investigation_Report.pdf)

Broadribb, M. P. (2006). Lessons from Texas city: A case history. *Center for Chemical Process Safety 21st annual international conference*. Orlando.

Center for Chemical Process Safety (CCPS). (2005). *Building process safety culture: tools to enhance process safety performance*. New York: Center for chemical process safety of the American Institute of Chemical Engineers.

Crowl, D. A., & Louvar, J. F. (2001). *Chemical process safety: fundamentals with applications*. New Jersey: Prentice Hall PTR.

Davis, S. G., Hinze, P., Hansen, O. R., & Van Wingerden, K. (2010). Investigation techniques used to determine the massive vapour cloud explosion at the Buncefield fuel Depot. *ISFI meeting*. Hyattsville.

GEXCON. (2010). FLACS v9.1 user's manual. Retrieved from [www.bp.com/sectiongenericarticle.do?categoryId=9034902&contentId=7064891](http://www.bp.com/sectiongenericarticle.do?categoryId=9034902&contentId=7064891)

Hanna, S. R., Hansen, O. R., & Dharmavaram, S. (2004). FLACS CFD air quality model performance evaluation with Kit Fox, Must, Prairie Grass, and EMU observations. *Atmospheric environment*, 38, 4675-4687.

Health and Safety Executive (HSE). (2010). Review of FLACS version 9.0 dispersion modeling capabilities. Retrieved from [www.hse.gov.uk/research/rrpdf/rr779.pdf](http://www.hse.gov.uk/research/rrpdf/rr779.pdf)

Høiset, S., Hjertager, B. H., Solberg, T., & Malo, K. A. (2000). Flixborough revisited- an explosion simulation approach. *Journal of hazardous materials*, 77, 1-9.

Huser, A., Foyn, T., & Skottene, M. (2009). A CFD based approach to the correlation of maximum overpressure to process plant parameters. *Journal of Loss Prevention in the Process Industries*, 22, 324-331.

Kalantarnia, M., Khan, F., & Hawboldt, K. (2010). Modeling of BP Texas City refinery accident using dynamic risk assessment approach. *Process Safety and Environmental Protection*, 88, 191-199.

Khan, F. I., & Abbasi, S. A. (1999). The world's worst industrial accident of the 1990s; what happened and what might have been: A quantitative study. *Process Safety Progress*, 18, 135-145.

Khan, F. I., & Amyotte, P. R. (2007). Modeling of BP Texas City refinery incident. *Journal of Loss Prevention in the Process Industries*, 20, 387-395.

Lauder, B. E., & Spalding, D. P. (1974). The numerical computation of turbulent flows. *Computer Methods in Applied Mechanics and Engineering*, 3, 269-289.

Mannan, S. (2005). *Lees' Loss Prevention in the Process Industries* (3rd ed., Vols. 1-3). Burlington: Elsevier Butterworth-Heinemann. Retrieved from [http://knovel.com/web/portal/browse/display?\\_EXT\\_KNOVEL\\_DISPLAY\\_bookid=1470&VerticalID=0](http://knovel.com/web/portal/browse/display?_EXT_KNOVEL_DISPLAY_bookid=1470&VerticalID=0)

Middha, J. R., & Wingerden, K. V. (2010). A study on the effects of threes on gas explosions. *2nd international conference on reliability*. Mumbai.

Middha, P., Hansen, O. R., Grune, J., & Kotchourko, L. (2010). CFD calculations of gas leak dispersion and subsequent gas explosions: validation against ignited impinging hydrogen jet experiments. *Journal of Hazardous Materials*, 179, 84-89.

Moros, A., Tam, V., Webb, S., Paterson, K., & Coulter, C. (1996). The effect of ventilation and gas cloud size on explosion overpressure. *International conference on health, safety and environment*. New Orleans.

OSHA. (1990). *Philips 66 Company Houston chemical complex explosion and fire: A report to the president*. Washington, DC: U.S. Dept. Of Labor.

Pate-Conell, M. E. (1993). Learning from the Piper Alpha accident: a post-mortem analysis of technical and organizational factors. *Journal of Risk Analysis*, 13, 215-232.

Prugh, R. W. (n.d.). Evaluation of unconfined vapour cloud explosions. *Proceedings of the International Conference on Vapour Cloud Modeling*. Boston.

Qiao, A., & Zhang, S. (2010). Advanced CFD modeling on vapour dispersion and vapour cloud explosion. *Journal of Loss Prevention in the Process Industries*, 23, 843-848.

Sadee, C., Samuels, D. E., & O'Brien, T. P. (1977). The characteristics of the explosion of cyclohexane at the Nypro (UK) Flixborough plant on 1st June 1974. *Journal of occupational accidents*, 1, 203-235.

U. S. Chemical Safety Board (CSB). (2007). *BP Texas city refinery explosion and fire*. final investigation report. Retrieved from [http://www.csb.gov/investigations/detail.aspx?SID=20&Type=2&pg=1&F\\_AccidentTypeId=12](http://www.csb.gov/investigations/detail.aspx?SID=20&Type=2&pg=1&F_AccidentTypeId=12)

U. S. Environmental Protection Agency (USEPA). (2001). Giant oil rig sinks. *The Journal of the U.S. EPA Oil Program Center*, 5, 1-3.

Venart, J. E. (2007). Flixborough: A final footnote. *Journal of loss prevention in the process industries*, 20, 621-634.

Wingerden, K. V., & Salvesen, H. C. (1995). Simulation of an accidental vapour cloud explosion. *Process safety progress*, 14, 173-181.

## 6 An Integrated Approach for Fire and Explosion Consequence

### Modelling

Mohammad Dadashzadeh<sup>1</sup>, Faisal Khan<sup>1</sup>, Kelly Hawboldt<sup>1</sup>, Paul Amyotte<sup>2</sup>

1. Process Engineering, Faculty of Engineering and Applied Science, Memorial University, St. John's, NL, Canada, A1B 3X5

2. Department of Process Engineering and Applied Science, Dalhousie University, Halifax, NS, Canada, B3J 2X4

#### Abstract

Fire and explosion are accidents which potentially can occur in oil and gas processing facilities. While fire and explosion could occur as a consequence of each other, most published work has assessed fire and explosion separately, ignoring interactions between the two phenomena.

The current study proposes a novel approach to model the entire sequences involved in a potential accident using liquid and gas release incidents as two test cases. The integrated scenario is modeled using Computational Fluid Dynamics (CFD) codes FLACS and FDS. An integrated approach is adopted to analyze and represent the effects (injuries/death) of the accident. The proposed approach can be used in designing safety measures to minimize the adverse impacts of such accidents. It can also serve as an important tool to develop safety training to improve emergency preparedness plans.

\* Dadashzadeh, M., Khan, F., Hawboldt, K., Amyotte, P. (2013). An Integrated Approach for Fire and Explosion Consequence Modeling. Fire Safety Journal (under review).

**Keywords: Liquid release, Gas release, Vapour cloud explosion, Pool fire, Accident modelling, CFD, Integrated scenario**

## **6.1 Introduction**

Several studies have modeled the consequences involved in the release of hydrocarbons. These studies range from advanced CFD modelling to comparison of different tools in accident modelling [Hansen et al., 2009; Koo et al., 2009; Gavelli et al., 2010; Kim and Salvesen, 2002; Skarsbo, 2011].

In a study conducted by Hansen et al. (2009), a FLACS CFD modelling was developed and compared with experimental data for liquefied natural gas (LNG) release and dispersion. As it is a cold dense cloud and is strongly affected by the field characteristics, simulating the dispersion of LNG vapour requires a complex model that considers the influencing factors. Using the FLACS CFD code and comparing the results with experimental data confirmed that FLACS is a suitable model to simulate the dispersion of LNG vapour

Koo et al. (2009) conducted a study to model various accident scenarios at an LNG terminal using the PHAST software. Six different scenarios were constructed based on the LNG release hole sizes. Early and late pool fire effects were evaluated through this study. The study concluded that the accident would have an impact on areas outside the plant boundary, and that the late pool fire is a greater hazard than the early one. However, the focus of this study was only on pool fire modelling, ignoring the other

more credible scenarios, such as Vapour Cloud Explosion (VCE) and potential interactions. The use of CFD models to better simulate such accidents was recommended by Koo et al. (2009).

In a study conducted by Gavelli et al. (2010), the consequences resulting from the ignition of a flammable vapour cloud dispersed after the release of LNG during an offloading process were evaluated. FLACS CFD code was used to simulate the LNG spill, pool spreading and vapourization, vapour cloud dispersion and ignition leading to the vapour cloud explosion. The study demonstrated that the FLACS application was able to predict the consequences of accidents; the sequences of events led to a pool fire after the release of LNG and the possibilities of ignition and explosion.

In a study by Kim and Salvesen (2002), the explosivity of LNG vapour after the release and formation of a liquid pool was modeled using FLACS. The LNG release occurred in a dike and dispersed to the process area where the source of ignition was located. The explosion overpressure was estimated and mitigation processes to decrease the explosion effects were presented. Reducing the thermal conductivity of the subsoil and increasing the height of the dike wall were the mitigation measures proposed to decrease the overpressure as a result of the explosion. While the vapour cloud explosion was addressed, no consideration was given to the pool fire which is a likely scenario occurring after the explosion.

Skarsbo (2011) used CFD models FLACS and FDS to model the pool fire phenomenon. Simulation results were compared to experimental data from different sources. The study

demonstrated that both models over-estimate the flame temperature. This study focused only on the effects of fire, ignoring the entire sequences involved in such accidents and more importantly interactions of fire and explosion.

LNG release consequences were extensively studied by Marry O'Connor Process Safety Center. The effects of parameters such as high expansion foam, dike wall height and floor conductivity on pool fire behaviour were investigated through these studies [Suardin et al., 2009; Yun et al., 2011]. The modelling of LNG vapour dispersion and its validation against medium-scale LNG spill tests were also studied [Qi et al., 2010].

There are also comprehensive studies on the chain of accidents starting from one unit and spreading to different units such as reactors, pipelines, or storage vessels in chemical industries (domino effects) [HSE, 1981; Bagster and Pitblado, 1991; Khan and Abbasi, 1998; Cozzani et al., 2006; Cozzani and Zanelli, 2001; Antonioni et al., 2009; Reniers et al., 2009]. One of the earliest attempts to study the domino effects was the Canvey report, prepared in a proposal of the construction of a new refinery on Canvey Island, UK. Through this study, all interactions between installations in the area were considered to determine risk associated with health and safety [HSE, 1981]. In 1991, data from the Canvey report were used by Bagster and Pitblado to define a procedure of treatment of the domino effect. There was a gap of developing domino effect studies until 1998 when Khan and Abbasi (1998) developed a framework of the domino effect analysis (DEA). In this study, a "DEA" procedure was also coded and its application to several case studies was demonstrated. Subsequently, Cozzani and coworkers worked on domino effect

analysis using new data [Cozzani et al., 2006; Cozzani and Zanelli, 2001; Antonioni et al., 2009]. In the recent study conducted by Reniers et al. [2009], a game-theory approach was developed to investigate the investments of different industries on domino effect prevention.

The above studies consider only individual events such as fire or explosion [Gavelli et al., 2010; Kim and Salvesen, 2002; Skarsbo, 2011]. Combination of the events is more important as one event may lead to another, escalating the overall consequences. In the current study, the authors highlight the importance of integrated accident scenarios and their use in detailed consequence analysis using LNG and methane as hydrocarbons of interest in two test cases. The study is equally applicable to other similar compressed and refrigerated systems involving gases such as liquefied petroleum gas (LPG), natural gas liquids (NGLs) and propane. The major difference between the current study and the domino effect studies is that the current study is focusing on an evolving accident scenario which includes one unit and the occurrence of more than one event. The domino effect focuses on the escalation of events from one unit to other units and may include different hazardous chemicals.

### **6.1.1 Hazards caused due to the release of hydrocarbons**

Release of flammable hydrocarbons to the surrounding environment could cause several types of hazards. If a flammable gas leak occurs, a quick ignition may lead to different types of fire such as a fire ball, jet fire or flash fire. The flammable gas could also be dispersed over the area and form a flammable vapour cloud. Then, a delayed ignition

could cause Vapour Cloud Explosion (VCE) depending on the level of congestion/confinement. On the other hand, a liquid leak of hydrocarbon could lead to a harmful accident. It may form a pool of liquid followed by vapourization due to the surrounding temperature. An immediate ignition may cause a pool fire. Another possible scenario is the dispersion of volatilized flammable vapour over the area causing the formation of a flammable vapour cloud at a distance from the pool leading to VCE due to a delayed ignition [Assael and Kakosimos, 2010].

In a usual accident occurrence, such events do not occur individually. There are interactions among different events causing evolving scenarios. For example, a vapour cloud explosion occurs at a distance from the source of release, the heat load caused by the explosion causes ignition at the release location and a jet fire occurs. Another good example of an evolving scenario is the interaction between the VCE and pool fire due to the release of a liquefied hydrocarbon such as LNG. The release of LNG to land or water could cause a rapidly evaporating pool and subsequent formation of a vapour cloud. An ignition source at any point in the vapour cloud could burn and cause a flash fire. The flash fire does not typically exceed a few tens of seconds; however, if the flash fire burns back to the pool or the ignition starts at the pool, a pool fire occurs. Further, a delayed ignition would provide enough time for the fuel vapour to disperse and form a vapour cloud which if ignited would cause a VCE and resulting overpressure. The heat load after the explosion enhances the vapourization over the liquid pool causing a pool fire [Ramos et al., 2011; Woodward and Pitblado, 2010].

In this study, the interaction between the fire and explosion and the resulting consequences are modeled. This type of model can be used to design effective safety measures to prevent and mitigate consequences and to develop efficient safety training and emergency preparedness.

### **6.1.2 Past major accidents and their analysis**

On October 1944, an LNG tank in Cleveland, Ohio failed and released all its contents to the surrounding area including streets and sewers. The LNG then vapourized and formed a vapour cloud. An unknown source of ignition contacted the vapour cloud and a massive fire and consequent explosion in the residential area followed. The explosion led to the deaths of 131 people [Yang et al., 2011].

Another LNG accident occurred in the Skikda LNG plant, Algeria in 2004. After a release of LNG, the fuel vapour entered an adjacent boiler through an inlet fan. The fuel mixed with air and the resulting increase in the pressure led to an explosion. The heat load from the explosion reached the fuel vapour near the leak area and caused the second explosion [Achour and Hached, 2004].

Other LNG accidents have also been reported by The California Energy Commission [The California Energy Commission, 2012]. In August 1987, at U.S. Department of Energy Test Site, Nevada, an LNG vapour release occurred and the vapour was ignited by an unknown source. In another LNG accident in Indonesia in 1983, the failure of a heat exchanger due to overpressurization in an LNG plant led to an explosion. In New

York in 1973, during the repair of an empty LNG storage tank, a fire accidentally started. The fast pressure increase inside the tank then led to the falling of the concrete dome on the tank and caused the death of 37 people.

In March 2005 at BP's Texas City refinery an explosion resulted in the loss of 15 lives and 180 injuries [CSB, 2007]. In this accident, a flammable liquid hydrocarbon was released to the ground around a knockout drum stack. The flammable liquid was vapourized, forming a vapour cloud at the top of the liquid pool. Atmospheric wind pushed the vapours and droplets downwind, causing them to mix with air. The vapour cloud then reached an ignition source which was most likely an idling pickup truck near the area, causing VCE. The heat load through the VCE reached the accumulated vapour above the liquid pool and caused a pool fire and subsequent explosions [Kalantarnia, 2010; Khan and Amyotte, 2007]. According to Broadribb (2006), the failure to control the release and the failure to respond appropriately resulted in the explosion.

In an accident at the McKee refinery, Texas (2007), the escaped propane from a high-pressure system formed a vapour cloud which caught fire when exposed to an ignition source. The released liquid from a cracked elbow rapidly formed a flammable vapour cloud due to the weather conditions. The flammable vapour spread to a boiler house due to the wind direction and an explosion occurred. Consequently, the resulting flames reached the leak source and intensified the fuel vapourization and the flame propagation in the area. Due to the size and the intensity of the fire, the access to the manual shut-off

valves and pump on-off switches were blocked, and this led to a continuous discharge of propane and a jet fire [CSB, 2008].

A review of past accidents and models [Yang et al., 2011; Achour and Hached, 2004; The California Energy Commission, 2012; CSB, 2007; CSB, 2008] demonstrates the need to evaluate the entire accident sequence to mitigate the impact, develop appropriate response methods, and prevent accidents by designing safety into the system.

## 6.2 Proposed methodology

The methodology is outlined in Figure 6.1. The **first step** in the model is the release of hydrocarbon and subsequent pool formation (of liquid fuel). Then, the evaporation (of liquid fuel) and dispersion of hydrocarbon as per the ambient conditions are simulated, followed by the delayed ignition and explosion of the dispersed vapour. FLACS is used to model these steps. FLACS is a 3-dimensional CFD simulation tool. On a structured, fixed, rectangular grid, FLACS uses a backward Euler time integration scheme. The pressure-velocity coupling is solved by the SIMPLE algorithm of Patankar while the linear equations are solved by efficient solvers. The evaporation is modeled using the heat transfer from the substrate, wind speed, turbulence and vapour pressure above the pool. For the LNG source model, the 2D shallow water equations are used [Hansen et al., 2009].

In the **second step**, the energy released from the explosion is used as a source to evaporate and ignite the rest of fuel. Temperatures and other useful parameters are extracted from the first step in fire simulation which is modeled with Fire Dynamic

Simulator (FDS). Developed by the National Institute of Standards and Technology (NIST) of the United States Department of Commerce, FDS uses partial differential equations to describe the transportation of mass, momentum and energy for the fire and its impact in the surrounding area [NIST, 2010]. Using the Large-Eddy Simulation (LES) method, FDS solves the conservation equations and updates the solutions based on time on a three-dimensional grid. The finite volume technique is used to estimate the thermal radiation [Gavelli et al., 2010].

In the **third step**, the probit model ( $Pr = c_1 + c_2 \ln D$ ) is used to calculate probabilities of effects for the heat and overpressure load [16].

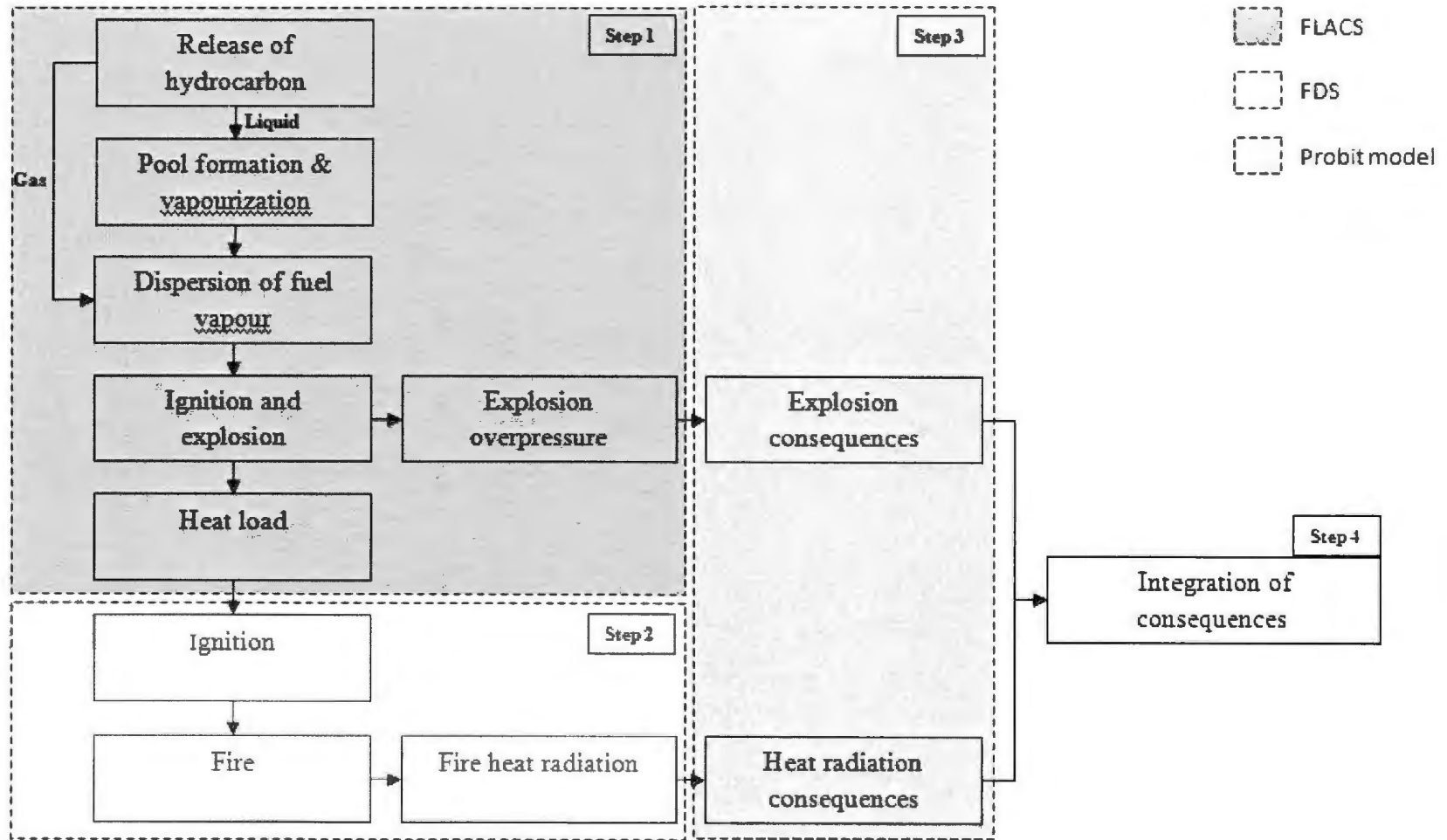


Figure 6.1. Applied methodology to model the sequences of an evolving accident scenario and the integrated effect

The **fourth step** integrates the effects through a grid-based approach. To simplify the consequence assessment process, consequence severity is mapped as an index. This index illustrates the severity of consequences at any location in the accident area.

**Table 6.1. Major human effects caused by fire and explosion [Assail and Kakosimos, 2010]**

Accident type	Effect type	Damage
Fire	Probability of injury from 1 <sup>st</sup> degree burn	<ul style="list-style-type: none"> <li>1<sup>st</sup> degree burns affect only the epidermis or outer layer of skin. The burn site is red, painful, dry, and with no blisters. Mild sunburn is an example. Long-term tissue damage is rare and usually consists of an alteration of the skin colour.</li> </ul>
	Probability of injury from 2 <sup>nd</sup> degree burn	<ul style="list-style-type: none"> <li>2<sup>nd</sup> degree burns involve the epidermis and part of the dermis layer of skin (0.7 – 0.12 mm depth). The burn site appears red, blistered, and may be swollen and painful.</li> </ul>
	Probability of death	
Explosion	Probability of injury from eardrum rupture	<ul style="list-style-type: none"> <li>Eardrum rupture is a direct effect of overpressure difference during an explosion.</li> </ul>
	Probability of death from lung damage	<ul style="list-style-type: none"> <li>The explosion can cause a sudden pressure difference between the inside and outside of the lungs, as the pressure to which the human body is subjected suddenly increases. As a consequence, the thorax is pressed inwards, causing lung damage and possible death. Since the inward pressure process is associated with a finite time, in addition to the value of the overpressure, its duration is also important.</li> </ul>
	Probability of death from head impact	<ul style="list-style-type: none"> <li>The shock wave can push the head of a person backwards, resulting in skull rupture or fracture, or even the collision of the head with another stationary or non-stationary object.</li> </ul>
	Probability of death from whole body displacement	<ul style="list-style-type: none"> <li>The shock wave can throw the whole body backwards, causing death because of its impact with other objects.</li> </ul>

Based on damages caused by different effects (Table 6.1) and experts' judgment, they are ranked on a scale of 1 to 10 as given in Table 6.2.

**Table 6.2. Scores (S) for seven major human effects caused by fire and explosion**

Hazard	Fire			Explosion						
Effects	1st degree	2nd degree	death	lung damage (death)	eardrum rupture (injury)	head impact (death)	whole body displacement (death)			
Score (S)	2	5	10	8	5	10	10	10		

The severity index for each type of effects at any location at the plant is calculated as follows:

$$Risk_i = S_i \times P_i \quad 6.1$$

where,  $Risk_i$  denotes the risk index for each type of effect. In the next stage, the maximum  $Risk_i$  for the fire and explosion are estimated ( $Risk_f$  and  $Risk_e$ ).

$$Risk_t = \sum Risk_f + Risk_e \quad 6.2$$

Therefore, any location at the plant has a  $Risk_t$  enabling the creation of contour-based risk considering cumulative effects.

## **6.3 Case studies**

### **6.3.1 Case study 1: LNG vapour cloud explosion and the consequent pool fire**

#### **6.3.1.1 Scenario definition**

In this scenario 200 kg/s of natural gas is released at a LNG processing plant. The release duration is 100 s and the wind speed was 3 m/s with an ambient temperature of 25 °C. A pool of LNG is formed at the release location and vapourization occurred due to ambient conditions. The vapourized LNG is then dispersed by the wind and fuel vapour cloud formed at the process area. At 60 s, a delayed ignition occurs in the process area which leads to a destructive VCE in the process. The energy released due to the explosion enhances the LNG vapourization over the LNG pool and causes a pool fire at the release location. The required parameters are defined according to Middha and Melheim [Middha and Melheim, 2010].

#### **6.3.1.2 Application of the methodology**

##### **6.3.1.2.1 Step 1: Release, pool formation and spreading, vapourization and dispersion of LNG vapour**

The geometry considered in this study is shown in Figure 6.2. The simulation volume is considered as 80 m × 40 m × 20 m with the grid resolution of 2 m for x and y directions and 1 m for z direction. Sensitivity analysis was used to select the grid resolution to make the solutions independent of the mesh sizes [Ichard et al., 2010]. Around the leak location, the grid resolution was adjusted to 0.5 m while at the locations far from the pool

area, grids were stretched. The finer grid around the leak takes into account the need for more information in the areas of the greatest impact, while the coarser grid is used in areas where the impact is much less in severity. Having denser meshes around the leak area was also previously advised by Gjesdal (2000) and Hanna et al. (2004). The total number of grids during the dispersion simulation was 31000 control volumes.

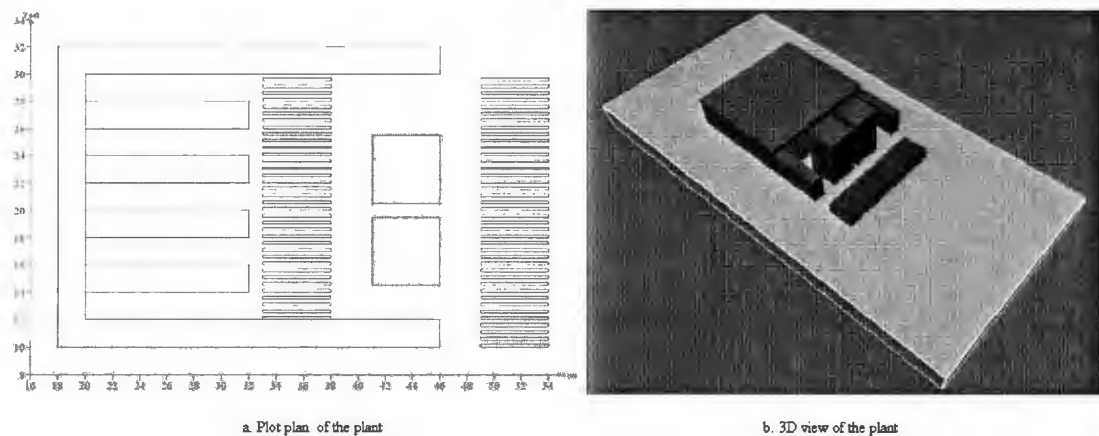


**Figure 6.2. The considered geometry**

Following the release, it required 100 s for enough vapour to be formed (ambient temperature = 25 °C; ground roughness = 0.01; Pasquill class = D; gas composition = 95% methane, 3% ethane and 2% propane). Pool characteristics and the fuel concentration were monitored during the dispersion simulation and are plotted in Figure 6.3.

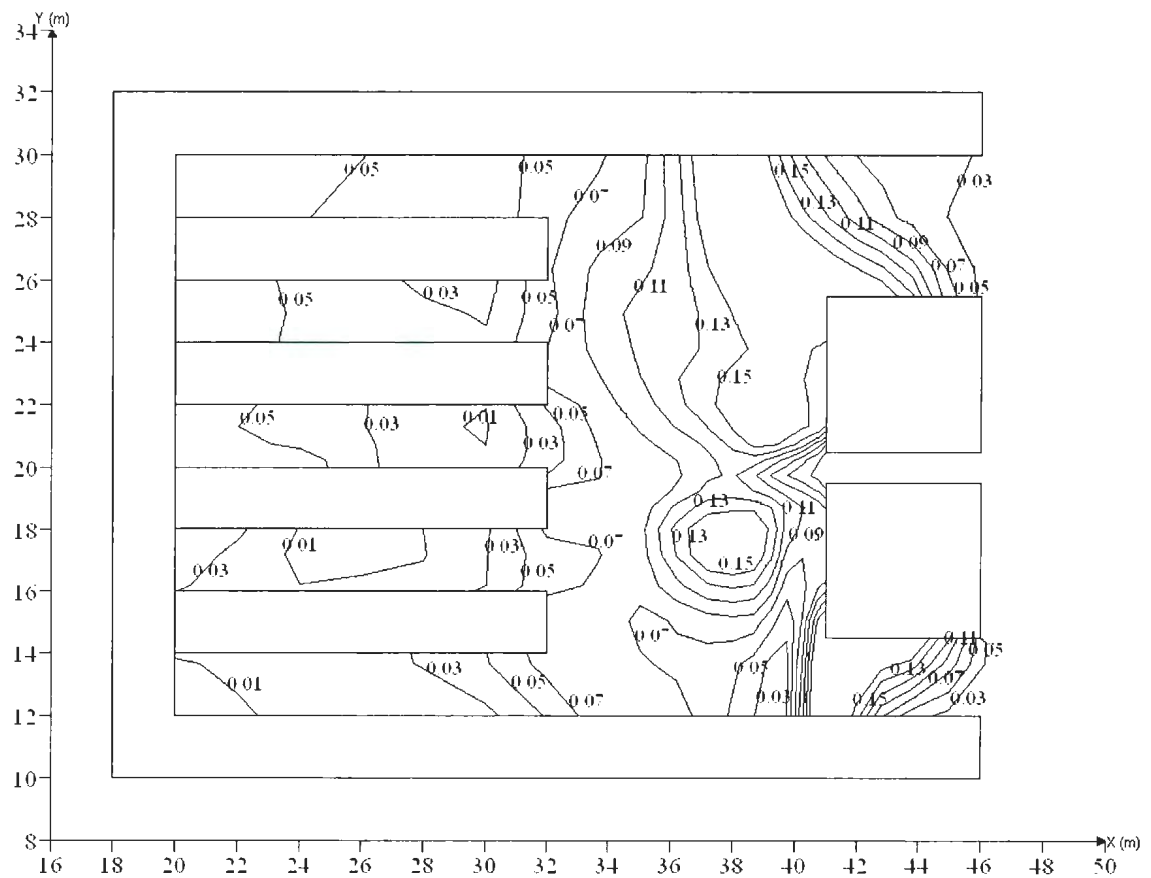


Figure 6.3. Dispersion of vapourized fuel over the plant (-)

#### 6.3.1.2.2 Step1-continued: Modeling the explosion of LNG vapour

Figure 6.3 demonstrates the mass fraction of fuel in the mixture of fuel, air, and combustion products over the plant. The engine room under the shelter is a potential ignition source. Thus, the ignition location is defined under the shelter. Based on the dispersion results (Figure 6.3), the time of ignition is selected at 50 s when the maximum amount of fuel vapour is monitored. The geometry is adjusted to simulate the explosion.

The simulation volume is 70 m × 40 m × 20 m with the grid dimension of 1 m in all directions.

### 6.3.1.2.3 Step 2: Modeling the pool fire

The output data including the temperature change due to the explosion and the pool diameter and depth (Figure 6.4) were extracted from FLACS and used as input parameters for pool fire modelling in FDS. The LNG pool depth ranges from 2 mm on the outer boundary of the liquid pool to 6 mm at the release location. The same geometry in Figure 6.2 was also created in FDS with grid dimension of 1 m in all directions. A hot surface was defined over the pool to model the enhanced vapourization due to the heat load after the explosion. The average temperature of the hot surface is extracted from FLACS explosion output.

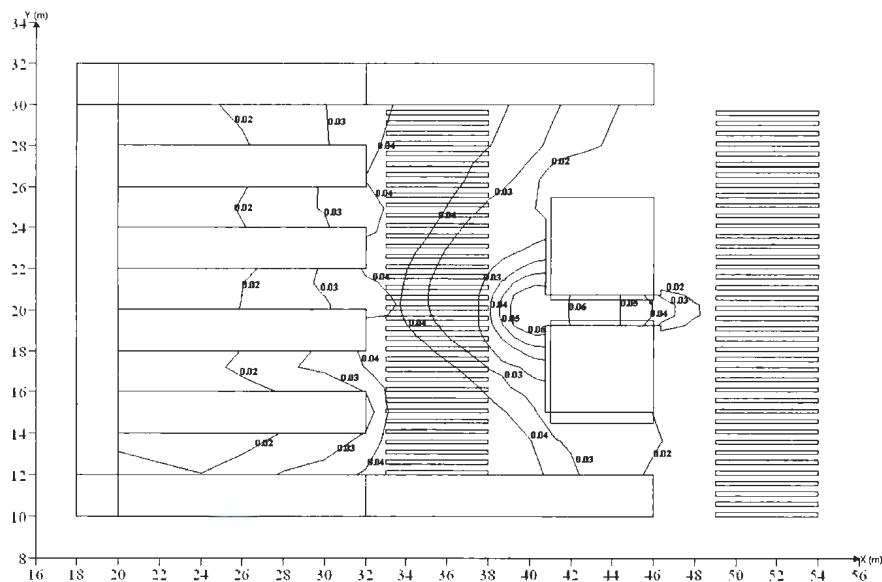


Figure 6.4. LNG pool diameter and depth after the explosion (m)

### **6.3.2 Case study 2: BP Deepwater Horizon vapour cloud explosion and the consequent fire**

#### **6.3.2.1 Scenario definition**

In 2010, the BP Deepwater Horizon blowout resulted in the release of flammable vapour over the platform causing the explosion and fire which led to 11 lost lives. According to the BP investigation report, the most important release locations were defined as the riser bore at the drill floor, the mud gas separator vent at the top of the rig, the mud gas separator (MGS) rupture disk/diverter outlet, the slip joint below the moon pool and the mud processing system (tanks and mud pit room exhaust vent) [BP, 2010]. The flammable vapour dispersed over the plant due to the wind. Through ventilation inlets, the flammable gas found its way to engine rooms where the most likely sources of ignition are located. The flame propagation resulting from the consequent explosion reached the flammable vapour dispersed over the platform and led to the fire at the source of release around the drilling floor.

#### **6.3.2.2 Application of the methodology**

##### **6.3.2.2.1 Step 1: Release, dispersion and explosion of flammable vapour**

The geometry considered in this study is shown in Figure 6.5. The simulation volume was assumed to be 116 m×71 m×104 m and the grid size was set as 1 (m). Sensitivity analysis was used to eliminate the dependency of the results on the mesh size. Grids were refined around the leak areas and some ventilation points. The time of simulation was

assumed to be 570 s, while the first 60 s were the start up period where only the ventilation points were in operation. The release of flammable gas started after 60 s. The total number of grids during the dispersion simulation was 31000 control volumes.

In order to control the time steps, Courant-Friedrich-Levy (CFLC and CFLV) numbers of 5 and 0.5 were selected, respectively. CFLC and CFLV are based on the sound velocity and the fluid flow velocity, respectively. The CFLC and CFLV control the sound waves and the fluid flow propagation distance in each time step, which is the average control volume length multiplied by the value of CFLC and CFLV. As an example, by defining a CFLC value of 5 and a CFLV value of 0.5, the pressure will propagate 5 cells while the fluid flow propagates 0.5 cells in each time step [GEXCON, 2010]. The CFLC and CFLV numbers determined were optimized to guarantee convergence. Figure 6.5 outlines the geometry based on the data available in BP's investigation report for this modelling scenario.

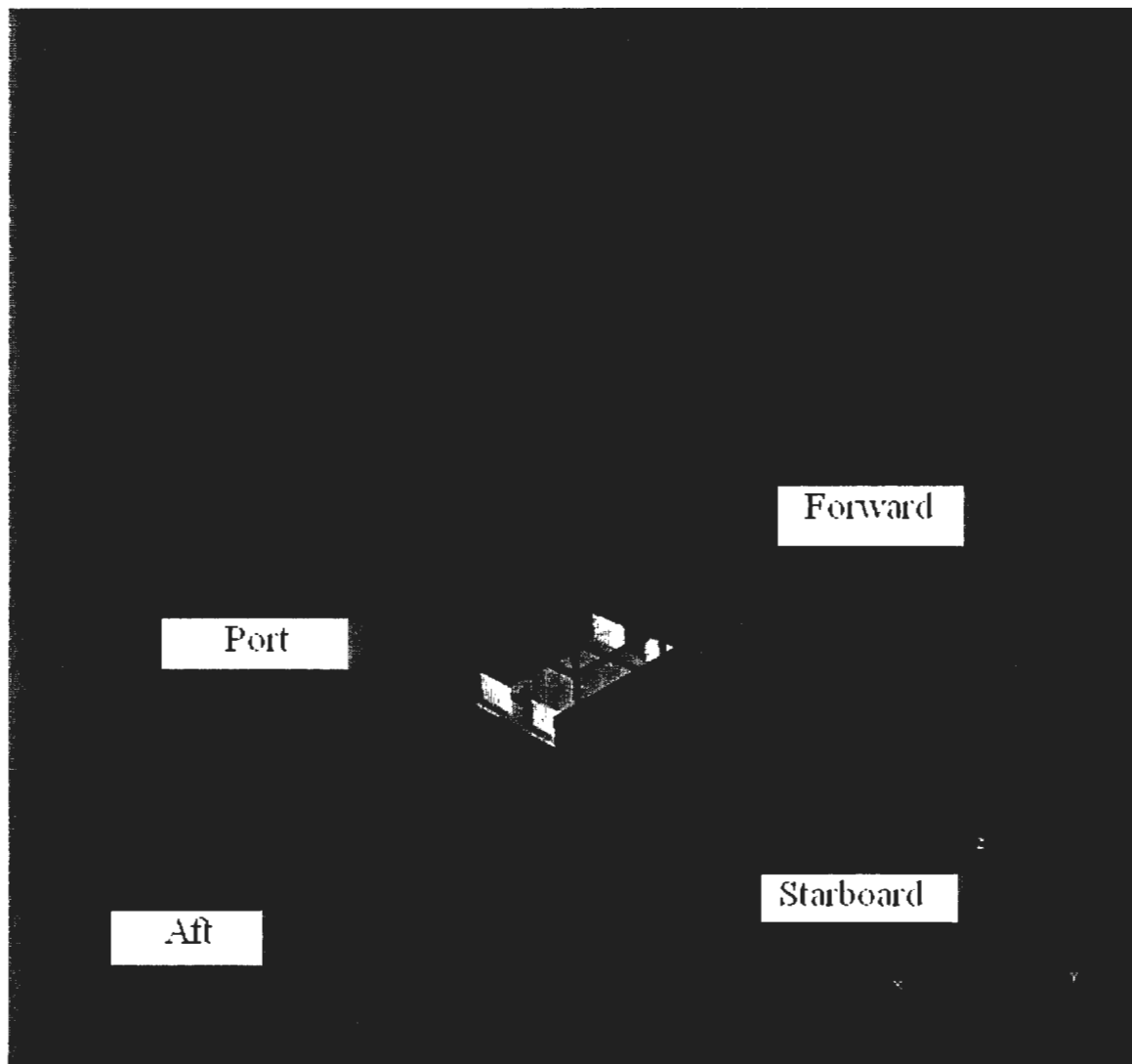


**Figure 6.5. BP Deepwater Horizon geometry used for dispersion/explosion simulation**

After the dispersion simulation, geometry details were changed in order to initiate the explosion simulation of the flammable vapour cloud which was the focus of this study. The fuel cloud formed through the dispersion simulation should be in the flammable limit. The gas composition [BP, 2010] had a Lower Flammable Limit (LFL) of 0.02 and an Upper Flammable Limit of 0.12. The flammable cloud within this limit was used in

explosion simulation. The maximum gas concentration was observed after 320 s and this was set as the time of ignition. The ignition location was set in engine room 6 where the highest concentration of flammable gas was observed. After 320 s, the simulation was re-started to observe the overpressure caused by the ignition. Figure 6.6 illustrates the location of engine rooms.

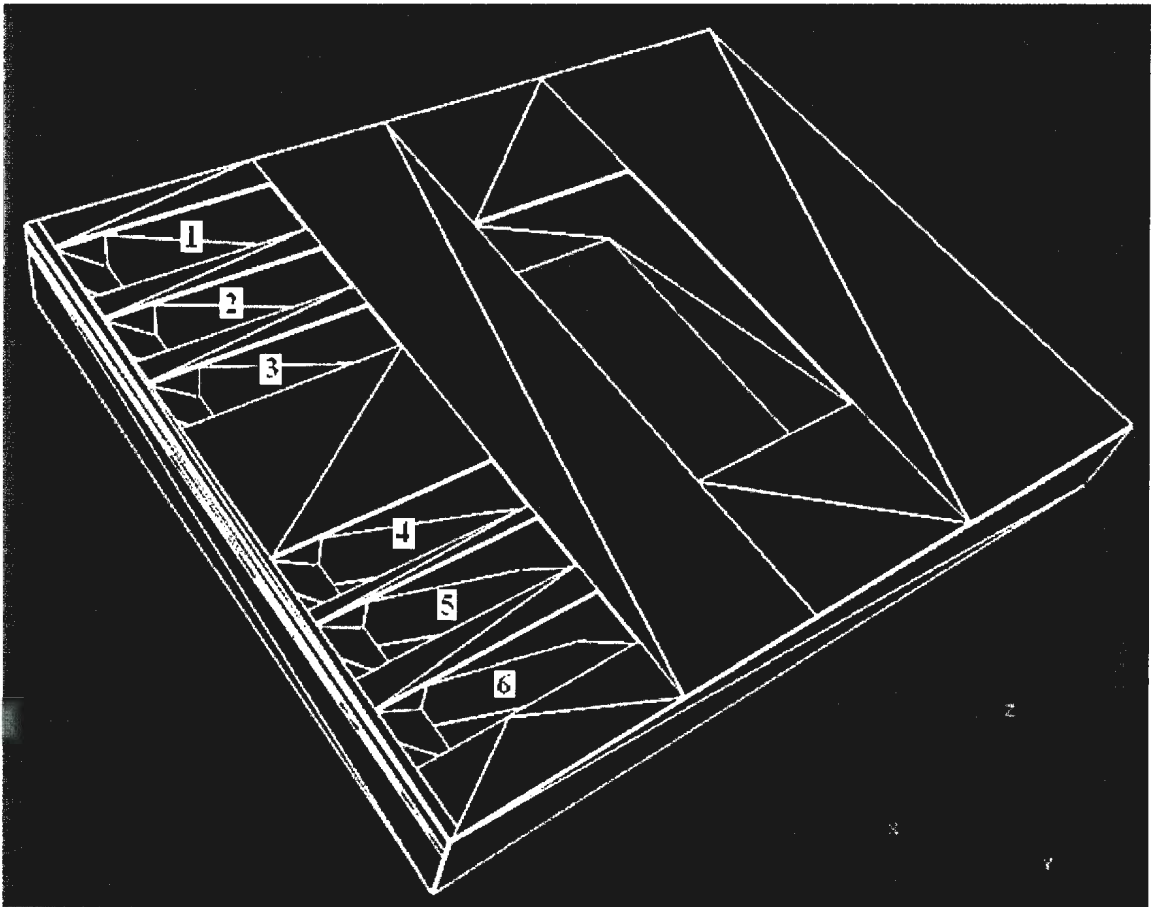


**Figure 6.6. Second deck, configuration of engine rooms #1 to #6**

Highly congested areas result in turbulence generation. Consequently, the combustion rate is enhanced leading to higher overpressure. The congestion parameter is an

important factor in complex geometries and is calculated by dividing the total length (m) of all items on the main deck (cylinders and boxes) by the total volume ( $\text{m}^3$ ) of the area of interest. Extracting the total length of cylinders and boxes on the main deck, the congestion parameter of the BP Deepwater Horizon oil rig was estimated to be 0.48 ( $\text{m}/\text{m}^3$ ) which is categorized as a low congested level [Huser et al., 2009].

#### **6.3.2.2.2 Step 2: Modelling the jet fire**

For the jet fire modelling, the release rate of flammable vapour on the drilling floor was selected as the jet release rate. Extracting the geometry data from FLACS, FDS code was used to model the consequent jet fire. The time of simulation was selected as 5 s with a mesh size of 0.5 m in all directions.

### **6.4 Results and discussions**

#### **6.4.1 Case study 1: Explosion**

The overpressure that resulted from the explosion was not significant over the plant; 0 bar at open areas and 0.5 bar at the edges of the shelter in an enclosed area (Figure 6.7). The existence of the complex confined geometry leads to high explosion overpressure. Thus, the low overpressure due to the low level of confinement/congestion in the current study is consistent with past studies and experimental observations [Huser et al., 2009]. However, low values of explosion overpressure do not have an impact on this study as the integration of consequences is of concern and not only the individual event.

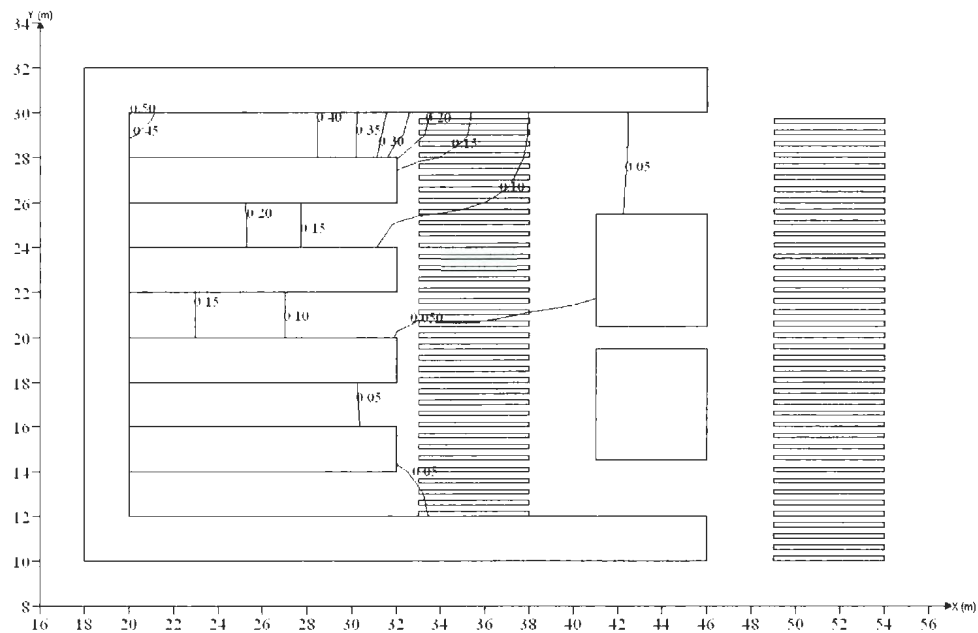


**Figure 6.7. Explosion overpressure over the plant (bar)**

Using the probit model (Step 3), the probabilities of injuries/death caused by the explosion overpressure were calculated. Then, as step 4 of the approach, the explosion risk index ( $Risk_e$ ) was estimated and plotted for the plant (Figure 6.8). While higher values of  $Risk_e$  (0.5) are located under the shelter, lower values are seen in open areas (0.1). The low values of  $Risk_e$  over the plant are in accordance with low overpressure over the plant due to the low level of congestion/confinement in the current study [Huser et al., 2009; Hansen et al., 2010].

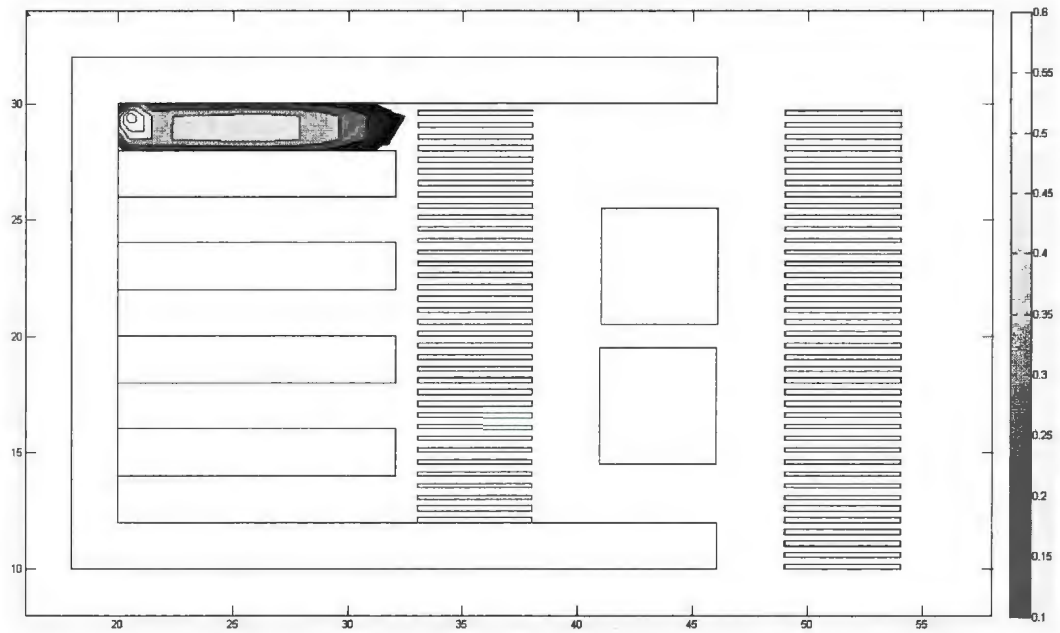


Figure 6.8. Explosion risk profile (-)

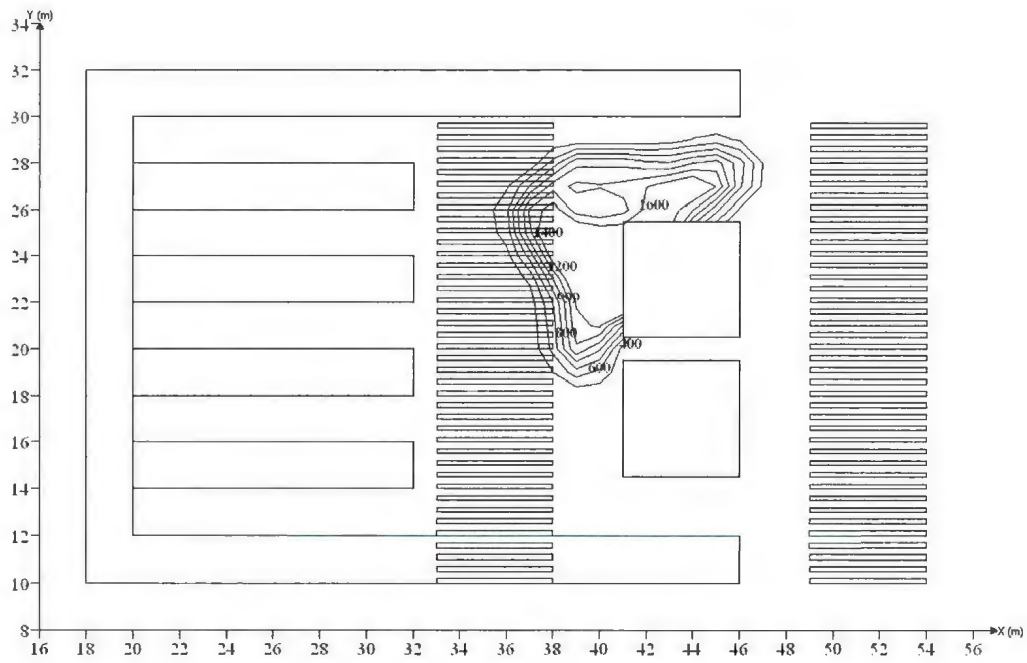
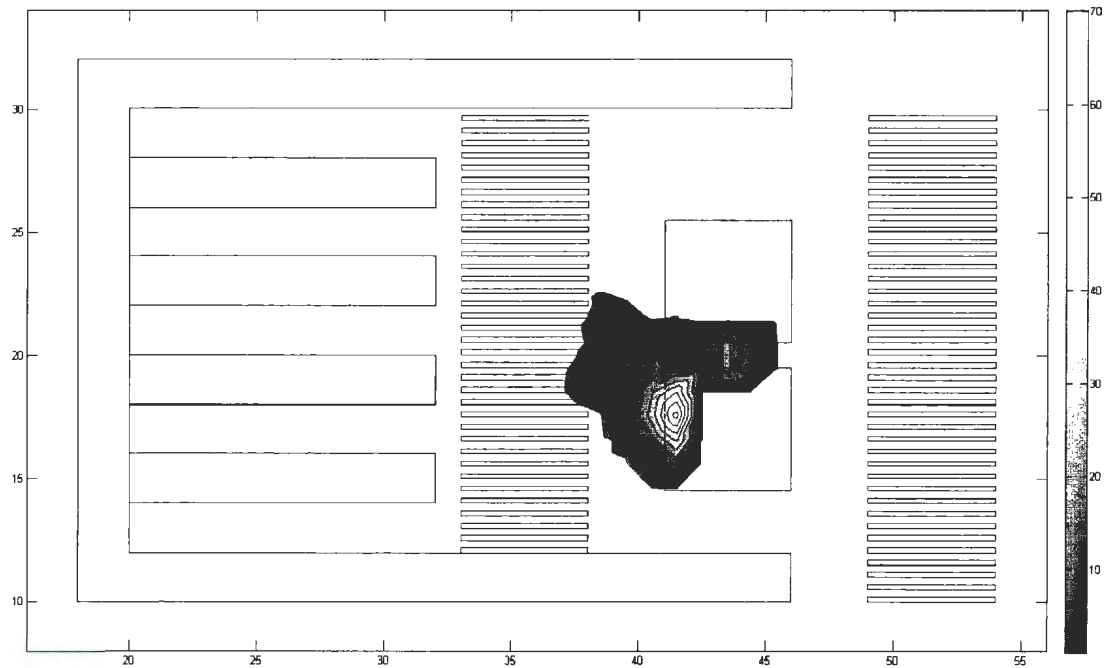


Figure 6.9. Temperature after the explosion over the pool of LNG (K)

The other output monitored during the explosion was the temperature over the LNG pool. The temperature of 300 K is observed far from the explosion point, whereas 1600 K is observed at the areas close to the explosion location (Figure 6.9). The flame temperature of 1500 K is reported for LNG burning by Assael and Kakosimos (2010). The extracted temperature shown in Figure 6.9 is used as input data in pool fire modelling.

#### **6.4.2 Case study 1: Pool fire**

The heat radiation vs. distance profile was developed as shown in Figure 10. The radiation values were in a range between 0 and 70 kW/m<sup>2</sup>. According to Assael and Kakosimos (2010), the low thermal radiation intensity limit is 1 kW/m<sup>2</sup>. Thus, heat radiation values less than this limit are neglected in Figure 6.10.



**Figure 6.10. Heat radiation caused by the pool fire over the plant (kW/m<sup>2</sup>)**

The probability of first and second degree injury and the probability of death at different locations of the plant were calculated (Step 3). Subsequently, the fire risk index ( $Risk_f$ ) of all grid points was estimated and plotted over the plant. The range of these values varies from 1 at the furthest distance from the fire location to the maximum value of 10 at the flame surface (Figure 6.11). This illustrates the higher risk closer to the release location.

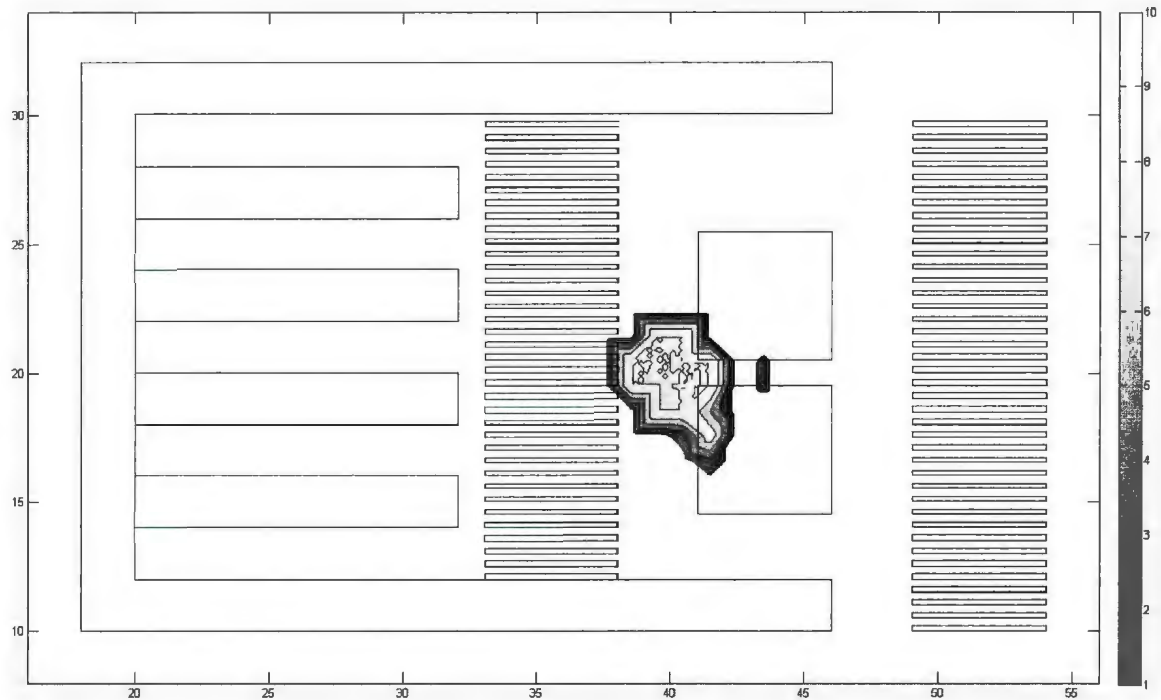


**Figure 6.11. Pool fire risk profile (-)**

#### **6.4.3 Case study 1: Integration of effects**

Finally, the estimated effects for both fire and explosion were integrated as per step 4 of the proposed methodology (Figure 6.12). As there is a certain distance between the location of the pool (where the fire occurs) and the ignition source (where the explosion happens), Figure 12 shows the integrated contours in two different places of the plant. The range of contour values is between 0 and 20. While there are negligible values around the explosion area, the values over the LNG pool are high showing more effects for fire than explosion over the plant. As one moves further from the LNG pool, the values are lower, due to lower confinement/congestion. The amount of released fuel also affects the risk values due to enhancement of the explosion overpressure and heat load.

Assael and Kakosimos (2010) studied the effects of fuel mass increase on increasing overpressure. The results of the new methodology confirm the effectiveness of an integrated approach to consider the hazardous area over the plant. It is noteworthy that while an individual phenomenon (explosion) does not have high risk index values, considering both the explosion and the consequent pool fire shows a higher risk index over the plant, which is useful for safety design and emergency preparedness.

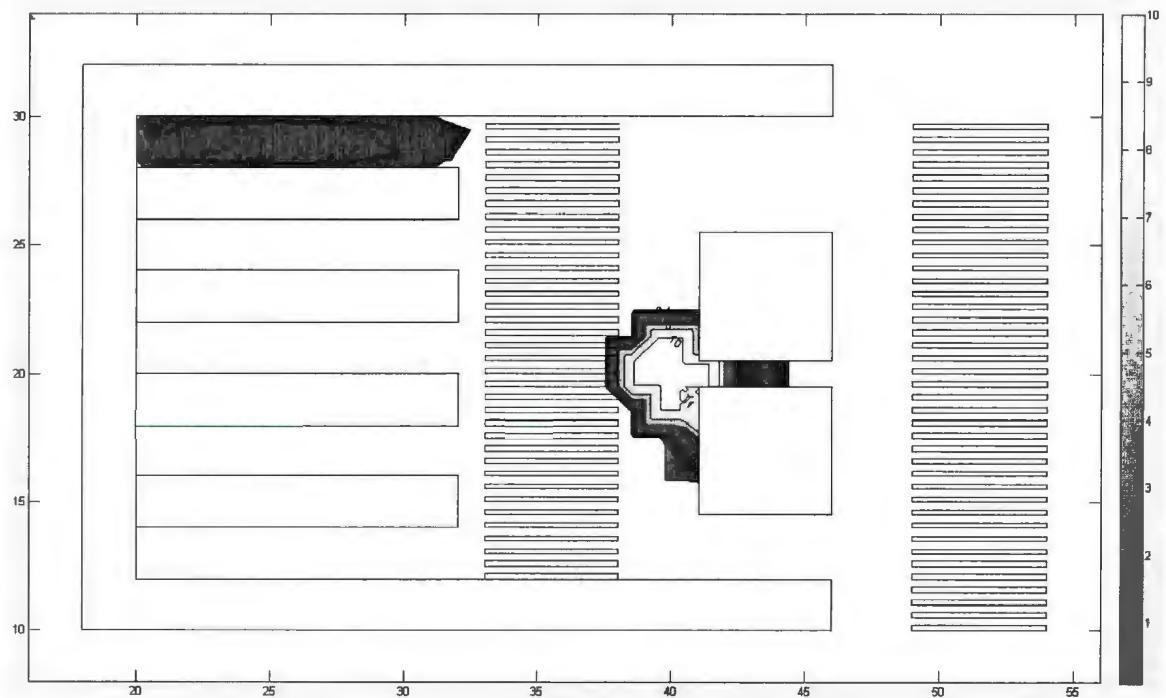
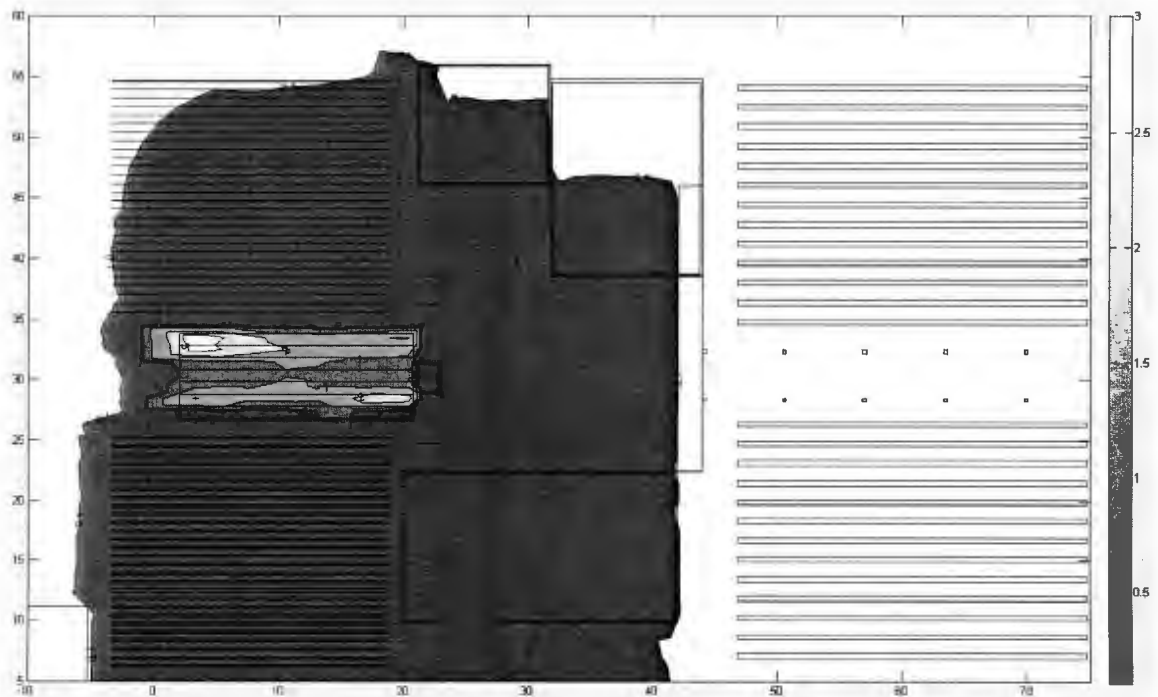


Figure 6.12. Integrated risk profile (-)

#### 6.4.4 Case study 2: Explosion

The explosion overpressure ranges between 0 to 3 bar over the platform. It is evident from Figure 6.13 that there is high overpressure around the pipe racks where the level of

congestion is high due to the storage of pipes. The effect of high congestion/confinement on explosion overpressure was discussed by Husser et al. (2009). Further from the pipe racks, the explosion overpressure decreases gradually, reaching its lowest value over the platform (0.1 bar). This is due to less congestion/confinement causing less turbulence, and the flammable vapour is also dispersed over the open area.



**Figure 6.13. Explosion overpressure over the plant (bar)**

Using the probit model (Step 3), the probabilities of injuries/death caused by the explosion overpressure were calculated. Then, as step 4, the explosion risk index ( $Risk_e$ ) was estimated and plotted over the facility (Figure 6.14). While high values of  $Risk_e$  (10) are located in pipe rack areas, further from the highly congested area, the  $Risk_e$

approaches a value of around 2. The ranges of Risk<sub>e</sub> were set from 2 to 10, thus, a lower value of explosion risk is not demonstrated in Figure 6.14.

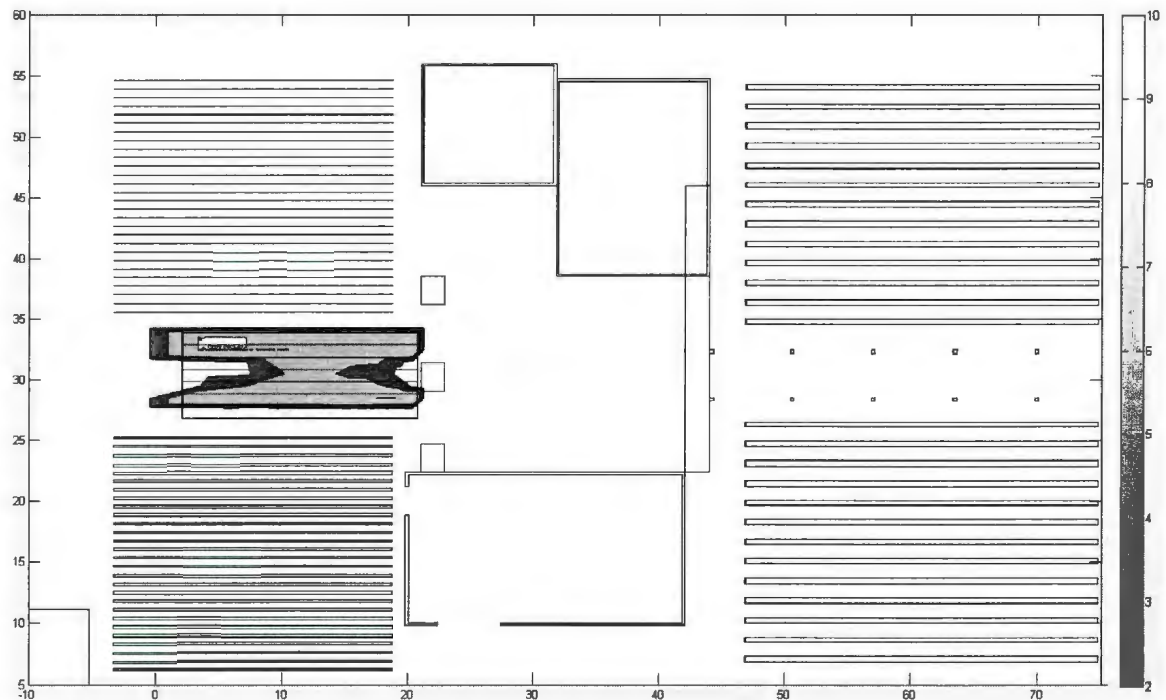


Figure 6.14. Explosion risk profile (-)

#### 6.4.5 Case study 2: Jet fire

Modelling the consequent jet fire after the explosion (Step 2), the heat radiation profile versus distance was developed (Figure 6.15). The radiation values are in a range between 0 and 80 kW/m<sup>2</sup>. The jet fire occurs at the release location on the drilling floor, thus the highest heat radiation value (80 kW/m<sup>2</sup>) was observed on the flame surface.

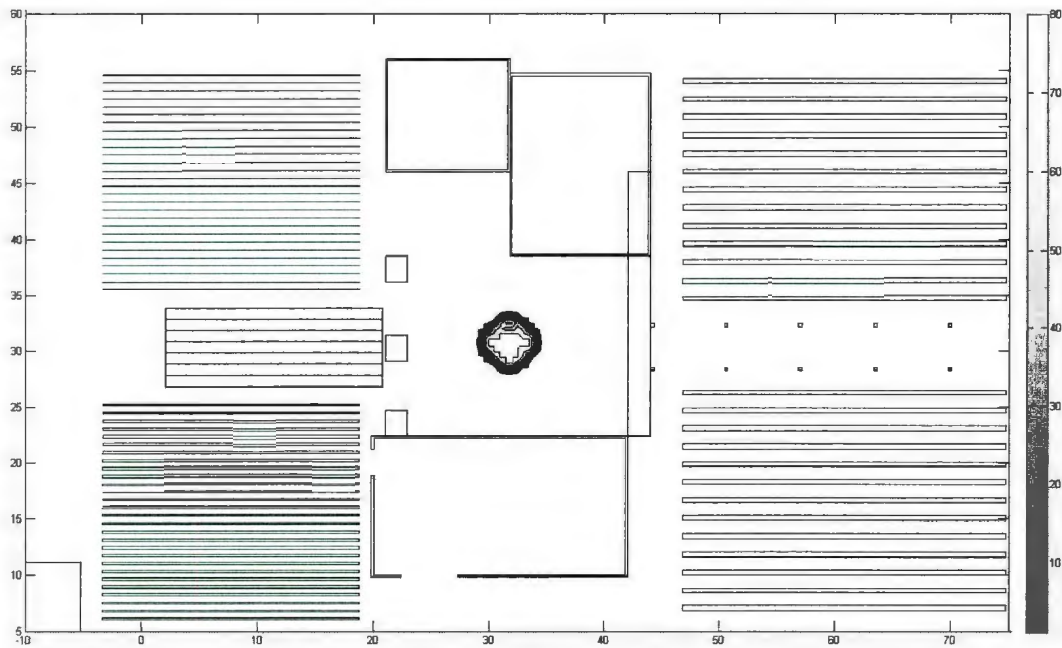


Figure 6.15. Heat radiation caused by the jet fire over the plant (kW/m2)

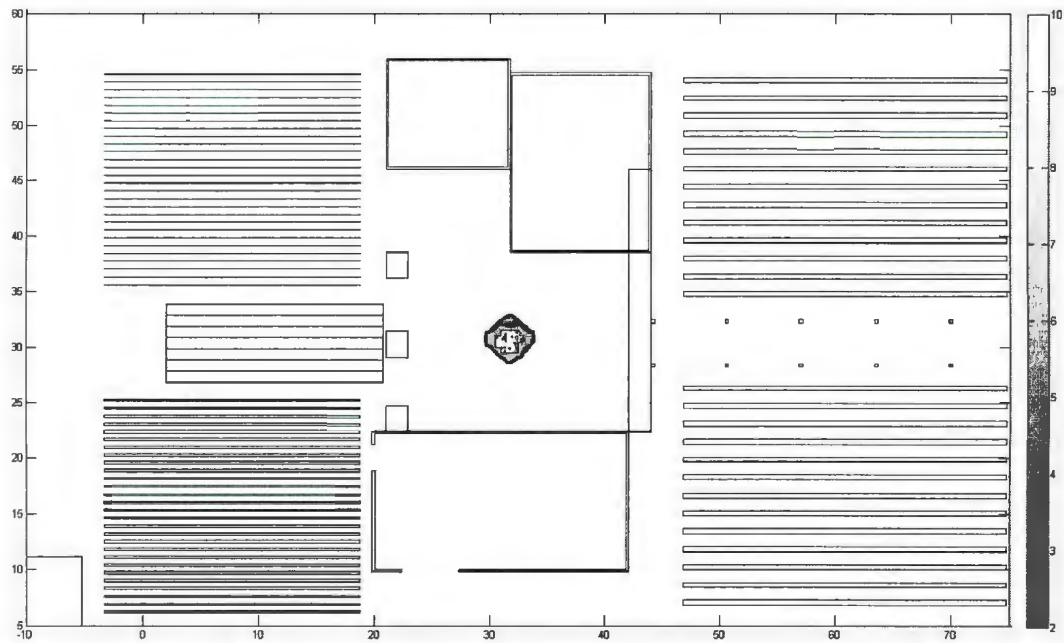


Figure 6.16. Jet fire risk profile (-)

Applying step 3, the probability of injury and death at different locations in the plant were calculated and the fire risk index ( $Risk_f$ ) on all grid points was plotted for the plant. The range of these values varies from 2 at the furthest distance from the fire location to the maximum value of 10 at the flame surface (Figure 6.16). This illustrates the higher risk closer to the release location.

#### **6.4.6 Case study 2: Integration of effects**

The effects of both fire and explosion were integrated as per step 4 of the methodology (Figure 6.17). As there is a significant distance between the release location (where the fire occurs) and the main explosion area (where the existence of pipe racks leads to significant overpressure), Figure 6.17 demonstrates the integrated contours in two different places in the plant. The range of contour values is between 0 and 20. It is clear from Figure 6.17 that there is a high risk value for both fire and explosion phenomena at different locations of the plant. The results of the applied methodology confirm the effectiveness of an integrated approach. It is worth reemphasizing that while individual phenomena (explosion and fire) have high risks, considering both the explosion and the consequent jet fire shows more portions of the facility with high values of risk. This information is useful for safety design and emergency preparedness.

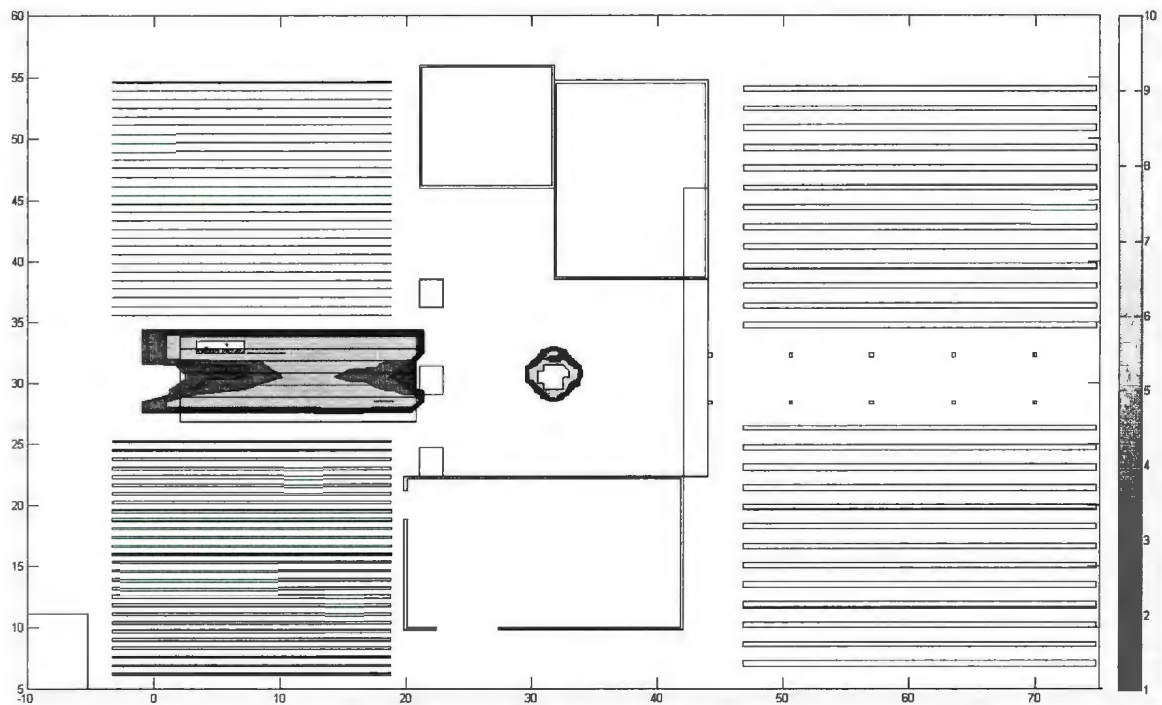


Figure 6.17. Integrated risk profile (-)

## 6.5 Conclusion

A new methodology using CFD codes was proposed to model the consequences due to hydrocarbon release. Using CFD codes FLACS and FDS, the vapour cloud explosion and the consequent fire were modeled. To evaluate the cumulative impact of explosion overpressure and the fire heat load, an integrated approach was adopted to predict the level of risk over the entire sequence; the level of risk over the plant was presented by a total risk index ( $Risk_t$ ). Applying the developed methodology to two case studies, the integrated level of risk was estimated; VCE and pool fire for LNG release and VCE and jet fire for methane gas release. In the LNG case, the explosion risk was insignificant, but the integrated risk was high due to pool fire effects. In the methane gas case, both the

explosion and jet fire have significant level of risk (10) and the integrated risk was observed to be high at two different locations due to the explosion and jet fire. Due to considering the interaction between events, the integrated methodology is more conservative when compared with existing methods. The results demonstrate the advantage of using the integrated approach over the modelling of a single phenomenon. While other related studies [Gevelli et al., 2010; Kim and Salvesen, 2002; Skarsbo, 2011] focused only on modelling the effects of fire or explosion individually, the integrated scenario and assessed cumulative risk make the current study unique. Considering interactions in an evolving accident scenario and taking into account the integration of consequences is useful for safety measure design of process facilities and it is essential to design effective emergency preparedness plans.

**Acknowledgments:**

The authors thankfully acknowledge the financial support provided by Natural Sciences and Engineering Research Council of Canada (NSERC). Author, Mohammad Dadashzadeh thankfully acknowledges Dr. Rouzbeh Abbassi from Princeton University for his valuable support.

## 6.6 References

Achour, B., & Hached, A. (n.d.). The incident at the Skikda plant: description and preliminary conclusion. *LNG14, Session 1*. DOHA, Qatar.

Antonioni, G., Spadoni, G., & Cozzani, V. (2009). Application of domino effect quantitative risk assessment to an extended industrial area. *Journal of Loss Prevention in the Process Industries*, 22, 614-615.

Assael, M. J., & Kakosimos, K. E. (2010). *Fires, Explosions, and Toxic Gas Dispersions: Effects Calculation and Risk Analysis*. Boca Raton: CRC Press/Taylor and Francis.

Bagster, D. F., & Pitblado, R. M. (1991). The estimation of domino incident frequencies—an approach. *Trans. IChemE.*, 69, 195-199.

British Petroleum (BP). (2010). Deepwater Horizon Accident Investigation Report. Retrieved from [http://www.bp.com/liveassets/bp\\_internet/globalbp/globalbp\\_uk\\_english/gom\\_response/STAGING/local\\_assets/downloads\\_pdfs/Deepwater\\_Horizon\\_Accident\\_Investigation\\_Report.pdf](http://www.bp.com/liveassets/bp_internet/globalbp/globalbp_uk_english/gom_response/STAGING/local_assets/downloads_pdfs/Deepwater_Horizon_Accident_Investigation_Report.pdf)

Broadribb, M. P. (2006). Lessons from Texas city: A case history. *Center for Chemical Process Safety 21st annual international conference*. Orlando.

Cozzani, V., & Zanelli, S. (2001). An approach to the assessment of domino accidents hazards in quantitative area risk analysis. *Proc. 10th Int. Symp. On loss prevention and safety promotion in the process industries*. Amsterdam: Elsevier.

Cozzani, V., Gubinelli, G., & Salzano, E. (2006). Escalation threshold in the assessment of domino accidental events. *Journal of Hazardous Materials*, 129, 1-21.

CSB. (2008). *LPG fire at Vallero-McKee refinery*. Retrieved from <http://www.csb.gov/assets/document/CSBFinalReportValeroSunray.pdf>

Gavelli, F., Davis, S. G., & Hansen, O. R. (2010). Evaluating the potential for overpressures from the ignition of an LNG vapour cloud during offloading. *Journal of Loss Prevention in the Process Industries*, 24, 908-915.

GEXCON. (2010). FLACS v9.1 user's manual. Retrieved from [www.bp.com/sectiongenericarticle.do?categoryId=9034902&contentId=7064891](http://www.bp.com/sectiongenericarticle.do?categoryId=9034902&contentId=7064891)

Gjesdal, T. (2000). Local grid refinement for improved description of leaks in industrial gas safety analysis. *Computing and Visualization in Science*, 3, 25-32.

Hanna, S. R., Hansen, O. R., & Dharmavaram, S. (2004). FLACS CFD air quality performance evaluation with KIT Fox, MUST, Prairie Grass, and EMU observations. *Atmospheric Environment*, 4675-4687.

Hansen, O. R., Hinze, P., Engel, D., & Davis, S. (2010). Using computational fluid dynamics (CFD) for blast wave predictions. *Journal of Loss Prevention in the Process Industries*, 23, 855-906.

Hansen, O. R., Ichard, M., & Davis, S. G. (2009). Validation of FLACS for Vapour Dispersion from LNG Spills: Model Evaluation Protocol. *Twelfth Annual Symposium, Mary Kay O'Connor Process Safety Center, Mary Kay O'Connor Process Safety Center* (pp. 712-743). College Station: Texas A&M University.

HSE. (1981). *CANVEY: A second report*. HMSO.

Huser, A., Foyn, T., & Skottene, M. (2009). A CFD based approach to the correlation of maximum overpressure to process plant parameters. *Journal of Loss Prevention in the Process Industries*, 22, 324-331.

Ichard, M., Hansen, O. R., & Melheim, J. A. (2010). Releases of pressurized liquefied gases: Simulations of the Desert Tortoise test series with the CFD model FLACS. *91st AMS annual meeting*. Atlanta, GA, USA.

Kalantarnia, M., Khan, F., & Hawboldt, K. (2010). Modeling of BP Texas City refinery accident using dynamic risk assessment approach. *Process Safety and Environmental Protection*, 88, 191-199.

Khan, F. I., & Abbasi, S. A. (1998). DOMIFECT (DOMIno Effect): User-friendly software for domino effect analysis. *Environmental Modelling & Software*, 13, 163-177.

- Khan, F. I., & Amyotte, P. R. (2007). Modeling of BP Texas City refinery incident. *Journal of Loss Prevention in the Process Industries*, 20, 387-395.
- Kim, W. K., & Salvesen, H. C. (2002). A Study for Prevention of Unconfined Vapour Cloud Explosion from Spilled LNG Confined in Dike. *CCPS Conference Proceedings*. Jacksonville Florida.
- Koo, J., Kim, H. S., So, W., Kim, K. H., & Yoon, E. S. (2009). Safety assessment of LNG terminal focused on the consequence analysis of LNG spills. *Proceeding of the 1st annual gas processing symposium*, (pp. 325-311). Doha.
- Middha, P., & Melheim, J. (2010). FLACS pool live exercise. *FLUG meeting*. Bergen, Norway. Retrieved from [http://www2.gexcon.com/file.php?src=secure/flug/flug\\_meetings/Live\\_pool.pdf&session=800587656](http://www2.gexcon.com/file.php?src=secure/flug/flug_meetings/Live_pool.pdf&session=800587656)
- National Institute of Standards and Technology (NIST). (2010). *Fire Dynamics Simulator (Version 5) User's Guide*. Retrieved from <http://fire.nist.gov/bfrlpubs/fire07/PDF/f07053.pdf>
- Qi, R., Ng, D., Cormier, B. R., & Mannan, M. S. (2010). Numerical simulations of LNG vapour dispersion in Brayton fire training field tests with ANSYS CFX. *Journal of Hazardous Materials*, 183, 51-61.

Ramos, M. A., Droguett, E. L., Martins, M. R., & Souza, H. P. (2011). Quantitative Risk Analysis and Comparison for Onshore and Offshore LNG Terminals: The Port of Suape - Brazil Case. *ASME 2011 30th International Conference on Ocean, Offshore and Arctic Engineering (OMAE2011)*. Rotterdam, The Netherlands.

Reniers, G., Dullaert, W., & Karel, S. (2009). Domino effects within a chemical cluster: a game-theoretical modeling approach by using Nash-equilibrium. *Journal of hazardous materials*, 167, 289-293.

Skarsbo, L. R. (2011). *An experimental study of pool fires and validation of different CFD fire models*. Master thesis submitted to the Department of physics and technology, University of Bergen, Bergen, Norway.

Suardin, J. A., Wang, Y., Willson, M., & Mannan, M. S. (2009). Field experiments on high expansion (HEX) foam application for controlling LNG pool fire. *Journal of Hazardous Materials*, 165, 612-622.

The California Energy Commission. (2012). *Liquefied natural gas safety*. Retrieved from <http://www.energy.ca.gov/lng/safety.html>

U. S. Chemical Safety Board (CSB). (2007). *BP Texas city refinery explosion and fire*. final investigation report. Retrieved from [http://www.csb.gov/investigations/detail.aspx?SID=20&Type=2&pg=1&F\\_AccidentTypeId=12](http://www.csb.gov/investigations/detail.aspx?SID=20&Type=2&pg=1&F_AccidentTypeId=12)

Woodward, J. L., & Pitblado, R. M. (2010). *LNG Risk Based Safety: Modelling and Consequence Analysis*. Hoboken, NJ: John Wiley and Sons.

Yang, X., Dinh, L. T., Castellanos, D., Amado, C. H., & Mannan, M. S. (2011). Common lessons learned from an analysis of multiple case histories. *Process Safety Progress*, 30, 143-147.

Yun, G., Ng, D., & Mannan, M. S. (2011). Key findings of liquefied natural gas pool fire outdoor tests with expansion foam application. *Industrial and Engineering Chemistry Research*, 50, 2359-2372.

## **7 Combustion Products Toxicity Risk Assessment in an Offshore Installation**

Mohammad Dadashzadeh<sup>1</sup>, Faisal Khan<sup>1</sup>, Rouzbeh Abbassi<sup>2</sup>, Kelly Hawboldt<sup>1</sup>

1. Process Engineering, Faculty of Engineering and Applied Science, Memorial University of Newfoundland, St. John's, NL, Canada, A1B 3X5

2. Department of Civil and Environmental Engineering, Princeton University, Princeton, NJ 08544

### **Abstract**

Products of a hydrocarbon fire accident have both chronic and acute health effects. They cause respiratory issues to lung cancer. While fire is the most frequent phenomenon among the offshore accidents, predicting the contaminants' concentration and their behaviour are key issues. Safety measures design, such as ventilation and emergency routes based only on predicted contaminants' concentration seems not to be the best approach. In a combustion process, various harmful substances are produced and their concentration cannot be added. The time duration that any individual spends in different locations of an offshore installation also varies significantly. A risk-based approach considers the duration a person is exposed to contaminants at various locations and also evaluates the hazardous impacts. A risk-based approach has also an additivity characteristic which helps to assess overall risk.

\* Dadashzadeh, M., Khan, F., Abbassi, R., Hawboldt, K. (2013). Combustion Products Toxicity Risk Assessment in an Offshore Installation. *Journal of Process Safety and Environmental Protection* (under review).

Through the current study, an approach is proposed to be used for risk assessment of combustion products dispersion phenomenon in a confined or semi-confined facility. Considering CO, NO<sub>2</sub> and CH<sub>4</sub> as the contaminants of concern, the dispersion of the substances over the layout of the facility after a LNG fire is modeled. Considering different exposure times for three major parts of the facility including the processing area, office area and the accommodation module, the risk contours of CO, NO<sub>2</sub> and CH<sub>4</sub> over the entire facility are developed. The additivity characteristic of the risk-based approach was used to calculate the overall risk. The proposed approach helps to better design safety measures to minimize the impacts and effective emergency evacuation planning.

**Key Words:** *CFD, Combustion products, Toxic dispersion, Risk-based approach*

## 7.1 Introduction

Harmful airborne contaminants in a process facility are a matter of concern. It is important to provide a safe environment for personnel working in a processing area. Predicting the risks caused from airborne toxicants is a useful approach to emergency preparedness.

Offshore personnel spend most of their time in a semi enclosed processing area or an enclosed office/residential area. Thus, it is important to minimize harmful effects during an accidental event. According to Pula et al. (2005), fire is the most frequent accident occurring on offshore installations. One of the main sources of concern is the combustion

of hydrocarbons due to fire accidents [Hartzell, 2001]. Thus, there is a need to carefully assess the hazards caused by a fire accident such as heat radiation and airborne toxic contaminants (combustion products).

An example of toxic dispersing in an industrial accident is the massive fire which occurred at oil storage in 2005 at Oil Storage Depots (Buncefield, Hertfordshire, England). The production of smoke and combustion products caused environmental problems and health issues over the plant and near-by areas showing the need to estimate the toxic substance concentration at and around the plant [Markatos et al., 2009]. The Piper Alpha explosion in the North Sea is another example of the hazards caused by combustion products. In 1988, the failure of a condensate injection pump caused a leak and was followed by a small explosion. Due to the failure of safety equipment, a series of major blasts occurred followed by a fireball. Then, the failure of the gas pipeline riser led to a massive explosion which was the reason for the collapse of the drilling derrick. The loss of 167 lives in the Piper Alpha disaster was demonstrated to be mainly from the smoke inhalation due to the massive fire [Knight and Pretty, 1997].

Safety measure design and emergency preparedness are not very effective when they are only based on contaminants' concentration. Personnel spend different time durations in various locations of an offshore facility (different exposure time) and the concentration of various toxic substances cannot be added. As a solution, a risk-based approach helps to consider the time duration when personnel are exposed to air pollutants at different

sections of a plant. Additionally, it helps to combine the harmful effects caused by various toxic substances [Markatos, 2012].

According to Srehic and Chen (2002), the application of Computational Fluid Dynamics (CFDs) is a common method of assessing air quality characteristics such as pollution concentration and air flow patterns. CFDs codes were extensively used in dispersion studies such as a liquefied natural gas (LNG) spill [Gavelli et al., 2008], heavy gas dispersion over large topographically complex areas [Scargiali et al., 2005] and indoor dispersion of toxic chemical substances [Kassomenos et al., 2008; McBride et al., 2001]. CFD codes have the advantages of low cost, high speed, capability to provide complete information and the ability to model ideal and realistic conditions [Bo and Guo-ming, 2010].

The focus of this study is to develop a methodology to apply a CFDs code to assess the dispersion of combustion products from a fire incident over a platform in combination with a risk-based approach to develop the risk profile. This is helpful for the safety measures design on offshore facilities. It is also useful to plan any emergency actions required on an installation during an accident.

## **7.2 Toxicity risk assessment approach**

Air borne combustion products cause adverse effects on both human health and the environment. These effects vary from primary ones (coughing and respiratory) to secondary long term effects (lung cancer and cardiovascular diseases).

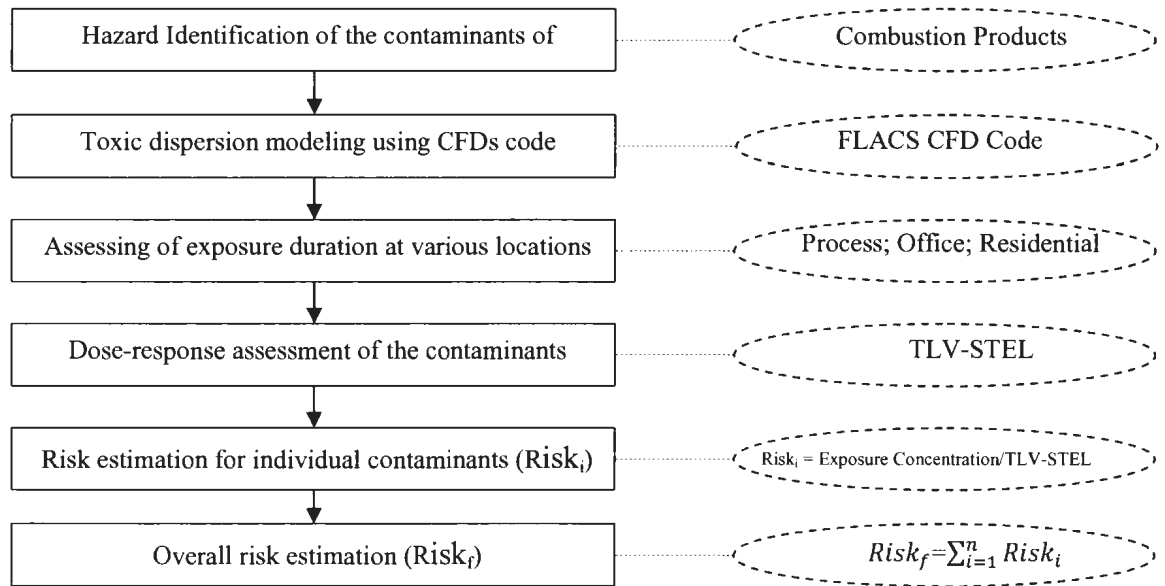


**Figure 7.1. A methodology of toxic risk assessment**

Toxicity risk assessment helps to develop a risk profile for the area of concern and also helps to plan risk minimization strategies. Figure 7.1 illustrates the risk assessment approach proposed by the current study. Hazard identification, dispersion modeling, exposure assessment, dose-response assessment and risk estimation are the main steps of the proposed risk assessment approach. Details of each step are given below.

## **7.2.1 Risk assessment**

### **7.2.1.1 Hazard identification**

Three major harmful combustion products produced due to an LNG fire are carbon monoxide (CO), nitrogen dioxide (NO<sub>2</sub>) and unburned methane (CH<sub>4</sub>) [Kajtar and

Leitner, 2007]. Table 7.1 shows the emission factors, fuel consumption and flow rates for natural gas combustion [USEPA, 1995; Assael and Kakosimos, 2010].

**Table 7.1. Emission factors, fuel consumption and the flow rate of CO and NO<sub>2</sub>**

Emission	Emission factor (gm <sup>-3</sup> )	Fuel consumption (m <sup>3</sup> s <sup>-1</sup> )	Flow rate (gs <sup>-1</sup> )
CO	4.48	0.5653	2.53
NO <sub>2</sub>	1.344	0.5653	0.76
CH <sub>4</sub>	0.0368	0.5653	0.021

Table 7.2 [Abbassi et al., 2012] shows the harmful effects associated with these three contaminants.

**Table 7.2. Adverse health effects [Abbassi et al., 2012; OSHA, 2003]**

Health hazard air pollution parameters	Adverse health effects
CO	<p>Cardiovascular effects: Low level CO is the most serious for those who suffer from heart disease such as angina, clogged arteries or congestive heart failure.</p> <p>Central nervous system effects: High levels of CO can result in vision problems, reduced ability to work or learn, reduced manual dexterity and difficulty performing complex tasks.</p> <p>Poisonous: At extremely high levels, CO is poisonous and can cause death.</p>
NO <sub>2</sub>	Respiratory effects: Chronic respiratory symptoms (cough and phlegm), more frequent in children.

	Poisonous: At extremely high levels, NO <sub>2</sub> is poisonous and can cause death.
CH <sub>4</sub>	Methane is an asphyxiant gas which displaces oxygen and causes hypoxia.

#### 7.2.1.2 Dispersion modeling using FLACS CFD code

Using FLACS CFDs code [GEXCON, 2010], the dispersion of the contaminants of concern on an offshore installation is modeled. Using a finite volume method in a Cartesian grid, the concentration equations of mass, momentum and enthalpy are solved using FLACS. For turbulence modelling, FLACS uses a Reynold-Averaged Navier–Stoke (RANS) approach based on the standard k-ε model [Mouilleau and Champassith, 2009]. Obstacles with small details play a significant role during confined dispersion of pollutants and as such the representation of these details is a key aspect of dispersion modelling. A distributed porosity concept is used in FLACS dispersion simulation as obstacles are represented by area and volume porosity [Hanna et al., 2004].

Compared to other dispersion models, FLACS has advantages such as better predictions that have been validated for different dispersion scenarios. The distributed porosity concept to create complex geometries and the Cartesian grid result in more rapid solutions in large and complex facilities when compared to conventional models. Additionally, the well-established turbulence model (k-ε) compared to other alternative models makes FLACS more appropriate to simulate dispersion phenomena [HSE, 2010].

#### **7.2.1.2.1 Geometry definition**

A typical offshore installation is selected as the geometry for the study (Figure 7.2). The considered offshore installation consists of three major parts including the process area, the office area and the residential area. An LNG pool fire was assumed to have occurred at the process area. The emission of combustion due to the LNG pool fire was modeled with the addition of 16 leak points over the pool area.

CFLC and CFLV are Courant–Friedrich–Levy numbers based on the sound velocity and the fluid flow velocity, respectively. By choosing the appropriate values of CFLC and CFLV, the sound waves and the fluid flow propagate a limited distance in each time step; the average control volume length multiplied by the value of CFLC and CFLV. In the current study, to control time steps, the CFLC and CFLV numbers were assumed to be 20 and 2, which is suggested by FLACS user's manual [GEXCON, 2010]. The simulation volume of  $57\text{ m} \times 40\text{ m} \times 6\text{ m}$  was selected with a grid size of 1 m, obtained as an optimum value through a sensitivity analysis. The time of simulation was chosen as 3,600 s for leak points during the entire simulation. There was no absorption of emissions by obstacles as the porosity of all objects was considered to be 1.

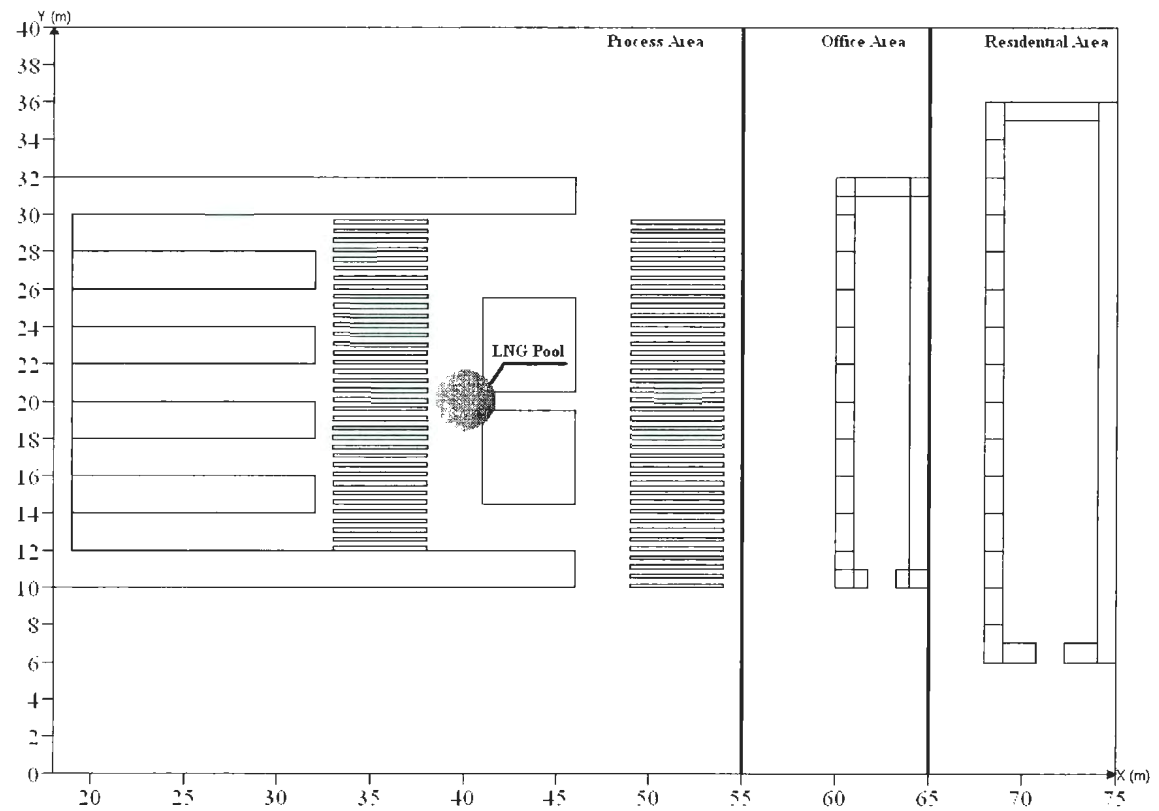


Figure 7.2. Schematic of offshore installation considered in modeling scenario

### 7.2.1.3 Exposure assessment

Time spent by the personnel at different locations of the offshore installation is the exposure time. Time spent by offshore personnel at different locations of the platform is demonstrated in Figure 7.3. According to HSE (2008), it was assumed that an individual spent 12 hours outside the residential area; 8 hours in the process area and 4 hours in the office area. The rest of the day is assumed to be spent in the residential area (12 hours).

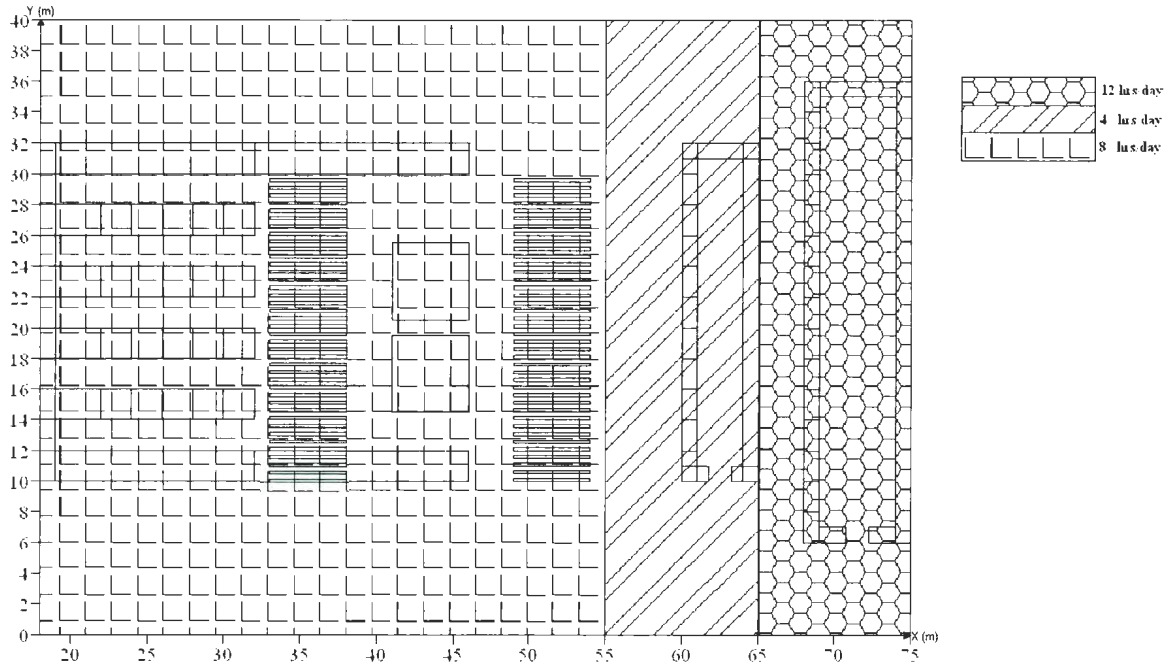


Figure 7.3. Time spent by a person during a day

#### 7.2.1.4 Dose-response assessment

The probability and severity of the damage to a person's health is related to the risk agent through the dose-response assessment. The threshold dose on the dose-response curve shows the highest concentration at which there is no adverse effect of inhaling the contaminant over a period of time. The American Conference of Governmental Industrial Hygienists (ACGIH) determines the threshold limit values (TLVs). TLV-STEL presents the short-term exposure limit for which an employee is exposed with no adverse effect.

In the current study, the values of TLV-STEL for CO, NO<sub>2</sub> and CH<sub>4</sub> are 440, 45 and 705 mg.m<sup>-3</sup>, respectively [ACGIH, 1991].

### 7.2.1.5 Risk estimation

For an individual contaminant, risk is calculated through the integration of the exposure and toxicity assessment (Equation 1). Then, the additive property of risk is estimated by summing the individual risk values for the mixture of contaminants (Equation 2).

$$RISK = \frac{\text{Exposure concentration}}{TLV - STEL} = \frac{\text{Concentration} \times \text{Time spent}/BW}{TLV - STEL/BW} \quad 7.1$$

$$RISK_f = \sum_0^i RISK_i \quad 7.2$$

where BW is the body weight.

## 7.3 Results

The natural ventilation caused by wind is the main reason for the dispersing of the contaminants of concern over the semi-confined area. The low vector velocities are seen in the engine rooms at the left end of the process area which is reasonable due to their being sheltered (Figure 7.4). Recirculation of air is seen around the vessels because of high congestion/confinement around this area. The same situation happens inside the office and the residential buildings. While the air enters the buildings through the openings, it hits the inside walls and trapped inside causing the recirculation. At the residential area, air is getting out through the entrance which is due to the negative pressure caused by the high velocity of wind outside the building.

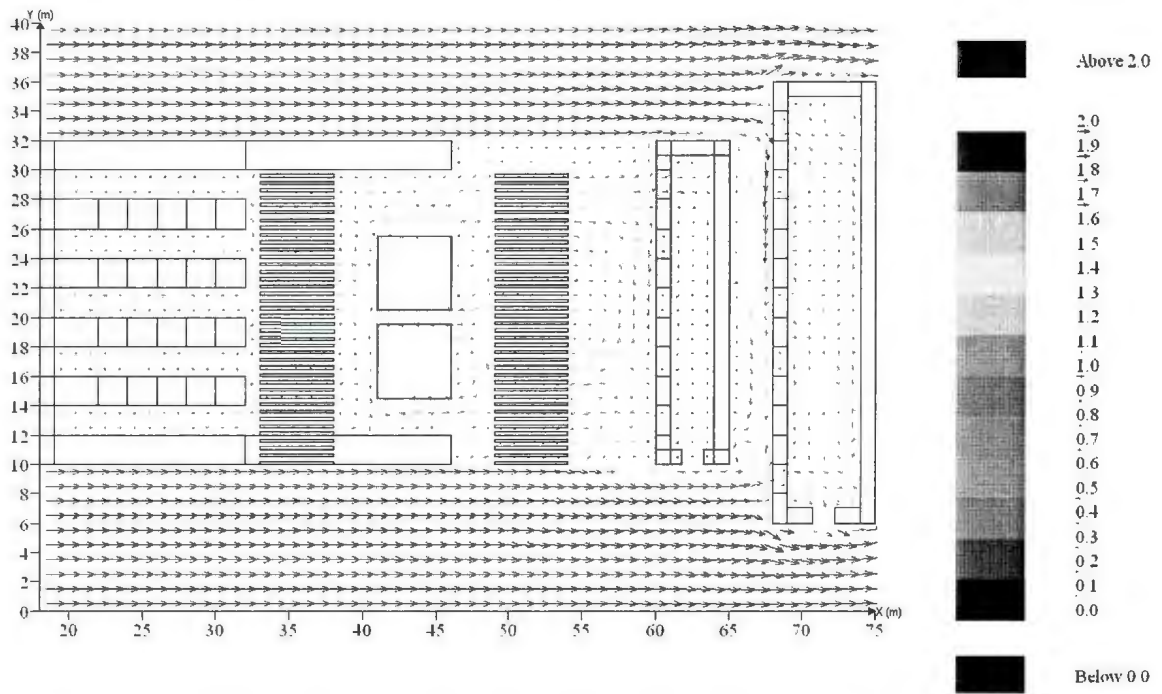


**Figure 7.4. Air flow over the plant due to wind effect**

According to Zhang and Zhao (2007), the average height for an individual inhaling air contaminants is 1.5 m. Thus, the CO, NO<sub>2</sub> and CH<sub>4</sub> concentration at 1.5 m from the ground was monitored (Figures 7.5, 7.6 and 7.7). The concentrations of contaminants are very high near the source of release. There are also high concentrations monitored at engine rooms where emissions trapped under the shelter. Wind velocity is the main reason for dispersing the contaminants of concern from the fire area to the office and residential area. The further distances of the office area and residential area from the source is the reason for their lower concentrations compared to other areas.

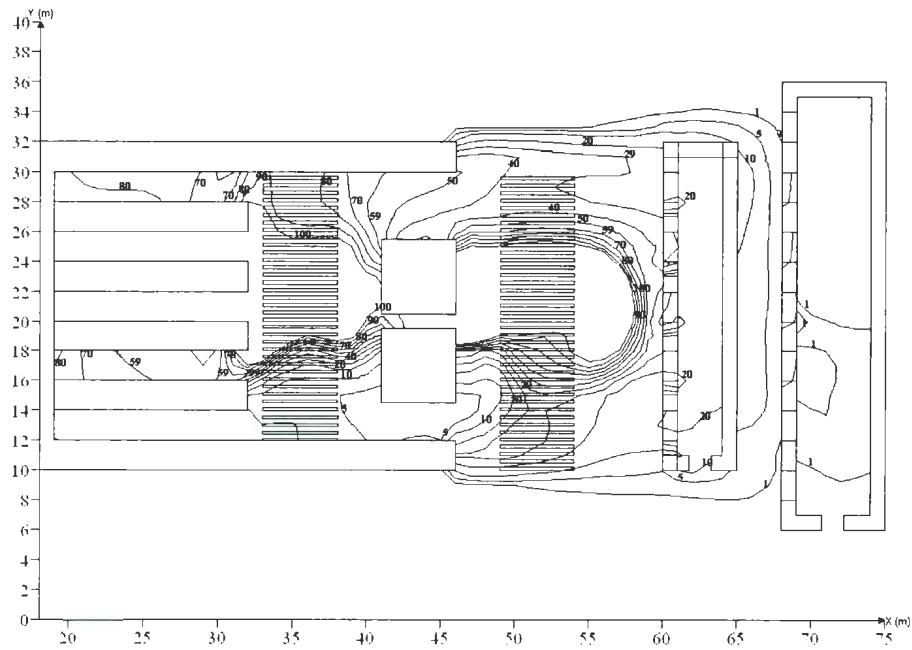


Figure 7.5. CO concentration ( $\text{mgm}^{-3}$ )

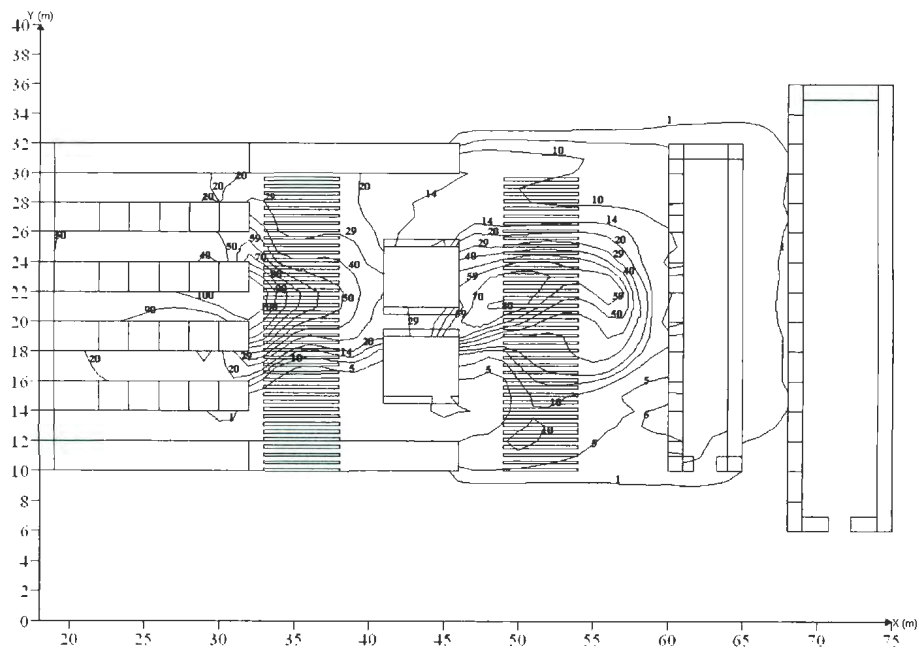


Figure 7.6.  $\text{NO}_2$  concentration ( $\text{mgm}^{-3}$ )

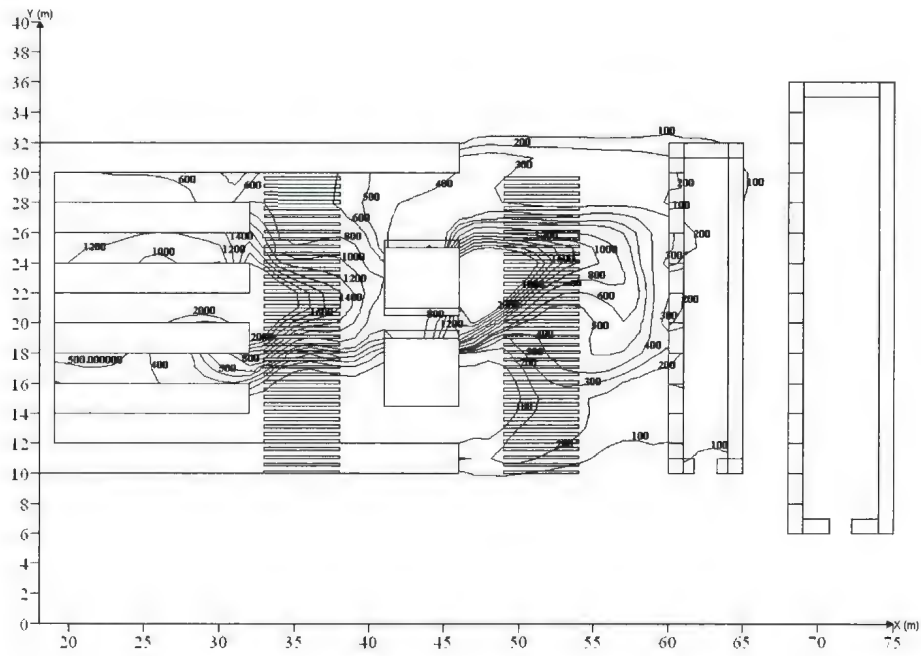


Figure 7.7. CH<sub>4</sub> concentration (mgm<sup>-3</sup>)

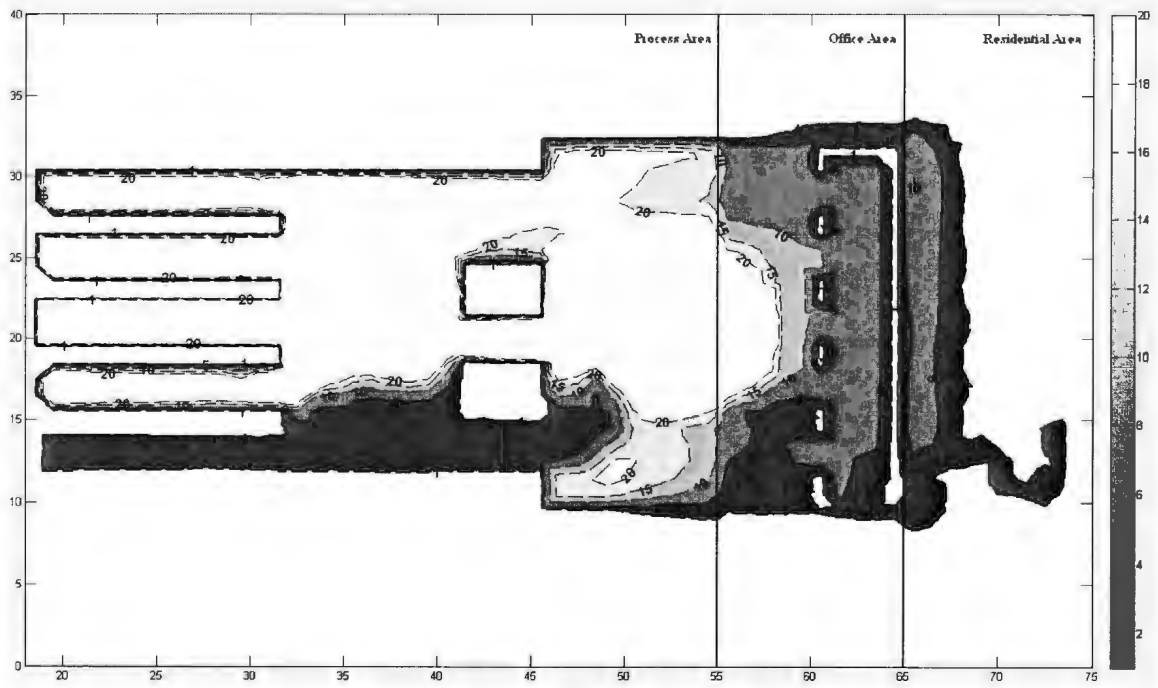


Figure 7.8. Hazard quotients (Risk<sub>CO</sub>) for CO inhalation over the plant

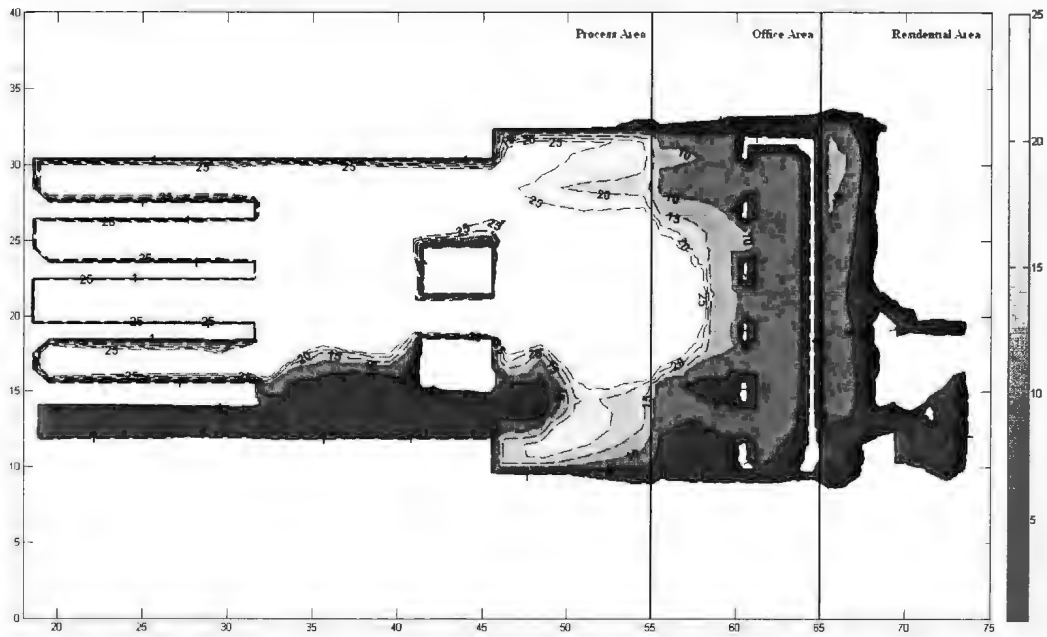


Figure 7.9. Hazard quotients ( $Risk_{NO_2}$ ) for  $NO_2$  inhalation over the plant

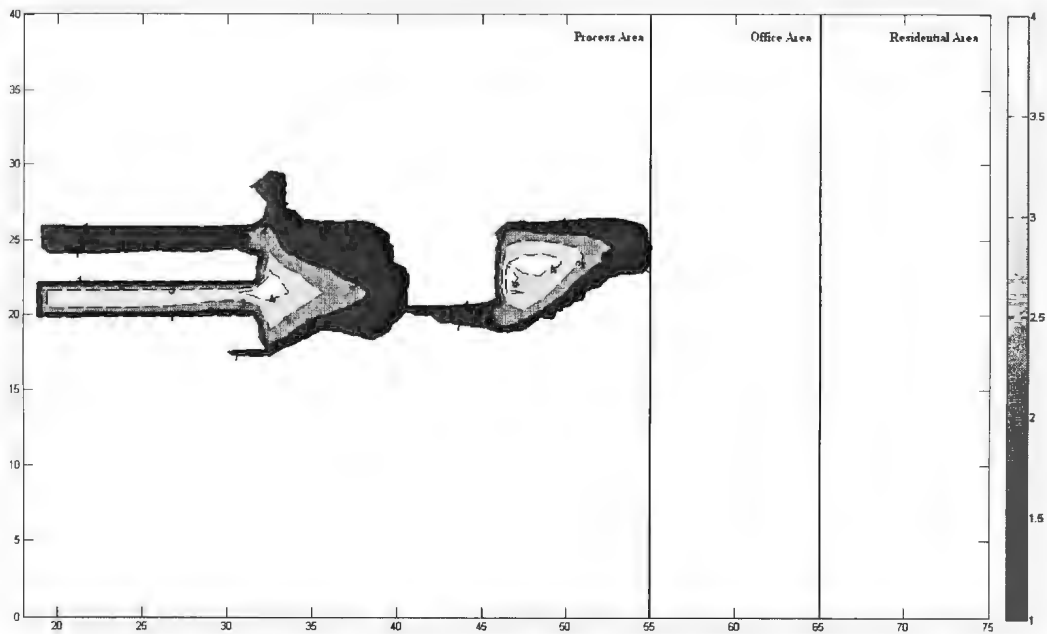


Figure 7.10. Hazard quotients ( $Risk_{CH_4}$ ) for  $CH_4$  inhalation over the plant

Risk values for the contaminants of concern were calculated based on the explained methodology. As shown in Figures 7.8-7.10, risk values are high around the release source which is due to the high concentration of contaminants in this area. However, it is observed that in the process area there are high values of risk for all contaminants, while lower ones are seen at office and residential areas. The longer exposure duration (12 hr.day<sup>-1</sup>) and the high concentration of the contaminants due to congestion/confinement are the reasons for these high risk values. It can be seen that the exposure duration plays a significant role in risk estimation as the concentrations of contaminants are to some extent high in the office area while the risk is negligible. On the other hand, from the individual risks shown in Figures 7.8-7.10, it is observed that the majority of the office area and the entire residential area are in a safe level of contaminants.

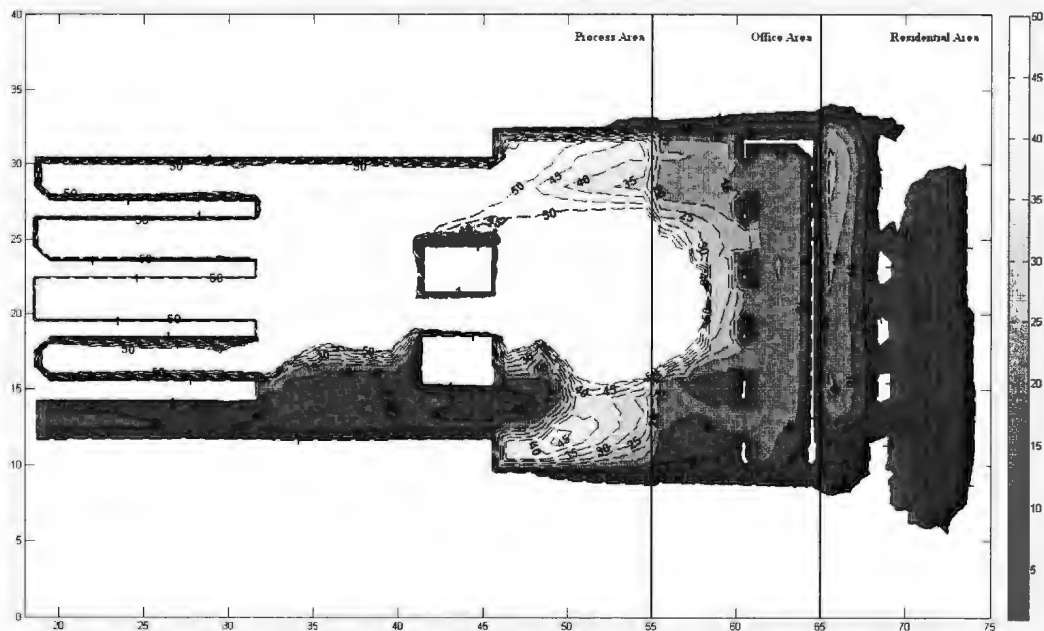


Figure 7.11. Final risk ( $Risk_f$ ) for  $NO_2$ , CO and  $CH_4$  inhalation over the plant

As explained by the methodology, one of the significant features of the risk assessment is its additivity characteristic for a mixture of contaminants. Figure 7.11 demonstrates the  $Risk_f$  considered for the combined effects of CO, NO<sub>2</sub> and CH<sub>4</sub> hazard quotients. While Figures 7.8-7.10 show a safe level for the majority of office and residential areas,  $Risk_f$  shows significant portions of the office area exceeding the acceptable level of risk, which is 1.

#### **7.4 Conclusion**

Fire accidents are among the most frequent accidents occurring on offshore facilities. While the heat radiation caused by the fire is the main reason for fatalities/injuries for offshore personnel, the toxic combustion products are a matter of concern due to their harmful effects, and they also seriously jeopardize evacuation. Predicting the concentration of toxic substances and their behaviour at the facility is therefore a key issue in safety measure design and evacuation planning. However, designing safety measures based on the predicted contaminants' concentration is not an appropriate approach, specifically when dealing with a mixture of contaminants which are combustion products. The problem arises from the fact that the concentration of different contaminants cannot be added. Moreover, the exposure duration which any person spends at different locations of the facility plays a significant role as well.

A risk-based approach is useful as it considers the time spent by any individual at various locations of an installation through an exposure assessment step. This approach is also

useful for the mixture of contaminants; the additivity characteristic of a risk-based approach enables the addition of risk values of different substances.

In the current study, a risk-based approach is proposed to model toxic dispersion at an offshore facility. Using FLACS CFDs code, the dispersion of the contaminants of concern (CO, NO<sub>2</sub> and CH<sub>4</sub>) after an LNG fire at an offshore installation was modeled. Then, considering the exposure time at different locations of the plant including the process area, the office area and the residential area, the Hazard Quotient (risk) for the contaminants of concern was estimated and shown as contours over the entire facility. While the process area (8 hr.day<sup>-1</sup> exposure time) has the highest value of individual risks, most of the office area (4 hr.day<sup>-1</sup> exposure time) and the entire residential area (12 hr.day<sup>-1</sup> exposure time) were observed to have lower risk values. Due to the higher concentration and longer exposure time, the higher values of risk are reasonable in the process area. The exposure time is higher than any other place in residential areas, but the risk is negligible due to low concentrations. The Risk<sub>f</sub> which is estimated through the addition of risks of all contaminants shows different results; significant portions of the office exceed the acceptable level of risk which is 1.

Considering the exposure time and its additivity characteristic, the risk-based approach is then more useful compared to any concentration-based approach in toxic dispersion assessment. It helps to design safety measures to minimize the harmful effects of the toxic substances and also provides a tool for effective emergency management.

### Acknowledgement

Authors gratefully acknowledge the financial support provided by Natural Science and Engineering Research Council (NSERC).

### 7.5 References

Abbassi, R., Dadashzadeh, M., Khan, F., Hawboldt, K. (2012). Risk-based prioritization of indoor air pollution monitoring using computational fluid dynamics. *Indoor and built environment*, 21, 663-673

American Conference of Governmental Industrial Hygienists (ACGIH) (1991). Threshold limits values for chemical substances and physical agents and biological exposure indices. ACGIH, Cincinnati, OH.

Assael, M.J., Kakosimos, K.E. (2010). Fires, explosions, and toxic gas dispersions: effects calculations and risk analysis. CRC Press Taylor and Francis Group, NY.

Bo, Z., Guo-ming, C. (2010). Quantitative risk analysis of toxic gas release caused poisoning—a CFD and dose-response model combined approach. *Process safety and environmental protection*, 88, 253-262.

Gavelli, F., Bullister, E., Kytömaa, H. (2008). Application of CFD (fluent) to LNG spills into geometrically complex environments. *Journal of hazardous materials*, 159, 158-168.

GEXCON (2010). FLACS v9.1 user's manual, Bergen, Norway.

Hanna, S.R., Hansen, O.R., Dharmavaram, S. (2004). FLACS CFD air quality performance evaluation with kit fox, MUST, prairie grass, and EMU observations. *Journal of atmospheric environment*, 38, 4675-4687.

Hartzell, G.E. (2001). Engineering analysis of hazards to life safety in fires: the fire effluent toxicity component. *Safety science*, 38, 147-155

Health and Safety Executive (HSE). (2008). Guidance for managing shiftwork and fatigue offshore. Retrieved from <http://www.hse.gov.uk/offshore/infosheets/is7-2008.htm>

Human and Safety Executive (HSE) (2010). Review of FLACS version 9.0. Dispersion modeling capabilities. Available at: [www.hse.gov.uk](http://www.hse.gov.uk).

Kajtar, L., Letner, A. (2007). CFD modeling of indoor environment quality affected by gas stoves. *Proceeding of climate change*, Helsinki, Finland, 10-14 June 2007.

Kassomenos, P., Karayannis, A., Panagopoulos, I., Karakitsios, S., Petrakis, M. (2008). Modeling the dispersion of a toxic substance at a workplace. *Environmental modeling and software*, 23, 82-89.

Knight, R.F., Pretty, D.J. (1997). The impact of catastrophes on shareholder value: a research report sponsored by Sedgwick Group, The oxford executive research briefings, Templeton College, Oxford, 1997.

Markatos, N.C. (2012). Dynamic computer modeling of environmental systems for decision making, risk assessment and design. *Asia-Pacific journal of chemical engineering*, 7, 182-205.

Markatos, N.C., Christolis, C., Argyropoulos, C. (2009). Mathematical modeling of toxic pollutants dispersion from large tank fires and assessment of acute effects for fire fighters. *International journal of heat and mass transfer*, 52, 4021-4030.

Mcbride, M.A., Reeves, A.B., Vanderheyden, M.D., Lea, C.J., Zhou, X.X. (2001). Use of advanced techniques to model the dispersion of chlorine in complex terrain. *Process safety and environmental protection*, 79, 89-102.

Moulilleau, Y., Champassith, A. (2009). CFD simulations of atmospheric gas dispersion using the fire dynamics simulator (FDS). *Journal of loss prevention in the process industries*, 22, 316-323.

Occupational Safety and Health Administration (OSHA). (2003). Safety and health topics: methane. Retrieved from [http://www.osha.gov/dts/chemicalsampling/data/CH\\_250700.html](http://www.osha.gov/dts/chemicalsampling/data/CH_250700.html)

Pula, R., Khan, F.I., Veitch, B, Amyotte, P. (2005). Revised fire consequence models for offshore quantitative risk assessment. *Journal of loss prevention in the process industries*, 18, 443-454.

Scargiali, F., Di Rienzo, E., Ciofalo, M., Grisafi, F., Brucato, A. (2005). Heavy gas dispersion modeling over a topographically complex mesoscale: a CFD based approach. *Process safety and environmental protection*, 83, 242-256.

Srebic, J., Chen, Q. (2002). Simplified numerical models for complex air supply diffusers. *HVAC and Research*, 8, 277-294.

U.S.Environmental Protection Agency (USEPA) (1995). Protocol for equipment leak emission estimates. EPA-453/R-95-017, Office of air quality planning and standards, research triangle park, NC 27711.

Zhang, Y., Zhao, B. (2007). Simulation and health risk assessment of residential particle pollution by coal combustion in China. *Building environment*, 42, 614-622.

## **8 Conclusions, and recommendations**

### **8.1 Conclusions**

The main conclusions of this study are:

#### **8.1.1 New equations to model emission factors**

This study concluded that applying a non-linear regression in order to develop correlation equation for estimating emission factors is a more effective way than the linear regression used by USEPA studies. The results obtained through the current study demonstrate a better estimation of emission leak rates in four categories of components including pump-seals, flanges, open-ended lines and others. Thus, the new sets of equations developed through the current research can replace USEPA correlation equations.

Although the results obtained for other categories including connectors and valves were almost similar in both approaches, the qualitative comparison of both approaches highlights better accuracy using the new methodology proposed in this thesis.

#### **8.1.2 Systematic approach to model vapour cloud explosion**

A systematic approach to model the VCE in oil and gas facilities was proposed through the current study. While CFD codes are commonly used to simulate the VCE phenomenon in offshore/onshore oil and gas facilities, there is no agreed standard systematic procedure to do the analysis. This causes significant variability in the modeling approaches and also in the results of such analysis. Thus, the current study

proposed an approach to highlight the various steps involved in the VCE modeling. These steps were divided into two major sections; dispersion modeling and explosion simulation. The required sub-steps, including various parameter definitions and sensitivity analysis, were also discussed in detail to better explain the VCE modeling.

### **8.1.3 Integration of the dispersion of flammable vapour with explosion modeling**

Here, the importance of the dispersion characteristics of flammable vapour release is discussed. Dispersion of flammable vapour is an important step in consequence assessment and it significantly influences the low and high limits of the flammable vapour, which control the explosion characteristics. Although these days CFD codes are used in VCE modeling, the major limitation of these studies is the consideration of the uniform stoichiometric volume of flammable vapour, ignoring the dispersion phenomenon. In this research, the dispersion simulation was integrated with the VCE modeling which makes this work unique.

### **8.1.4 Integrated modeling of fire and explosion consequences**

The study introduced a novel approach using CFD codes to model consequences after hydrocarbon release. While consequence modeling has been extensively studied for individual fire and explosion accidents and also for domino effects, the interaction between events (fire and explosion) in a unit has been missing. In the present work, a novel systematic methodology to model the evolving accident scenario is developed and applied to two case studies. This methodology used CFD codes FLACS and FDS to model explosion and fire consequences, respectively. An integrated approach was

subsequently adopted to create the cumulative risk profile of an offshore installation. Through this study, it has been confirmed that the integrated methodology is more effective in assessing damage potential, if an accident occurs. This study helps in designing safety measures and developing an effective emergency management system.

#### **8.1.5 Risk-based approach for toxicity assessment**

This study developed a risk-based approach to assess the effects of combustion products dispersion in semi-confined and confined areas of an offshore installation. Toxic assessment based only on concentrations of contaminants lacks the rigour required. Safety measure design based on such an approach may be less effective. An individual spends different durations in various locations of an offshore installation, making the exposure time an important parameter. Combustion products vary significantly in their compositions, depending on source and type of combustion. To assess exposure, concentrations of different contaminants cannot be added. A risk-based approach, however, considers the time that an individual spends in different locations of a platform in estimating the risk. In addition, risk has an additive characteristic that enables a risk-based approach to take into account the cumulative effects caused from various toxic constituents. The proposed methodology is tested with a case study; the overall risk profile of an offshore installation has been developed and analyzed for safety measure design including emergency management. The case study has confirmed the more effective use of a risk-based approach over a concentration-based one.

## **8.2 Recommendations**

The present work introduces new approaches and attempts to address some of the limitations of existing techniques related to consequence modeling and risk assessment of oil and gas industries. This study can be further improved and extended. Below is a list of important recommendations to extend the present work.

### **8.2.1 CFD explosion modeling**

The study has shown the effective use of CFD codes in VCE accident modeling. However, the use of CFD codes to prevent accidents or at least decrease the harmful effects of accidents has not been studied in this work. Using CFD codes to analyze the effects of natural and mechanical ventilation rates at an installation to prevent the formation of flammable vapour is an effective way to prevent a fire and explosion. This could be further explored. In addition, different configurations of confinement/congestion at a platform also affect the severity of the explosion overpressure that can be analyzed through the application of CFD codes. Blast walls are effective ways of reducing the harmful effects of explosion overpressure. Thus, the configuration and technical characteristics of blast walls/relief valves can be evaluated using the proposed approaches and CFD codes.

### **8.2.2 Integrated consequence modeling**

The study has demonstrated the effective use of an integrated approach of consequence modeling. Further studies could consider stronger dependence and interactions between events and also take into account the cumulative effects caused by various damage types.

Considering other events involved in offshore accidents such as the combustion products inhaled by individuals or damages to the offshore structures combined with the mentioned events (fire and explosion) is recommended for further study.

The effective use of CFD codes in accident modeling was also shown through various case studies in the current work. However, it should be mentioned that the current available CFD codes are only capable of modeling individual events; in the current study FLACS has been used to model the explosion and FDS has been exploited to simulate the fire. There is no tool available that could model an evolving accident scenario. Thus, further studies on developing a new generation of CFD codes capable of modeling evolving accident scenarios are recommended.

### **8.2.3 Toxic dispersion modeling**

The study has confirmed the priority of a risk-based approach in combustion products toxicity assessment over concentration-based methods. Future studies can focus on an extensive evaluation of combustion products to provide a comprehensive cumulative toxic risk profile for offshore installations.

Taking into account the cumulative risk caused by the combination of toxic contaminants, fire heat load and explosion overpressure is also recommended for future study. This will be very useful for safety measures design and emergency preparedness actions.

#### **8.2.4 Data uncertainty analysis**

Different approaches and models proposed in the present work require a large set of data. Procuring such a large set of precise data is often very difficult. It is recommended to integrate data uncertainty and a sensitivity analysis approach to the currently proposed models. This would help to identify critical data needed, and thus a focused approach to collect essential data. It will also help to quantify the uncertainty associated with the estimated results based on the uncertainty of the input data.





